Coulomb ポテンシャル

$$V_{ij} = V(r_{ij}) = \frac{q_i q_j}{r_{ij}} \tag{1.1}$$

Schrödinger方程式

$$\mathbf{H}\Psi = i\hbar\frac{\partial\Psi}{\partial \mathrm{t}} \tag{1.3}$$

$$\begin{aligned}
&\mathbf{H}(\mathbf{r},t) = \mathbf{H}(\mathbf{r}) \\
&\Psi(\mathbf{r},t) = \Psi(\mathbf{r})\mathrm{e}^{-iEt/\hbar} \\
&\mathbf{H}(\mathbf{r})\Psi(\mathbf{r}) = E\Psi(\mathbf{r})
\end{aligned} \tag{1.4}$$

時間に依存しない Schrödinger方程式

$$\begin{aligned}
&\mathbf{H} = \mathbf{T} + \mathbf{V} \\
&\mathbf{T} = \sum_{i=1}^{N}\mathbf{T}_i = -\sum_{i=1}^{N}\frac{\hbar^2}{2m_i}\nabla_i^2 \qquad \text{運動エネルギー} \\
&\nabla_i^2 = \left(\frac{\partial^2}{\partial x_i^2} + \frac{\partial^2}{\partial y_i^2} + \frac{\partial^2}{\partial z_i^2}\right) \\
&\mathbf{V} = \sum_{i=1}^{N}\sum_{j>1}^{N} V_{ij} \qquad \text{ポテンシャル}
\end{aligned} \tag{1.5}$$

電子と原子核からなる系のHamiltonian

$$\mathbf{H}_{\mathrm{tot}} = \mathbf{T}_{\mathrm{n}} + \mathbf{T}_{\mathrm{e}} + \mathbf{V}_{\mathrm{ne}} + \mathbf{V}_{\mathrm{ee}} + \mathbf{V}_{\mathrm{nn}} \tag{3.2}$$

重心系

mass polarization

$$\begin{aligned}
&\mathbf{H}_{\mathrm{tot}} = \mathbf{T}_{\mathrm{n}} + \mathbf{H}_{\mathrm{e}} + \mathbf{H}_{\mathrm{mp}} \\
&\mathbf{H}_{\mathrm{e}} = \mathbf{T}_{\mathrm{e}} + \mathbf{V}_{\mathrm{ne}} + \mathbf{V}_{ee} + \mathbf{V}_{\mathrm{nn}} \quad (\text{電子ハミルトニアン}) \\
&\mathbf{H}_{\mathrm{mp}} = -\frac{1}{2M_{\mathrm{tot}}}\left(\sum_{i=1}^{N}\nabla_i\right)^2
\end{aligned} \tag{3.3}$$

$\mathbf{H}_{\mathrm{e}}$について厳密解が求まったとすると、

$$\mathbf{H}_{\mathrm{e}}(\mathbf{R})\Psi_i(\mathbf{R},\mathbf{r}) = E_i(\mathbf{R})\Psi_i(\mathbf{R},\mathbf{r}),\ i = 1,2\ldots\infty \tag{3.4}$$

$$\begin{aligned}
&\int \Psi_i^*(\mathbf{R},\mathbf{r})\Psi_j(\mathbf{R},\mathbf{r})\mathrm{d}\mathbf{r} = \delta_{ij} \\
&\delta_{ij} = 1, \quad i = j \\
&\delta_{ij} = 0, \quad i \neq j
\end{aligned} \tag{3.5}$$

ととけ、全波動関数(核と電子合わせたもの)は

$$\Psi_{\mathrm{tot}}(\mathbf{R},\mathbf{r}) = \sum_{i=1}^{\infty}\Psi_{ni}(\mathbf{R})\Psi_i(\mathbf{R},\mathbf{r}) \tag{3.6}$$

とかける。

$\mathbf{H}_{\mathrm{tot}}\Psi = E_{\mathrm{tot}}\Psi$ に代入

$$\sum_{i=1}^{\infty}(\mathbf{T}_{\mathrm{n}} + \mathbf{H}_{\mathrm{e}} + \mathbf{H}_{\mathrm{mp}})\Psi_{ni}(\mathbf{R})\Psi_i(\mathbf{R},\mathbf{r}) = E_{\mathrm{tot}}\sum_{i=1}^{\infty}\Psi_{ni}(\mathbf{R})\Psi_i(\mathbf{R},\mathbf{r}) \tag{3.7}$$

$$\begin{aligned}
&\mathbf{T}_{\mathrm{n}} = \sum_a -\frac{1}{2M_a}\nabla_a^2 = \nabla_{\mathrm{n}}^2 \\
&\nabla_a = \left(\frac{\partial}{\partial X_a}, \frac{\partial}{\partial Y_a}, \frac{\partial}{\partial Z_a}\right) \\
&\nabla_a^2 = \left(\frac{\partial^2}{\partial X_a^2} + \frac{\partial^2}{\partial Y_a^2} + \frac{\partial^2}{\partial Z_a^2}\right)
\end{aligned} \tag{3.8}$$

$$\begin{aligned}
&\int \Psi^*\mathbf{H}\Psi\mathrm{d}v = \langle\Psi|\mathbf{H}|\Psi\rangle \\
&\int \Psi^*\Psi\mathrm{d}v = \langle\Psi|\Psi\rangle
\end{aligned} \tag{3.10}$$

∇_{n}^2, $\langle\Psi|\hat{H}|\Psi\rangle$, $\langle\Psi|\Psi\rangle$を使うと、$\langle\Psi_{ni}|$を(3.7)に作用させて

$$\begin{aligned}
&\nabla_{\mathrm{n}}^2\Psi_{ni} + E_j\Psi_{ni} + \sum_{i=1}^{\infty}\{2\langle\Psi_j|\nabla_{\mathrm{n}}|\Psi_i\rangle(\nabla_{\mathrm{n}}\Psi_{ni}) + \langle\Psi_j|\nabla_{\mathrm{n}}^2|\Psi_i\rangle\Psi_{ni} \\
&\quad + \langle\Psi_j|\mathbf{H}_{\mathrm{mp}}|\Psi_i\rangle\Psi_{ni}\} = E_{\mathrm{tot}}\Psi_{nj}
\end{aligned} \tag{3.12}$$

断熱近似（1/Mの項は無視）
原子核は無限にゆっくり運動する（電子に比べて）という考え

$$(\nabla_n^2 + E_j + \langle\Psi_j|\nabla_n^2|\Psi_j\rangle + \langle\Psi_j|\mathbf{H}_{mp}|\Psi_j\rangle)\Psi_{nj} = E_{tot}\Psi_{nj} \qquad (3.13)$$

mass polarization の項を無視して

$$(\mathbf{T}_n + E_j + \langle\Psi_j|\nabla_n^2|\Psi_j\rangle)\Psi_{nj} = E_{tot}\Psi_{nj} \qquad (3.14)$$

$\langle \Psi_i | \nabla_n^2 | \Psi_j \rangle = O(\frac{m_e}{M})$ なので無視（Born-Oppenheimer近似）

$$(\mathbf{T}_n + E_j(\mathbf{R}))\Psi_{nj}(\mathbf{R}) = E_{tot}\Psi_{nj}(\mathbf{R})$$
$$(\mathbf{T}_n + \mathrm{V}_j(\mathbf{R}))\Psi_{nj}(\mathbf{R}) = E_{tot}\Psi_{nj}(\mathbf{R}) \qquad (3.16)$$

核をとめて電子の問題を解いてから核の運動を論じる（大体よい）

注：Born-Oppenheimer近似がだめなとき

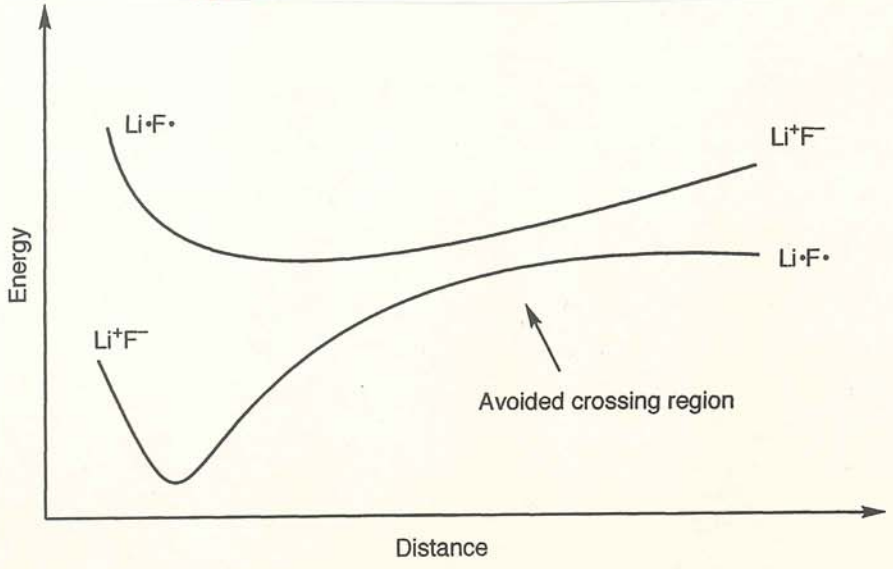

Figure 3.1 Avoided crossing of potential energy surfaces for LiF

電子スピン

$$\langle\alpha|\alpha\rangle = \langle\beta|\beta\rangle = 1$$
$$\langle\alpha|\beta\rangle = \langle\beta|\alpha\rangle = 0 \qquad (3.18)$$

変分法

$$E_e = \frac{\langle\Psi|\mathbf{H}_e|\Psi\rangle}{\langle\Psi|\Psi\rangle} \qquad (3.19)$$

Slater 行列式

$$\Phi_{SD} = \frac{1}{\sqrt{N!}}\begin{vmatrix} \phi_1(1) & \phi_2(1) & \dots & \phi_N(1) \\ \phi_1(2) & \phi_2(2) & \dots & \phi_N(2) \\ \dots & \dots & \dots & \dots \\ \phi_1(N) & \phi_2(N) & \dots & \phi_N(N) \end{vmatrix}, \quad \langle\phi_i|\phi_j\rangle = \delta_{ij} \qquad (3.20)$$

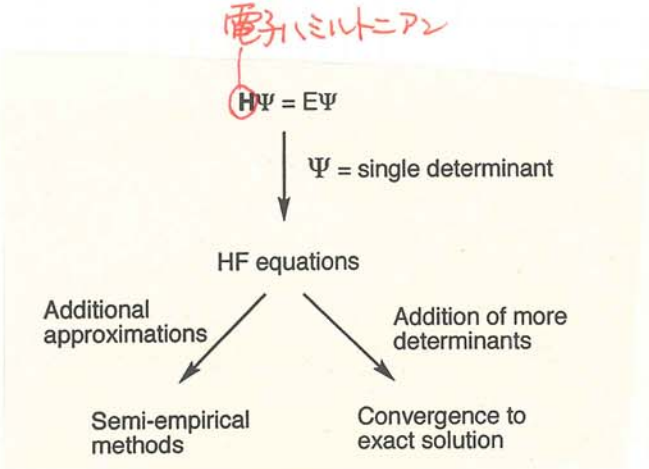

Figure 3.2 The HF model as a starting point for either more approximate or more accurate treatments

分子軌道法では，原子核の動きを左右する核のポテンシャルエネルギー（＝電子エネルギー）を求めている

Slater行列式 Φ

$$\Phi = \mathbf{A}[\phi_1(1)\phi_2(2)\ldots\phi_N(N)] = \mathbf{A}\Pi$$
$$\mathbf{A} = \frac{1}{\sqrt{N!}}\sum_{p=0}^{N-1}(-1)^p\mathbf{P} = \frac{1}{\sqrt{N!}}[\mathbf{1} - \sum_{ij}\mathbf{P}_{ij} + \sum_{ijk}\mathbf{P}_{ijk} - \ldots] \quad (3.21)$$

Âの性質

$$\mathbf{AH} = \mathbf{HA}$$
$$\mathbf{AA} = \sqrt{N!}\mathbf{A} \quad (3.22)$$

電子ハミルトニアン Ĥe

$$\mathbf{H}_e = \mathbf{T}_e + \mathbf{V}_{ne} + \mathbf{V}_{ee} + \mathbf{V}_{nn}$$
$$\mathbf{T}_e = -\sum_i^N \frac{1}{2}\nabla_i^2$$
$$\mathbf{V}_{ne} = -\sum_i^N\sum_a \frac{Z_a}{|\mathbf{R}_a - \mathbf{r}_i|} \quad (3.23)$$
$$\mathbf{V}_{ee} = \sum_i^N\sum_{j>i}^N \frac{1}{|\mathbf{r}_i - \mathbf{r}_j|}$$
$$\mathbf{V}_{nn} = \sum_a\sum_{b>a} \frac{Z_aZ_b}{|\mathbf{R}_a - \mathbf{R}_b|}$$

$$\mathbf{h}_i = -\frac{1}{2}\nabla_i^2 - \sum_a \frac{Z_a}{|\mathbf{R}_a - \mathbf{r}_i|}$$
$$\mathbf{g}_{ij} = \frac{1}{|\mathbf{r}_i - \mathbf{r}_j|} \quad (3.24)$$
$$\mathbf{H}_e = \sum_{i=1}^N \mathbf{h}_i + \sum_{i=1}^N\sum_{j>i}^N \mathbf{g}_{ij} + \mathbf{V}_{nn}$$

1電子演算子　2電子演算子　核間

電子エネルギー E

$$\begin{aligned} E &= \langle\Phi|\mathbf{H}|\Phi\rangle \\ &= \langle\mathbf{A}\Pi|\mathbf{H}|\mathbf{A}\Pi\rangle \\ &= \sqrt{N!}\langle\Pi|\mathbf{H}|\mathbf{A}\Pi\rangle \\ &= \sum_p(-1)^p\langle\Pi|\mathbf{H}|\mathbf{P}\Pi\rangle \end{aligned} \quad (3.25)$$

核

$$\langle\Phi|\mathbf{V}_{nn}|\Phi\rangle = V_{nn}\langle\Phi|\Phi\rangle = V_{nn} \quad (3.26)$$

1電子

$$\begin{aligned} \langle\Pi|\mathbf{h}_1|\Pi\rangle &= \langle\phi_1(1)\phi_2(2)\ldots\phi_N(N)|\mathbf{h}_1|\phi_1(1)\phi_2(2)\ldots\phi_N(N)\rangle \\ &= \langle\phi_1(1)|\mathbf{h}_1|\phi_1(1)\rangle\langle\phi_2(2)|\phi_2(2)\rangle\ldots\langle\phi_N(N)|\phi_N(N)\rangle \\ &= \langle\phi_1(1)|\mathbf{h}_1|\phi_1(1)\rangle = h_1 \end{aligned} \quad (3.27)$$

$$\begin{aligned} \langle\Pi|\mathbf{h}_1|\mathbf{P}_{12}\Pi\rangle &= \langle\phi_1(1)\phi_2(2)\ldots\phi_N(N)|\mathbf{h}_1|\phi_2(1)\phi_1(2)\ldots\phi_N(N)\rangle \\ &= \langle\phi_1(1)|\mathbf{h}_1|\phi_2(1)\rangle\langle\phi_2(2)|\phi_1(2)\rangle\ldots\langle\phi_N(N)|\phi_N(N)\rangle \end{aligned} \quad (3.28)$$

2電子

$$\begin{aligned} \langle\Pi|\mathbf{g}_{12}|\Pi\rangle &= \langle\phi_1(1)\phi_2(2)\ldots\phi_N(N)|\mathbf{g}_{12}|\phi_1(1)\phi_2(2)\ldots\phi_N(N)\rangle \\ &= \langle\phi_1(1)\phi_2(2)|\mathbf{g}_{12}|\phi_1(1)\phi_2(2)\rangle\ldots\langle\phi_N(N)|\phi_N(N)\rangle \\ &= \langle\phi_1(1)\phi_2(2)|\mathbf{g}_{12}|\phi_1(1)\phi_2(2)\rangle = J_{12} \end{aligned} \quad (3.29)$$

$$\begin{aligned} \langle\Pi|\mathbf{g}_{12}|\mathbf{P}_{12}\Pi\rangle &= \langle\phi_1(1)\phi_2(2)\ldots\phi_N(N)|\mathbf{g}_{12}|\phi_2(1)\phi_1(2)\ldots\phi_N(N)\rangle \\ &= \langle\phi_1(1)\phi_2(2)|\mathbf{g}_{12}|\phi_2(1)\phi_1(2)\rangle\ldots\langle\phi_N(N)|\phi_N(N)\rangle \\ &= \langle\phi_1(1)\phi_2(2)|\mathbf{g}_{12}|\phi_2(1)\phi_1(2)\rangle = K_{12} \end{aligned} \quad (3.30)$$

$$E = \sum_{i=1}^N h_i + \sum_{i=1}^N\sum_{j>i}^N (J_{ij} - K_{ij}) + V_{nn} \quad (3.31)$$

または

$$E = \sum_{i=1}^N h_i + \frac{1}{2}\sum_{i=1}^N\sum_{j=1}^N (J_{ij} - K_{ij}) + V_{nn} \quad (3.32)$$

電子エネルギーEを演算子を使ってかく

$$E = \sum_i^N \langle\phi_i|\mathbf{h}_i|\phi_i\rangle + \frac{1}{2}\sum_{ij}^N (\langle\phi_j|\mathbf{J}_i|\phi_j\rangle - \langle\phi_j|\mathbf{K}_i|\phi_j\rangle) + V_{\mathrm{nn}} \tag{3.33}$$

$$\mathbf{J}_i|\phi_j(2)\rangle = \langle\phi_i(1)|\mathbf{g}_{12}|\phi_i(1)\rangle|\phi_j(2)\rangle$$
$$\mathbf{K}_i|\phi_j(2)\rangle = \langle\phi_i(1)|\mathbf{g}_{12}|\phi_j(1)\rangle|\phi_i(2)\rangle$$

Lagrangeの未定定数法を使って極値を求める(変分法)

$$L = E - \sum_{ij}^N \lambda_{ij}(\langle\phi_i|\phi_j\rangle - \delta_{ij})$$
$$\delta L = \delta E - \sum_{ij}^N \lambda_{ij}(\langle\delta\phi_i|\phi_j\rangle + \langle\phi_i|\delta\phi_j\rangle) = 0 \tag{3.34}$$

$$\delta E = \sum_i^N (\langle\delta\phi_i|\mathbf{h}_i|\phi_i\rangle + \langle\phi_i|\mathbf{h}_i|\delta\phi_i\rangle)$$
$$+\frac{1}{2}\sum_{ij}^N (\langle\delta\phi_i|\mathbf{J}_i - \mathbf{K}_j|\phi_i\rangle + \langle\phi_i|\mathbf{J}_j - \mathbf{K}_j|\delta\phi_i\rangle \tag{3.35}$$
$$+ \langle\delta\phi_j|\mathbf{J}_i - \mathbf{K}_i|\phi_j\rangle + \langle\phi_j|\mathbf{J}_i - \mathbf{K}_i|\delta\phi_j\rangle)$$

$$\delta E = \sum_i^N \langle\delta\phi_i|\mathbf{h}_i|\phi_i\rangle + \langle\phi_i|\mathbf{h}_i|\delta\phi_i\rangle + \sum_{ij}^N (\langle\delta\phi_i|\mathbf{J}_j - \mathbf{K}_j|\phi_i\rangle + \langle\phi_i|\mathbf{J}_j - \mathbf{K}_j|\delta\phi_i\rangle)$$
$$\delta E = \sum_i^N (\langle\delta\phi_i|\mathbf{F}_i|\phi_i\rangle + \langle\phi_i|\mathbf{F}_i|\delta\phi_i\rangle)$$
$$\mathbf{F}_i = \mathbf{h}_i + \sum_j^N (\mathbf{J}_j - \mathbf{K}_j) \tag{3.36}$$

Fock演算子

Fock演算子を使うと

$$\delta L = \sum_i^N (\langle\delta\phi_i|\mathbf{F}_i|\phi_i\rangle + \langle\phi_i|\mathbf{F}_i|\delta\phi_i\rangle) - \sum_{ij}^N \lambda_{ij}(\langle\delta\phi_i|\phi_j\rangle + \langle\phi_i|\delta\phi_j\rangle) \tag{3.37}$$

$$\delta L = \sum_i^N \langle\delta\phi_i|\mathbf{F}_i|\phi_i\rangle - \sum_{ij}^N \lambda_{ij}\langle\delta\phi_i|\phi_j\rangle$$
$$+ \sum_i^N \langle\delta\phi_i|\mathbf{F}_i|\phi_i\rangle^* - \sum_{ij}^N \lambda_{ij}\langle\delta\phi_j|\phi_i\rangle^* = 0 \tag{3.38}$$

$\delta\phi_i$は任意だから

$$\mathbf{F}_i\phi_i = \sum_j^N \lambda_{ij}\phi_j \tag{3.40}$$

unitary変換により対角化してやると、

$$\mathbf{F}_i\phi_i' = \varepsilon_i\phi_i' \tag{3.41}$$

$\langle\phi_i'|\times$

$$\varepsilon_i = \langle\phi_i'|\mathbf{F}_i|\phi_i'\rangle \tag{3.42}$$

軌道エネルギー

まとめて、

$$E = \sum_i^N \varepsilon_i - \frac{1}{2}\sum_{ij}^N (J_{ij} - K_{ij}) + V_{\mathrm{nn}}$$
$$\varepsilon_i = \langle\phi_i|\mathbf{F}_i|\phi_i\rangle = h_i + \sum_j^N (J_{ij} - K_{ij}) \tag{3.43}$$

N電子とN-1電子のエネルギー

$$E_N = \sum_{i=1}^{N} h_i + \frac{1}{2}\sum_{i=1}^{N}\sum_{j=1}^{N}(J_{ij} - K_{ij}) + V_{\mathrm{nn}}$$
$$E_{N-1}^{k} = \sum_{i=1}^{N-1} h_i + \frac{1}{2}\sum_{i=1}^{N-1}\sum_{j=1}^{N-1}(J_{ij} - K_{ij}) + V_{\mathrm{nn}} \qquad (3.44)$$

差

$$E_N - E_{N-1}^{k} = h_k + \frac{1}{2}\sum_{i=1}^{N}(J_{ik} - K_{ik}) + \frac{1}{2}\sum_{j=1}^{N}(J_{kj} - K_{kj}) \qquad (3.45)$$

$$E_N - E_{N-1}^{k} = h_k + \sum_{i=1}^{N}(J_{ki} - K_{ki}) = \varepsilon_k \qquad (3.46)$$

すなわち、Koopmansの定理が得られた
($\varepsilon_k < 0$に注意)
(イオン化エネルギー) $= -\varepsilon_k$

LCAO近似(基底関数系を使った展開)

$$\phi_i = \sum_{\alpha}^{M} c_{\alpha i}\chi_\alpha \qquad (3.48)$$

$$\mathbf{F}_i \sum_{\alpha}^{M} c_{\alpha i}\chi_\alpha = \varepsilon_i \sum_{\alpha}^{M} c_{\alpha i}\chi_\alpha \qquad (3.49)$$

Roothaan-Hall方程式

$$\mathbf{FC} = \mathbf{SC}\boldsymbol{\varepsilon}$$
$$F_{\alpha\beta} = \langle\chi_\alpha|\mathbf{F}|\chi_\beta\rangle \quad \text{Fock 行列要素}$$
$$S_{\alpha\beta} = \langle\chi_\alpha|\chi_\beta\rangle \quad \text{重なり 行列要素} \qquad (3.50)$$

いっしょうけんめい計算すると、

$$\langle\chi_\alpha|\mathbf{F}|\chi_\beta\rangle = \langle\chi_\alpha|\mathbf{h}|\chi_\beta\rangle + \sum_{\gamma}^{\mathrm{AO}}\sum_{\delta}^{\mathrm{AO}} D_{\gamma\delta}(\langle\chi_\alpha\chi_\gamma|\mathbf{g}|\chi_\beta\chi_\delta\rangle - \langle\chi_\alpha\chi_\gamma|\mathbf{g}|\chi_\delta\chi_\beta\rangle)$$
$$D_{\gamma\delta} = \sum_{j}^{\mathrm{occ.\ MO}} c_{\gamma j}c_{\delta j} \quad : \text{密度行列要素} \qquad (3.51)$$

$$F_{\alpha\beta} = h_{\alpha\beta} + \sum_{\gamma\delta} G_{\alpha\beta\gamma\delta}D_{\gamma\delta}$$
$$\mathbf{F} = \mathbf{h} + \mathbf{G}\cdot\mathbf{D} \quad \text{テンソルの縮約} \qquad (3.52)$$

電子エネルギーもいっしょうけんめい計算すると

$$E = \sum_{\alpha\beta}^{M} D_{\alpha\beta}h_{\alpha\beta} + \frac{1}{2}\sum_{\alpha\beta\gamma\delta}^{M}(D_{\alpha\beta}D_{\gamma\delta} - D_{\alpha\delta}D_{\gamma\beta})\langle\chi_\alpha\chi_\gamma|\mathbf{g}|\chi_\beta\chi_\delta\rangle + V_{\mathrm{nn}} \qquad (3.54)$$

記法(書き方)について

$$h_{\alpha\beta} = \langle\chi_\alpha|\mathbf{h}|\chi_\beta\rangle = \int\chi_\alpha(1)\left(-\frac{1}{2}\nabla^2\right)\chi_\beta(1)\mathrm{d}\mathbf{r}_1 + \sum_a\int\chi_\alpha(1)\frac{Z_a}{|\mathbf{R}_a - \mathbf{r}_1|}\chi_\beta(1)\mathrm{d}\mathbf{r}_1$$
$$\langle\chi_\alpha\chi_\gamma|\mathbf{g}|\chi_\beta\chi_\delta\rangle = \int\chi_\alpha(1)\chi_\gamma(2)\frac{1}{|\mathbf{r}_1 - \mathbf{r}_2|}\chi_\beta(1)\chi_\delta(2)\mathrm{d}\mathbf{r}_1\mathrm{d}\mathbf{r}_2 \qquad (3.55)$$

physisist の記法

$$\int\chi_\alpha(1)\chi_\gamma(2)\frac{1}{|\mathbf{r}_1 - \mathbf{r}_2|}\chi_\beta(1)\chi_\delta(2)\mathrm{d}\mathbf{r}_1\mathrm{d}\mathbf{r}_2 = \langle\chi_\alpha\chi_\gamma|\mathbf{g}|\chi_\beta\chi_\delta\rangle$$
$$= \langle\chi_\alpha\chi_\gamma|\chi_\beta\chi_\delta\rangle = \langle\alpha\gamma|\beta\delta\rangle \qquad (3.56)$$

chemist, Mullikenの記法

$$\int\chi_\alpha(1)\chi_\beta(1)\frac{1}{|\mathbf{r}_1 - \mathbf{r}_2|}\chi_\gamma(2)\chi_\delta(2)\mathrm{d}\mathbf{r}_1\mathrm{d}\mathbf{r}_2 = (\chi_\alpha\chi_\beta|\chi_\gamma\chi_\delta) \qquad (3.57)$$

$$\langle\chi_\alpha\chi_\beta\|\chi_\gamma\chi_\delta\rangle = \langle\chi_\alpha\chi_\beta|\chi_\gamma\chi_\delta\rangle - \langle\chi_\alpha\chi_\beta|\chi_\delta\chi_\gamma\rangle$$
$$(\chi_\alpha\chi_\beta\|\chi_\gamma\chi_\delta) = (\chi_\alpha\chi_\beta|\chi_\gamma\chi_\delta) - (\chi_\alpha\chi_\gamma|\chi_\beta\chi_\delta) \qquad (3.58)$$

↖ 全てかかない記法

SCF法の流れ

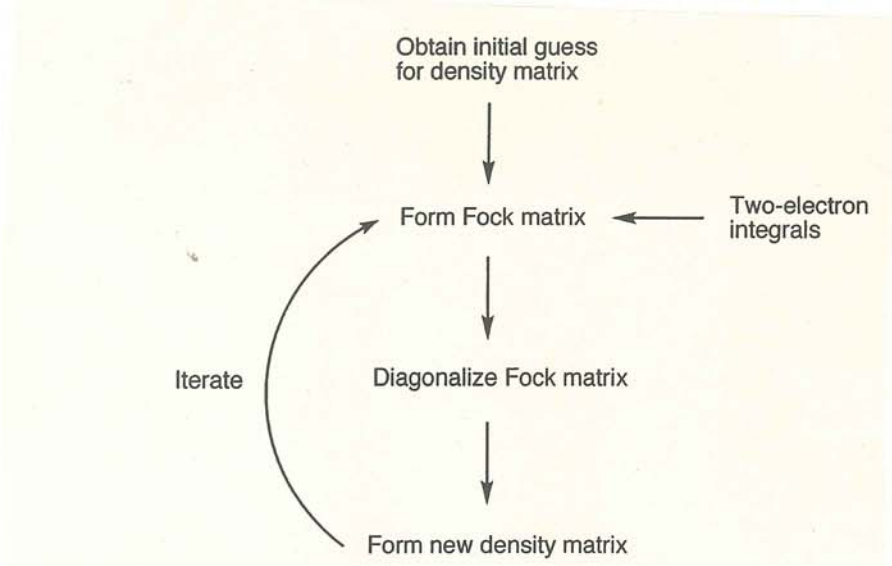

Figure 3.3 Illustration of the SCF procedure

(1) Calculate all one- and two-electron integrals.
(2) Generate a suitable start guess for the MO coefficients.
(3) Form the initial density matrix
(4) Form the Fock matrix as the core (one-electron) integrals + the density matrix times the two-electron integrals.
(5) Diagonalize the Fock matrix (see Chapter 13 for details). The eigenvectors contain the new MO coefficients.
(6) Form the new density matrix. If it is sufficiently close to the previous density matrix, we are done, otherwise go to step (4).

Gauss関数がab initio計算で使われる訳

$$
\begin{aligned}
G_A(\mathbf{r}) &= \left(\frac{2\alpha}{\pi}\right)^{3/4} e^{-\alpha(\mathbf{r}-\mathbf{R}_A)^2} \\
G_B(\mathbf{r}) &= \left(\frac{2\beta}{\pi}\right)^{3/4} e^{-\beta(\mathbf{r}-\mathbf{R}_B)^2} \\
G_A(\mathbf{r})G_B(\mathbf{r}) &= Ke^{-\gamma(\mathbf{r}-\mathbf{R}_c)^2} \\
\gamma &= \alpha+\beta \\
\mathbf{R}_c &= \frac{\alpha\mathbf{R}_A+\beta\mathbf{R}_B}{\alpha+\beta} \\
K &= \left(\frac{2}{\pi}\right)^{3/2}(\alpha\beta)^{3/4}e^{-\frac{\alpha\beta}{\alpha+\beta}(\mathbf{R}_A-\mathbf{R}_B)^2}
\end{aligned}
\tag{3.59}
$$

RHFとUHF

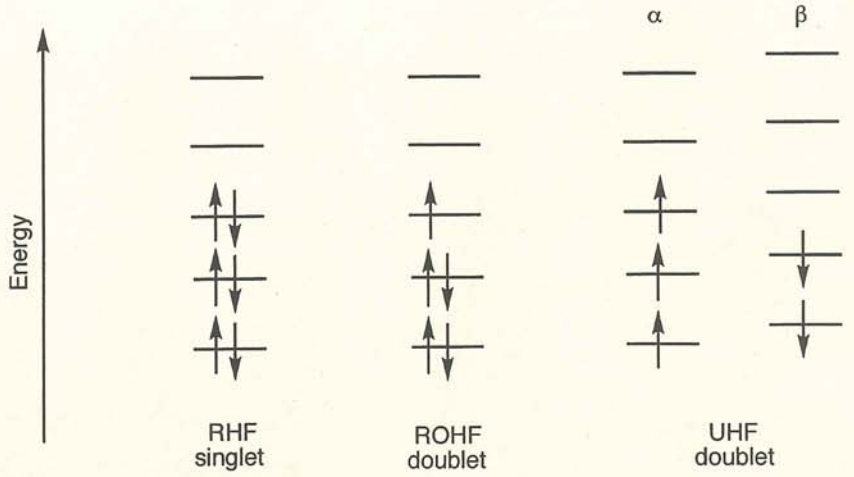

Figure 3.4 Illustrating an RHF singlet, and ROHF and UHF doublet states

半経験的方法 … ZDO(Zero differential Overlap)
$\mu_A(i)\cdot\lambda_B(i)\simeq 0$

Fock行列要素

$$F_{\mu\nu} = h_{\mu\nu} + \sum_{\lambda\sigma}^{\mathrm{AO}} D_{\lambda\sigma}[\langle\mu\nu|\lambda\sigma\rangle - \langle\mu\lambda|\nu\sigma\rangle] \qquad (3.71)$$
$$h_{\mu\nu} = \langle\mu|\mathbf{h}|\nu\rangle$$

Neglect of Diatomic Differential Overlap Approximation (NDDO)

重なり積分

$$S_{\mu\nu} = \langle\mu_\mathrm{A}|\nu_\mathrm{B}\rangle = \delta_{\mu\nu}\delta_{\mathrm{AB}} \qquad (3.72)$$

一電子演算子

$$\mathbf{h} = -\tfrac{1}{2}\nabla^2 - \sum_a \frac{Z'_a}{|\mathbf{R}_a - \mathbf{r}|} = -\tfrac{1}{2}\nabla^2 - \sum_a \mathbf{V}_a \qquad (3.73)$$

一電子積分

$$\langle\mu_\mathrm{A}|\mathbf{h}|\nu_\mathrm{A}\rangle = \langle\mu_\mathrm{A}| -\tfrac{1}{2}\nabla^2 - \mathbf{V}_\mathrm{A}|\nu_\mathrm{A}\rangle - \sum_{a\neq\mathrm{A}}\langle\mu_\mathrm{A}|\mathbf{V}_a|\nu_\mathrm{A}\rangle$$
$$\langle\mu_\mathrm{A}|\mathbf{h}|\nu_\mathrm{B}\rangle = \langle\mu_\mathrm{A}| -\tfrac{1}{2}\nabla^2 - \mathbf{V}_\mathrm{A} - \mathbf{V}_\mathrm{B}|\nu_\mathrm{B}\rangle \qquad (3.74)$$
$$\langle\mu_\mathrm{A}|\mathbf{V}_d|\nu_\mathrm{B}\rangle = 0 \quad (d\neq\mathrm{A},\mathrm{B})$$

$$\langle\mu_\mathrm{A}| -\tfrac{1}{2}\nabla^2 - \mathbf{V}_\mathrm{A}|\nu_\mathrm{A}\rangle = \delta_{\mu\nu}\langle\mu_\mathrm{A}| -\tfrac{1}{2}\nabla^2 - \mathbf{V}_\mathrm{A}|\mu_\mathrm{A}\rangle \qquad (3.75)$$

二電子積分

$$\langle\mu_\mathrm{A}\nu_\mathrm{B}|\lambda_\mathrm{C}\sigma_\mathrm{D}\rangle = \delta_{\mathrm{AC}}\delta_{\mathrm{BD}}\langle\mu_\mathrm{A}\nu_\mathrm{B}|\lambda_\mathrm{A}\sigma_\mathrm{B}\rangle \qquad (3.76)$$

μ, ν, λ, σ：原子軌道（価電子のみ）
A, B, C, D：原子（中心）

Intermediate Neglect of Differential Overlap Approximation (INDO)

NDDOにさらに

$$\langle\mu_\mathrm{A}|\mathbf{h}|\nu_\mathrm{A}\rangle = -\delta_{\mu\nu}\sum_a \langle\mu_\mathrm{A}|\mathbf{V}_a|\mu_\mathrm{A}\rangle$$
$\langle\mu_\mathrm{A}|\mathbf{V}_a|\mu_\mathrm{A}\rangle$ is independent of orbital type (s or p) (3.77)

$$\langle\mu_\mathrm{A}\nu_\mathrm{B}|\lambda_\mathrm{C}\sigma_\mathrm{D}\rangle = \delta_{\mu_\mathrm{A}\lambda_\mathrm{C}}\delta_{\nu_\mathrm{B}\sigma_\mathrm{D}}\langle\mu_\mathrm{A}\nu_\mathrm{B}|\mu_\mathrm{A}\nu_\mathrm{B}\rangle$$
$\langle\mu_\mathrm{A}\nu_\mathrm{B}|\mu_\mathrm{A}\nu_\mathrm{B}\rangle$ is independent of orbital type (s or p) (3.78)

$$\langle\mu_\mathrm{A}\nu_\mathrm{A}|\mu_\mathrm{A}\nu_\mathrm{A}\rangle = \langle\mu_\mathrm{A}\mu_\mathrm{A}|\mu_\mathrm{A}\mu_\mathrm{A}\rangle = \gamma_{\mathrm{AA}}$$
$$\langle\mu_\mathrm{A}\nu_\mathrm{B}|\mu_\mathrm{A}\nu_\mathrm{B}\rangle = \gamma_{\mathrm{AB}} \qquad (3.79)$$

Coulomb型だけ残す

Complete Neglect of Differential Overlap Approximation (CNDO)

INDOにさらに

γ_{AB}

$$\langle\mu_\mathrm{A}\nu_\mathrm{B}|\lambda_\mathrm{C}\sigma_\mathrm{D}\rangle = \delta_{\mathrm{AC}}\delta_{\mathrm{BD}}\delta_{\mu\lambda}\delta_{\nu\sigma}\langle\mu_\mathrm{A}\nu_\mathrm{B}|\mu_\mathrm{A}\nu_\mathrm{B}\rangle$$
$\langle\mu_\mathrm{A}\nu_\mathrm{B}|\mu_\mathrm{A}\nu_\mathrm{B}\rangle$ is independent of orbital type (s or p) (3.80)

Pariser–Pople–Parr (PPP)法

π電子のみ考えたCNDO法

- NDDO > INDO > CNDO の順に
  近似が多くなる（計算は速いが、一般に精度が悪い）

Modified Intermediate Neglect of Differential Overlap (MINDO)

$$\begin{aligned}\langle\mu_A|\mathbf{h}|\nu_B\rangle &= \langle\mu_A|-\tfrac{1}{2}\nabla^2-\mathbf{V}_A-\mathbf{V}_B|\nu_B\rangle \\ &= S_{\mu\nu}\beta_{AB}(I_\mu+I_\nu) \qquad (3.81)\\ S_{\mu\nu} &= \langle\mu_A|\nu_B\rangle\end{aligned}$$

原子対について

MINDO/3 has been parameterized for H, B, C, N, O, F, Si, P, S and Cl, although certain combinations of these elements have been omitted.

Modified NDDO Models

The MNDO, AM1 and PM3 methods[30]

$$h_{\mu\nu} = \langle\mu_A|\mathbf{h}|\nu_A\rangle = \delta_{\mu\nu}U_\mu - \sum_{a\neq A} Z'_a\langle\mu_A s_a|\nu_A s_a\rangle \qquad (3.82)$$

$$U_\mu = \langle\mu_A|-\tfrac{1}{2}\nabla^2-\mathbf{V}_A|\mu_A\rangle$$

$$\begin{aligned}\langle\mu_A|\mathbf{h}|\nu_B\rangle &= \langle\mu_A|-\tfrac{1}{2}\nabla^2-\mathbf{V}_A-\mathbf{V}_B|\nu_B\rangle \\ &= S_{\mu\nu}\tfrac{1}{2}(\beta_\mu+\beta_\nu) \qquad (3.83)\\ S_{\mu\nu} &= \langle\mu_A|\nu_B\rangle\end{aligned}$$

原子それぞれについて (cf. MINDO)

$$\begin{aligned}\langle ss|ss\rangle &= G_{ss}\\ \langle sp|sp\rangle &= G_{sp}\\ \langle ss|pp\rangle &= H_{sp} \qquad (3.84)\\ \langle pp|pp\rangle &= G_{pp}\\ \langle pp'|pp'\rangle &= G_{p2}\end{aligned}$$

Each of the MNDO, AM1 and PM3 methods involves at least 12 parameters per atom: orbital exponents, $\zeta_{s/p}$; one-electron terms, $U_{s/p}$ and $\beta_{s/p}$; two-electron terms, G_{ss}, G_{sp}, G_{pp}, G_{p2}, H_{sp}; parameters used in the core–core repulsion, α; and for the AM1 and PM3 methods also a, b and c constants, as described below.

Modified Neglect of Diatomic Overlap (MNDO)

8

$$V_{nn}^{MNDO}(A,B) = Z'_A Z'_B\langle s_A s_B|s_A s_B\rangle(1+e^{-\alpha_A R_{AB}}+e^{-\alpha_B R_{AB}}) \qquad (3.85)$$

Interactions involving O–H and N–H bonds are treated differently

$$V_{nn}(A,H) = Z'_A Z_H\langle s_A s_H|s_A s_H\rangle\left(1+\frac{e^{-\alpha_A R_{AH}}}{R_{AH}}+e^{-\alpha_H R_{AH}}\right) \qquad (3.86)$$

$\zeta_s = \zeta_p$ for some of the lighter elements.

MNDO has been parameterized for the elements: H, B, C, N, O, F, Al, Si, P, S, Cl, Zn, Ge, Br, Sn, I, Hg and Pb. The G_{ss}, G_{sp}, G_{pp}, G_{p2}, H_{sp} parameters are taken from atomic spectra, while the others are fitted to molecular data. Although MNDO has been succeeded by the AM1 and PM3 methods, it is still used for some types of calculation where MNDO is known to give better results.

MNDOの注意点

(1) Sterically crowded molecules, like neopentane, are too unstable.
(2) Four membered rings are too stable.
(3) Weak interactions are unreliable, for example it does not predict hydrogen bonds.
(4) Hypervalent molecules, like sulfoxides and sulfones, are too unstable.
(5) Activation energies for bond breaking/forming reactions are too high.
(6) Non-classical structures are predicted to be unstable relative to classical structures (for example ethyl cation).
(7) Oxygenated substituents on aromatic rings are out-of-plane (for example nitrobenzene).
(8) Peroxide bonds are too short by $\sim$0.17 Å
(9) The C–X–C angle in ethers and sulfides is too large by $\sim 9°$.

3.10.4 Austin Model 1 (AM1)

MNDO

$$V_{nn}(A,B) = V_{nn}^{MNDO}(A,B) + \frac{Z'_A Z'_B}{R_{AB}} \times \left(\sum_k a_{kA} e^{-b_{kA}(R_{AB}-c_{kA})^2} + \sum_k a_{kB} e^{-b_{kB}(R_{AB}-c_{kB})^2} \right) \quad (3.87)$$

(kについての和は2項～4項)

parameterized for the elements: H, B, C, N, O, F, Al, Si, P, S, Cl, Zn, Ge, Br, I and Hg.

AM1の注意点

(1) AM1 does predict hydrogen bonds with a strength approximately correct, but the geometry is often wrong.
(2) Activation energies are much improved over MNDO.
(3) Hypervalent molecules are improved over MNDO, but still have significantly larger errors than other types of compound.
(4) Alkyl groups are systematically too stable by ~2 kcal/mol per CH_2 group.
(5) Nitro compounds are systematically too unstable.
(6) Peroxide bonds are too short by ~0.17 Å.
(7) Phosphor compounds have problems when atoms are ~3 Å apart, producing incorrect geometries. P_4O_6 for example is predicted to have P–P bonds differing by 0.4 Å, although experimentally they are identical.
(8) The *gauche* conformation in ethanol is predicted to be more stable than the *trans*.

3.10.5 Modified Neglect of Diatomic Overlap, Parametric Method Number 3 (MNDO-PM3)

"全パラメータを同時最適化したAM1"
(kについての和は2項)

PM3 has been parameterized for the elements: H, Li, C, N, O, F, Mg, Al, Si, P, S, Cl, Zn, Ga, Ge, As, Se, Br, Cd, In, Sn, Sb, Te, I, Hg, Tl, Pb, Bi, Po and At. Parameters for many of the (additional) transition metals are also being developed under the name PM3(tm), which includes d-orbitals.

PM3の注意点

(1) Almost all sp^3-nitrogens are predicted to be pyramidal, contrary to experimental observation.
(2) Hydrogen bonds are too short by ~0.1 Å.
(3) The *gauche* conformation in ethanol is predicted to be more stable than the *trans*.
(4) Bonds between Si and Cl, Br and I are underestimated, the Si-I bond in H_3SiI, for example, is too short by ~0.4 Å.
(5) H_2NNH_2 is predicted to have a C_{2h} structure, while the experimental is C_2, and ClF_3 is predicted to have a D_{3h} structure, while the experimental is C_{2v}.
(6) The charge on nitrogen atoms is often of "incorrect" sign and "unrealistic" magnitude.

MNDO, AM1, PM3 共通の注意点

Some common limitations to MNDO, AM1 and PM3 are:

(1) Rotational barriers for bonds which have partly double bond character are significantly too low. This is especially a problem for the rotation around the C–N bond in amides, where values of 5–10 kcal/mol are obtained. A purely *ad hoc* fix has been made for amides by adding a force field rotational term to the C–N bond which raises the value to 20–25 kcal/mol, and brings it in line with experimental data. Similarly, the barrier for rotation around the central bond in butadiene is calculated to be only 0.5–2.0 kcal/mol, in contrast to the experimental value of 5.9 kcal/mol.[35]
(2) Weak interactions, such as van der Waals complexes or hydrogen bonds, are poorly predicted. Either the interaction is too weak, or the minimum energy geometry is wrong.
(3) The bond length to nitrosyl groups is underestimated, the N–N bond in N_2O_3, for example, is ~0.7 Å too short.
(4) Although MNDO, AM1 and PM3 have parameters for some metals, these are often based on only a few experimental data. Calculations involving metals should thus be treated with care. The PM3(tm) set of parameters are determined exclusively from geometrical data (X-ray), since there are very few reliable energetic data available for transition metal compounds.

MNDO, AM1, PM3の比較

Table 3.1 Average heat of formation error in kcal/mol (number of compounds)

Compounds:	MNDO	AM1	PM3
H, C, N, O (276)	18.5	10.5	7.9
F (133)	84.2	49.5	11.2
Si (78)	22.9	20.8	14.2
All normal valent (607)	24.3	14.8	11.2
Hypervalent (106)	104.5	62.3	17.3
All (713)	46.2	27.6	11.6

Table 3.2 Average errors in bond distances (Å)

Bonds to:	MNDO	AM1	PM3
H	0.015	0.006	0.005
C	0.002	0.002	0.002
N	0.015	0.014	0.012
O	0.017	0.011	0.006
F	0.023	0.017	0.011
Si	0.030	0.019	0.045

Table 3.3 Mulliken charges in formamide with different methods

	MNDO	AM1	PM3	HF/6-31G(d,p)	MP2/6-31G(d,p)
C	0.37	0.26	0.16	0.56	0.40
O	−0.39	−0.40	−0.38	−0.56	−0.43
N	−0.49	−0.62	−0.13	−0.73	−0.63

生成熱を求める式（零点振動エネルギーは既に考慮されていることに注意）

$$\Delta H_f(\text{molecule}) = E_{elec}(\text{molecule}) - \sum^{\text{atoms}} E_{elec}(\text{atoms}) + \sum^{\text{atoms}} \Delta H_f(\text{atoms}) \quad (3.89)$$

Table 3.4 Average heat of formation error in kcal/mol (number of compounds)

Compounds	MNDO	AM1	PM3	MNDO/d	SAM1	SAM1d
Al (29)	22.1	10.5	16.4	4.9		
Si (84)	12.0	8.5	6.0	6.3	8.0	11.2
P (43)	38.7	14.5	17.1	7.6	14.4	15.0
S (99)	48.4	10.3	7.5	5.6	8.3	7.9
Cl (85)	39.4	29.1	10.4	3.9	11.1	4.7
Br (51)	16.2	15.2	8.1	3.4	8.7	5.2
I (42)	25.4	21.7	13.4	4.0	6.6	6.6
Zn (18)	21.0	16.9	14.7	4.9		
Hg (37)	13.7	9.0	7.7	2.2		
Al, Si, P, S, Cl, Br, I, Zn, Hg (488)	29.2	15.3	10.0	4.9		
Si, P, S, Cl, Br, I (404)	31.4	16.1	9.5	5.1	9.3	8.2

種々の方法により計算した各種分子の生成熱の誤差の比較

	誤差(kcal/mol)					
分　子	STO-3G[a]	3-21G[a]	6-31G*[a]	MINDO/3[b]	MNDO[c]	AM1[d]
誤差の絶対値平均	11.7	6.9	6.1	9.0	6.3	5.8
分子数	44	44	43	45	45	45

ab initio法　　半経験的方法

The apparent accuracy of 5–10 kcal/mol for calculating heats of formation with semi-empirical methods is slightly misleading. Normally the interest is in relative energies of different species, and since the heat of formation errors are essentially random, relative energies may not be predicted as well (two random errors of 10 kcal/mol may add up to an error of 20 kcal/mol). This is in contrast to *ab initio* methods, which usually are better at predicting relative rather than absolute energies, since errors using these methods tend to be systematic and at least partly cancel out when comparing similar systems.

拡張Hückel法

$$F_{\mu\mu} = -I_\mu \quad \text{(イオン化ポテンシャル)}$$
$$F_{\mu\nu} = -K\left(\frac{I_\mu + I_\nu}{2}\right)S_{\mu\nu} \tag{3.89}$$

ZDO近似が使われていない

通常 K=1.75

単純Hückel法

$$F_{\mu_A\mu_A} = \alpha_A$$
$$F_{\mu_A\nu_B} = \beta_{AB} \text{ (A and B are neighbours)}$$
$$F_{\mu_A\nu_B} = 0 \text{ (A and B are not neighbours)} \tag{3.93}$$

$$\alpha_A = \alpha_C + h_A\beta_{CC}$$
$$\beta_{AB} = k_{AB}\beta_{CC} \tag{3.94}$$

通常，一回の対角化で解が求まる

(Charge iteration (self-consistent) Hückel法
という原子上の電荷が self-consistent になるまで
繰返す方法もある)

基底関数系

STO

$$\chi_{\zeta,n,l,m}(r,\theta,\varphi) = NY_{l,m}(\theta,\varphi)r^{n-1}\,e^{-\zeta r} \tag{5.1}$$

GTO

$$\chi_{\zeta,n,l,m}(r,\theta,\varphi) = NY_{l,m}(\theta,\varphi)r^{(2n-2-l)}\,e^{-\zeta r^2}$$
$$\chi_{\zeta,l_x,l_y,l_z}(x,y,z) = N x^{l_x}y^{l_y}z^{l_z}\,e^{-\zeta r^2} \tag{5.2}$$

DZ基底の必要性

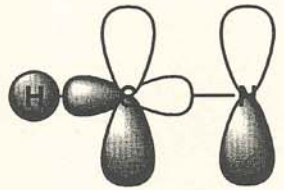

Figure 5.1 A double zeta basis allows for different bonding in different directions

Even-tempered

$$\zeta_i = \alpha\beta^i, \quad i = 1,2,\ldots,M$$
$$\ln(\ln\beta) = b\ln M + b'$$
$$\ln\alpha = a\ln(\beta - 1) + a' \tag{5.3}$$

Well-tempered

$$\zeta_i = \alpha\beta^{i-1}\left(1 + \gamma\left(\frac{i}{M}\right)^\delta\right), \quad i = 1,2,\ldots,M \tag{5.4}$$

縮約(contraction)

$$\chi(\text{CGTO}) = \sum_{i}^{k} a_i \chi_i\,(\text{PGTO}) \tag{5.3}$$

$$\begin{aligned}
\chi_1\,(\text{CGTO}) &= \sum_{i=1}^{6} a_i \chi_i\,(\text{PGTO}) \\
\chi_2(\text{CGTO}) &= \sum_{i=7}^{9} a_i \chi_i\,(\text{PGTO}) \\
\chi_3(\text{CGTO}) &= \chi_{10}\,(\text{PGTO})
\end{aligned} \tag{5.4}$$

$$\begin{aligned}
\chi_1(\text{CGTO}) &= \sum_{i=1}^{10} a_i \chi_i\,(\text{PGTO}) \\
\chi_2(\text{CGTO}) &= \sum_{i=1}^{10} b_i \chi_i\,(\text{PGTO}) \\
\chi_3(\text{CGTO}) &= \sum_{i=1}^{10} c_i \chi_i\,(\text{PGTO})
\end{aligned} \tag{5.5}$$

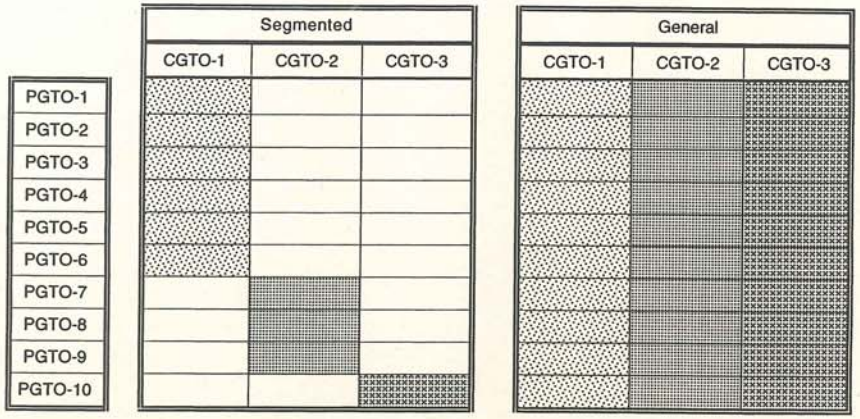

Figure 5.2 Segmented and general contraction

Table 5.1 Correlation consistent basis sets

Basis	Primitive functions	Contracted functions
cc-pVDZ	9s,4p,1d/4s,1p	3s,2p,1d/2s,1p
cc-pVTZ	10s,5p,2d,1f/5s,2p,1d	4s,3p,2d,1f/3s,2p,1d
cc-pVQZ	12s,6p,3d,2f,1g/6s,3p,2d,1f	5s,4p,3d,2f,1g/4s,3p,2d,1f
cc-pV5Z	14s,9p,4d,3f,2g,1h/8s,4p,3d,2f,1g	6s,5p,4d,3f,2g,1h/5s,4p,3d,2f,1g
cc-pV6Z	16s,10p,5d,4f,3g,2h,1i/ 10s,5p,4d,3f,2g,1h	7s,6p,5d,4f,3g,2h,1i/ 6s,5p,4d,3f,2g,1h

有効内殻ポテンシャル (**Effective Core Potential Basis Sets**)

$$U_{\text{ECP}}\,(r) = \sum_{i} a_i r^{n_i} \mathrm{e}^{-\alpha_i r^2} \tag{5.10}$$

内殻電子をポテンシャルにおきかえる

基底関数系重なり誤差

(**Basis Set Superposition Errors**)

複合体の構造を示す

$$\Delta E_{\text{complexation}} = E(\text{AB})^{*}_{\text{ab}} - E(\text{A})_{\text{a}} - E(\text{B})_{\text{b}} \tag{5.11}$$

$$\Delta E_{\text{CP}} = E(\text{A})^{*}_{\text{ab}} + E(\text{B})^{*}_{\text{ab}} - E(\text{A})^{*}_{\text{a}} - E(\text{B})^{*}_{\text{b}} \tag{5.12}$$

$\Delta E_{\text{complexation}} - \Delta E_{\text{CP}}$: counterpoise 補正した
複合体形成エネルギー

電子相関

$$\Psi = a_0\Phi_{\mathrm{HF}} + \sum_{i=1} a_i\Phi_i \qquad (4.1)$$

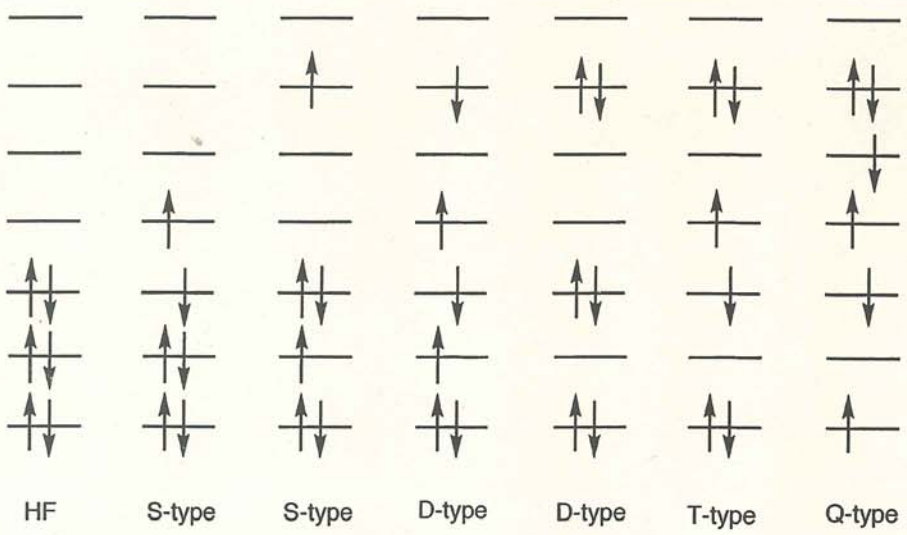

Figure 4.1 Excited Slater determinants generated from a HF reference

EC	Basic	Minimum	DZ	DZP	.....	Infinite
HF (0%)						HF limit
10%						
.....						
100%						"Exact"

Figure 4.2 Convergence to the exact solution

CI波動関数

$$\Psi_{\mathrm{CI}} = a_0\Phi_{\mathrm{SCF}} + \sum_{\mathrm{S}} a_{\mathrm{S}}\Phi_{\mathrm{S}} + \sum_{\mathrm{D}} a_{\mathrm{D}}\Phi_{\mathrm{D}} + \sum_{\mathrm{T}} a_{\mathrm{T}}\Phi_{\mathrm{T}} \ldots = \sum_{i=0} a_i\Phi_i \qquad (4.2)$$

$\Phi_{\mathrm{SCF}} = \Phi_{\mathrm{HF}}$

Lagrangeの未定定数法

$$L = \langle\Psi_{\mathrm{CI}}|\mathbf{H}|\Psi_{\mathrm{CI}}\rangle - \lambda[\langle\Psi_{\mathrm{CI}}|\Psi_{\mathrm{CI}}\rangle - 1] \qquad (4.3)$$

$$\begin{aligned}\langle\Psi_{\mathrm{CI}}|\mathbf{H}|\Psi_{\mathrm{CI}}\rangle &= \sum_{i=0}\sum_{j=0} a_i a_j\langle\Phi_i|\mathbf{H}|\Phi_j\rangle = \sum_{i=0} a_i^2 E_i + \sum_{i=0}\sum_{j\neq i} a_i a_j\langle\Phi_i|\mathbf{H}|\Phi_j\rangle \\ \langle\Psi_{\mathrm{CI}}|\Psi_{\mathrm{CI}}\rangle &= \sum_{i=0}\sum_{j=0} a_i a_j\langle\Phi_i|\Phi_j\rangle = \sum_{i=0} a_i^2\langle\Phi_i|\Phi_i\rangle = \sum_{i=0} a_i^2\end{aligned} \qquad (4.4)$$

停留値をとる条件

$$\begin{aligned}\frac{\partial L}{\partial a_i} &= 2\sum_j a_j\langle\Phi_i|\mathbf{H}|\Phi_j\rangle - 2\lambda a_i = 0 \\ a_i(\langle\Phi_i|\mathbf{H}|\Phi_i\rangle - \lambda) &+ \sum_{j\neq i} a_j\langle\Phi_i|\mathbf{H}|\Phi_j\rangle = 0 \\ a_i(E_i - \lambda) &+ \sum_{j\neq i} a_j\langle\Phi_i|\mathbf{H}|\Phi_j\rangle = 0\end{aligned} \qquad (4.5)$$

永年方程式　$H_{ij} = \langle\Phi_i|\mathbf{H}|\Phi_j\rangle$

$$\begin{pmatrix} H_{00}-E & H_{01} & \cdots & H_{0j} & \cdots \\ H_{10} & H_{11}-E & \cdots & H_{1j} & \cdots \\ \cdots & \cdots & \cdots & \cdots & \cdots \\ H_{j0} & \cdots & \cdots & H_{jj}-E & \cdots \\ \cdots & \cdots & \cdots & \cdots & \cdots \end{pmatrix}\begin{pmatrix} a_0 \\ a_1 \\ .. \\ a_j \\ .. \end{pmatrix} = \begin{pmatrix} 0 \\ 0 \\ .. \\ 0 \\ .. \end{pmatrix} \qquad (4.6)$$

行列とベクトルを使ってかくと

$$(\mathbf{H}-E\mathbf{I})\,\mathbf{a} = \mathbf{0} \qquad \mathbf{H}\mathbf{a} = E\mathbf{a}.$$

CSF
配置状態関数

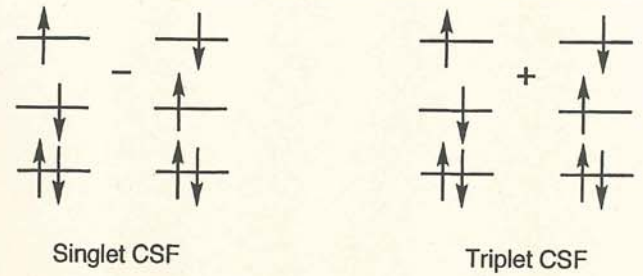

Figure 4.3 Forming configurational state functions from Slater determinants

Slater-Condonの規則

$\langle \Phi_0 | \hat{H} | \Phi_0 \rangle = E_0$

$$\langle \Phi_0 | \mathbf{H} | \Phi_i^a \rangle = \langle \phi_i | \mathbf{h} | \phi_a \rangle + \sum_j \left(\langle \phi_i \phi_j | \phi_a \phi_j \rangle - \langle \phi_i \phi_j | \phi_j \phi_a \rangle \right)$$
$$\langle \Phi_0 | \mathbf{H} | \Phi_{ij}^{ab} \rangle = \langle \phi_i \phi_j | \phi_a \phi_b \rangle - \langle \phi_i \phi_j | \phi_b \phi_a \rangle \qquad (4.7)$$

Brillouinの定理の証明

$$\langle \phi_i | \mathbf{h} | \phi_a \rangle + \sum_j \left(\langle \phi_i \phi_j | \phi_a \phi_j \rangle - \langle \phi_i \phi_j | \phi_j \phi_a \rangle \right) = \langle \phi_i | \mathbf{F} | \phi_a \rangle \qquad (4.8)$$

$$\mathbf{F}\phi_a = \varepsilon_a \phi_a$$
$$\langle \phi_i | \mathbf{F} | \phi_a \rangle = \varepsilon_a \langle \phi_i | \phi_a \rangle = \varepsilon_a \delta_{ia} \qquad (4.9)$$

$\therefore \langle \Phi_0 | \hat{A} | \Phi_1^a \rangle = 0$ (Brillouinの定理)

CI matrix	Φ_{HF}	Φ_S	Φ_D	Φ_T	Φ_Q	Φ_Q	...
Φ_{HF}	E_{HF}	0		0	0	0	0
Φ_S	0				0	0	0
Φ_D						0	0
Φ_T	0						0
Φ_Q	0	0					
Φ_Q	0	0	0				
...	0	0	0	0			

Figure 4.4 Structure of the CI matrix

積分変換 $O(M^5)$

$$\langle \phi_i | \mathbf{h} | \phi_j \rangle = \sum_\alpha^M \sum_\beta^M c_{\alpha i} c_{\beta j} \langle \chi_\alpha | \mathbf{h} | \chi_\beta \rangle$$
$$\langle \phi_i \phi_j | \phi_k \phi_l \rangle = \sum_\alpha^M \sum_\beta^M \sum_\gamma^M \sum_\delta^M c_{\alpha i} c_{\beta j} c_{\gamma k} c_{\delta l} \langle \chi_\alpha \chi_\beta | \chi_\gamma \chi_\delta \rangle \qquad (4.10)$$

$$\langle \phi_i \phi_j | \phi_k \phi_l \rangle = \sum_\alpha c_{\alpha i} \left(\sum_\beta c_{\beta j} \left(\sum_\gamma c_{\gamma k} \left(\sum_\delta c_{\delta l} \langle \chi_\alpha \chi_\beta | \chi_\gamma \chi_\delta \rangle \right) \right) \right) \qquad (4.11)$$

Consider a small system, H_2O with a 6-31G(d)

There are 10 electrons and 38 spin-MOs,

Slater行列式の数

$$\text{Number of SDs} = \sum_{n=0}^{10} K_{10,n} \cdot K_{28,n} = K_{38,10} = \frac{38!}{10! \cdot (38-10)!} \qquad (4.12)$$

Table 4.1 Number of singlet CSFs as a function of excitation level for H_2O with a 6-31G(d) basis

Excitation level n	Number of nth excited CSFs	Total number of CSFs ← 累積
1	71	71
2	2 485	2 556
3	40 040	42 596
4	348 530	391 126
5	1 723 540	2 114 666
6	5 033 210	7 147 876
7	8 688 680	15 836 556
8	8 653 645	24 490 201
9	4 554 550	29 044 751
10	1 002 001	30 046 752

In the general case of N electrons and M basis functions the total number of singlet CSFs that can be generated is given by

$$\text{Number of CSFs} = \frac{M!(M+1)!}{\left(\frac{N}{2}\right)!\left(\frac{N}{2}+1\right)!\left(M-\frac{N}{2}\right)!\left(M-\frac{N}{2}+1\right)!} \qquad (4.13)$$

For H_2O with the above 6-31G(d) basis there are $\sim 30 \times 10^6$ CSFs ($N = 10$, $M = 19$); with the larger 6-311G(2d,2p) basis there are $\sim 106 \times 10^9$ CSFs ($N = 10$, $M = 41$). For $H_2C{=}CH_2$ with the 6-31G(d) basis there are $\sim 334 \times 10^{12}$ CSFs ($N = 16$, $M = 38$).

小さい分子でもひじょうに多い

Table 4.2 Weights of excited configurations for the Neon atom

Excitation level	Weight
0	0.9644945073
1	0.0009804929
2	0.0336865893 ← 二電子励起配置が大切
3	0.0003662339
4	0.0004517826
5	0.0000185090
6	0.0000017447
7	0.0000001393
8	0.0000000011

↓ CISD

CIとRHF解の解離の問題

H_2の解離を考える。

$$\phi_1 = N_1(\chi_A + \chi_B)$$
$$\phi_2 = N_2(\chi_A - \chi_B)$$
$$\Phi_0 = \begin{vmatrix} \phi_1(1)\bar{\phi}_1(1) \\ \phi_1(2)\bar{\phi}_1(2) \end{vmatrix} \qquad (4.15)$$

HF 波動関数

Here N_1 and N_2 are suitable normalization constants, and the bar above the MO indicates that the electron has a β spin function, no bar indicates an α spin function.

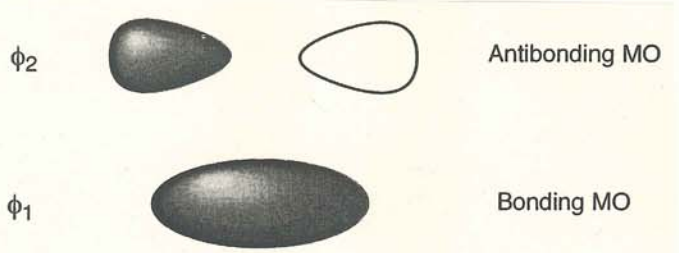

Figure 4.5 Molecular orbitals for H_2

$$\Phi_1 = \begin{vmatrix} \phi_2(1)\bar{\phi}_2(1) \\ \phi_2(2)\bar{\phi}_2(2) \end{vmatrix}$$
$$\Phi_2 = \begin{vmatrix} \phi_1(1)\bar{\phi}_2(1) \\ \phi_1(2)\bar{\phi}_2(2) \end{vmatrix}$$
$$\Phi_3 = \begin{vmatrix} \bar{\phi}_1(1)\phi_2(1) \\ \bar{\phi}_1(2)\phi_2(2) \end{vmatrix} \qquad (4.16)$$
$$\Phi_4 = \begin{vmatrix} \phi_1(1)\phi_2(1) \\ \phi_1(2)\phi_2(2) \end{vmatrix}$$
$$\Phi_5 = \begin{vmatrix} \bar{\phi}_1(1)\bar{\phi}_2(1) \\ \bar{\phi}_1(2)\bar{\phi}_2(2) \end{vmatrix}$$

$$\Phi_0 = \phi_1(1)\bar{\phi}_1(2) - \bar{\phi}_1(1)\phi_1(2) = \phi_1\phi_1(\alpha\beta - \beta\alpha)$$
$$\Phi_1 = \phi_2(1)\bar{\phi}_2(2) - \bar{\phi}_2(1)\phi_2(2) = \phi_2\phi_2(\alpha\beta - \beta\alpha) \qquad (4.17)$$

$$\Phi_0 = (\chi_A(1) + \chi_B(1))(\chi_A(2) + \chi_B(2)) = \chi_A\chi_A + \chi_B\chi_B + \chi_A\chi_B + \chi_B\chi_A$$
$$\Phi_1 = (\chi_A(1) - \chi_B(1))(\chi_A(2) - \chi_B(2)) = \chi_A\chi_A + \chi_B\chi_B - \chi_A\chi_B - \chi_B\chi_A \qquad (4.18)$$

$H^- H^+ \quad H^+ H^- \quad H^\cdot H^\cdot \quad H^\cdot H^\cdot$

	$^1\Phi_0(\sum_g)$	$^1\Phi_1(\sum_g)$	$^1(\Phi_2-\Phi_3)(\sum_u)$	$^3\Phi_4(\sum_u)$	$^3(\Phi_2+\Phi_3)(\sum_u)$	$^3\Phi_5(\sum_u)$
$^1\Phi_0(\sum_g)$			0	0	0	0
$^1\Phi_1(\sum_g)$			0	0	0	0
$^1(\Phi_2-\Phi_3)(\sum_u)$	0	0		0	0	0
$^3\Phi_4(\sum_u)$	0	0	0		0	0
$^3(\Phi_2+\Phi_3)(\sum_u)$	0	0	0	0		0
$^3\Phi_5(\sum_u)$	0	0	0	0	0	

Figure 4.6 Structure of the full CI matrix for the H_2 system in a minimum basis

したがって（対称性の異なるものは互いに混ざらない）

$$\Psi_{CI} = a_0\Phi_0 + a_1\Phi_1 = a_0(\phi_1\phi_1) + a_1(\phi_2\phi_2)$$
$$\Psi_{CI} = (a_0 + a_1)(\chi_A\chi_A + \chi_B\chi_B) + (a_0 - a_1)(\chi_A\chi_B + \chi_B\chi_A) \qquad (4.19)$$

The wrong dissociation limit for RHF wave functions has several consequences.

(1) The energy for stretched bonds is too high. Most transition structures have partly formed/broken bonds, thus activation energies are too high at the RHF level.

(2) The excessively steep increase in energy as a function of the bond length causes the minimum on a potential energy curve to occur too "early" for covalently bonded systems, and equilibrium bond lengths are too short at the RHF level.

(3) The excessively steep increase in energy as a function of the bond length causes the curvature of the potential energy surface near the equilibrium to be too large, and vibrational frequencies, especially those describing bond stretching, are in general too high.

(4) The wave function contains too much "ionic" character, and RHF dipole moments (and also atomic charges) are in general too large.

UHF解の解離の問題

$$\phi_1 = N(\chi_A + c\chi_B)\alpha$$
$$\bar{\phi}_1 = N(c\chi_A + \chi_B)\beta$$
$$\Phi_0^{UHF} = \left|\phi_1(1)\,\bar{\phi}_1(1)\right| \qquad (4.20)$$

The six RHF determinants can be expanded in terms of the AOs:

$$\Phi_0 = [\chi_A\chi_A + \chi_B\chi_B + \chi_A\chi_B + \chi_B\chi_A](\alpha\beta - \beta\alpha)$$
$$\Phi_1 = [\chi_A\chi_A + \chi_B\chi_B - \chi_A\chi_B - \chi_B\chi_A](\alpha\beta - \beta\alpha)$$
$$\Phi_2 = [\chi_A\chi_A - \chi_B\chi_B](\alpha\beta - \beta\alpha) - [\chi_A\chi_B - \chi_B\chi_A](\alpha\beta + \beta\alpha) \qquad (4.21)$$
$$\Phi_3 = [\chi_A\chi_A - \chi_B\chi_B](\alpha\beta - \beta\alpha) + [\chi_A\chi_B - \chi_B\chi_A](\alpha\beta + \beta\alpha)$$
$$\Phi_4 = [\chi_A\chi_B - \chi_B\chi_A](\alpha\alpha)$$
$$\Phi_5 = [\chi_A\chi_B - \chi_B\chi_A](\beta\beta)$$

$$^1\Phi_- = \Phi_2 - \Phi_3 = [\chi_A\chi_A - \chi_B\chi_B](\alpha\beta - \beta\alpha)$$
$$^3\Phi_+ = \Phi_2 + \Phi_3 = [\chi_A\chi_B - \chi_B\chi_A](\alpha\beta + \beta\alpha) \qquad (4.22)$$

$$\Phi_0^{UHF} = c[\chi_A\chi_A + \chi_B\chi_B](\alpha\beta - \beta\alpha)$$
$$+ [\chi_A\chi_B\alpha\beta - c^2\chi_A\chi_B\beta\alpha] \qquad (4.23)$$
$$+ [c^2\chi_B\chi_A\alpha\beta - \chi_B\chi_A\beta\alpha]$$

$^1\Phi$と$^3\Phi$で表せる

$$\Phi_0^{UHF} = [c(\chi_A\chi_A + \chi_B\chi_B) + (\chi_A\chi_B + \chi_B\chi_A)](\alpha\beta - \beta\alpha)$$
$$+ (1 - c^2)[\chi_A\chi_B\beta\alpha - \chi_B\chi_A\alpha\beta] \qquad (4.24)$$

^{3}Φ の一部

$$^1\Phi^{UHF} = a_1\,^1\Phi^{RHF} + a_3\,^3\Phi^{ROHF} + a_5\,^5\Phi^{ROHF} + \ldots \qquad (4.25)$$

Figure 4.8 Resonance structures for ozone

RHFでうまく表せない一重項の例

電子が2つの軌道に1個ずつ

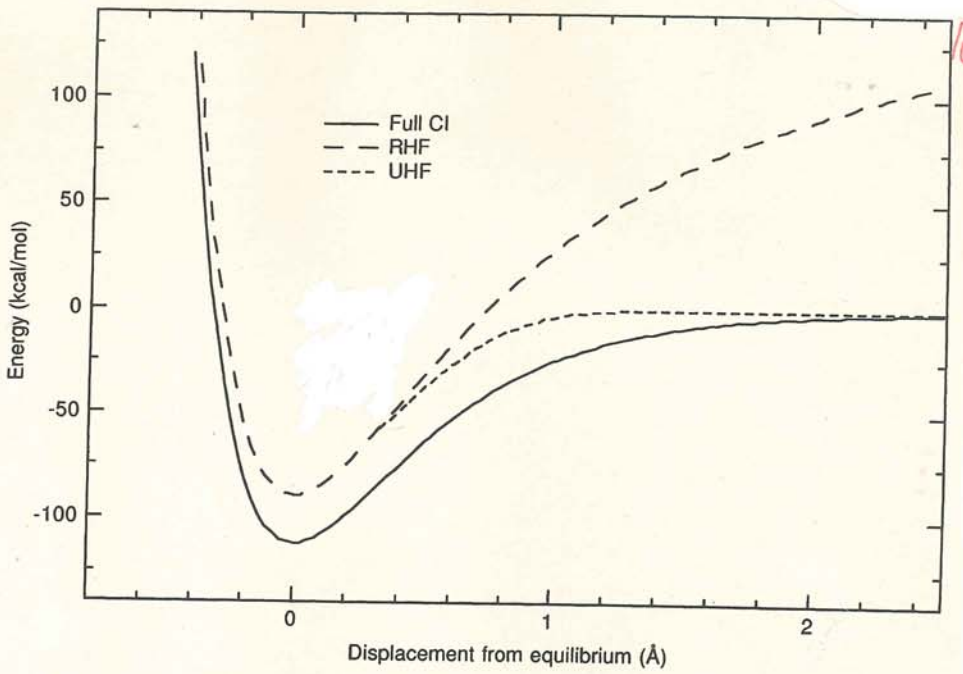

Figure 4.7 Bond dissociation curves for H_2

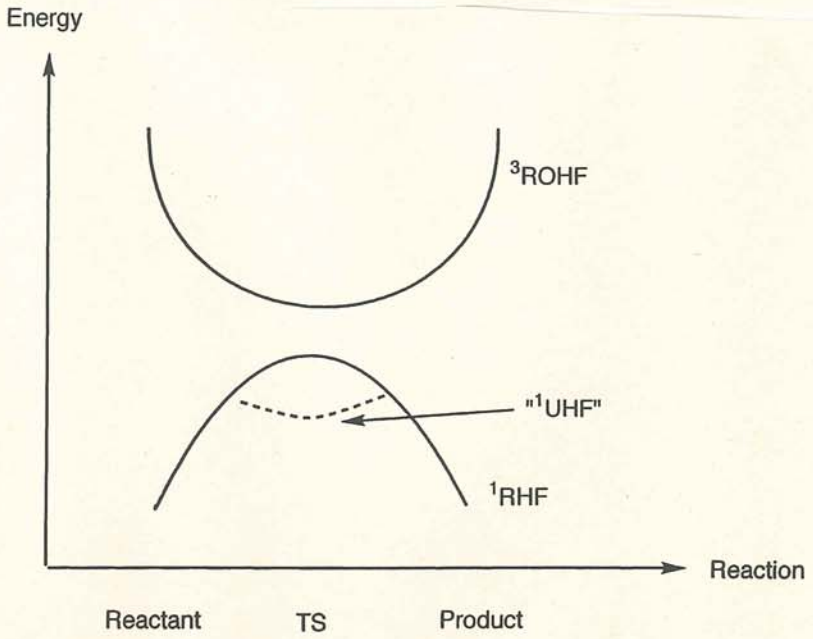

Figure 4.9 Mixing of pure singlet and triplet states may generate artificial minima on the UHF energy surface

CASSCF (Complete Active Space) SCF

Table 4.3 Number of configurations generated in a $[n,n]$-CASSCF wave function

n	Number of CSFs
2	3
4	20
6	175
8	1 764
10	19 404
12	226 512
14	2 760 615

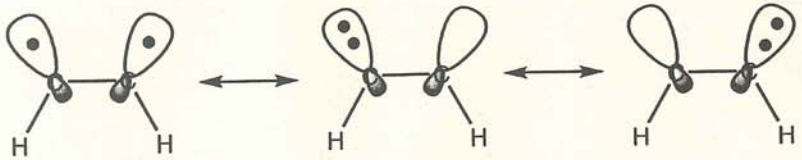

Figure 4.11 Important configurations for a bend acetylene model

Table 4.4 Natural orbital occupation numbers for the distorted acetylene model in Figure 4.11. Only the occupation numbers for the six "central" orbitals are shown

	n_5	n_6	n_7	n_8	n_9	n_{10}
RHF	2.00	2.00	2.00	0.00	0.00	0.00
UHF	2.00	1.72	1.30	0.70	0.28	0.01
[2,2]-CASSCF	2.00	2.00	1.62	0.38	0.00	0.00
[4,4]-CASSCF	2.00	1.85	1.67	0.33	0.14	0.00
[10,10]-CASSCF	1.97	1.87	1.71	0.30	0.13	0.02

The [4,4]-CASSCF also includes the two out-of-plane π-orbitals in the active space, while the [10,10]-CASSCF generates a full-valence CI wave function. The unbalanced description for the [2,2]-CASSCF is reminiscent of the spin contamination problem for UHF wave functions, although the effect is much less pronounced. Nevertheless, the overestimation may be severe enough to alter the qualitative shape of energy surfaces, for example turning transition structures into minima, as illustrated in Figure 4.9. MCSCF methods are therefore not "black box" methods like for example HF and MP (Section 4.8.1); selecting a proper number of configurations, and the correct orbitals, to give a balanced description of the problem at hand requires some experimentation and insight.

多体摂動論 *Many-Body Perturbation Theory* (MBPT)

$$\mathbf{H} = \mathbf{H}_0 + \lambda\mathbf{H}'$$
$$\mathbf{H}_0\Phi_i = E_i\Phi_i,\ i = 0,\ 1,\ 2,\ \ldots,\infty \tag{4.27}$$

$$\mathbf{H}\Psi = W\Psi \tag{4.28}$$

If $\lambda = 0$, then $\mathbf{H} = \mathbf{H}_0$, $\Psi = \Phi_0$ and $W = E_0$.

$$W = \lambda^0 W_0 + \lambda^1 W_1 + \lambda^2 W_2 + \lambda^3 W_3 + \ldots$$
$$\Psi = \lambda^0\Psi_0 + \lambda^1\Psi_1 + \lambda^2\Psi_2 + \lambda^3\Psi_3 + \ldots \tag{4.29}$$

$$\begin{aligned} \langle\Psi|\Phi_0\rangle &= 1 \\ \langle\Psi_0 + \lambda\Psi_1 + \lambda^2\Psi_2 + \ldots|\Phi_0\rangle &= 1 \\ \langle\Psi_0|\Phi_0\rangle + \lambda\langle\Psi_1|\Phi_0\rangle + \lambda^2\langle\Psi_2|\Phi_0\rangle + \ldots &= 1 \\ \langle\Psi_{i\neq 0}|\Phi_0\rangle &= 0 \end{aligned} \tag{4.30}$$

$$\begin{aligned} &(\mathbf{H}_0 + \lambda\mathbf{H}')(\lambda^0\Psi_0 + \lambda^1\Psi_1 + \lambda^2\Psi_2 + \ldots) = \\ &(\lambda^0 W_0 + \lambda^1 W_1 + \lambda^2 W_2 + \ldots)(\lambda^0\Psi_0 + \lambda^1\Psi_1 + \lambda^2\Psi_2 + \ldots) \end{aligned} \tag{4.31}$$

$$\begin{aligned} \lambda^0 &: \mathbf{H}_0\Psi_0 = W_0\Psi_0 \\ \lambda^1 &: \mathbf{H}_0\Psi_1 + \mathbf{H}'\Psi_0 = W_0\Psi_1 + W_1\Psi_0 \\ \lambda^2 &: \mathbf{H}_0\Psi_2 + \mathbf{H}'\Psi_1 = W_0\Psi_2 + W_1\Psi_1 + W_2\Psi_0 \\ \lambda^n &: \mathbf{H}_0\Psi_n + \mathbf{H}'\Psi_{n-1} = \sum_{i=0}^{n} W_i\Psi_{n-i} \end{aligned} \tag{4.32}$$

$\langle\Phi_0|\mathbf{H}_0|\Psi_i\rangle = \langle\Psi_i|\mathbf{H}_0|\Phi_0\rangle^*$ を使って

$$\begin{aligned} \langle\Phi_0|\mathbf{H}_0|\Psi_n\rangle + \langle\Phi_0|\mathbf{H}'|\Psi_{n-1}\rangle &= \sum_{i=0}^{n-1} W_i\langle\Phi_0|\Psi_{n-i}\rangle + W_n\langle\Phi_0|\Psi_0\rangle \\ E_0\langle\Phi_0|\Psi_n\rangle + \langle\Phi_0|\mathbf{H}'|\Psi_{n-1}\rangle &= W_n\langle\Phi_0|\Psi_0\rangle \\ W_n &= \langle\Phi_0|\mathbf{H}'|\Psi_{n-1}\rangle \end{aligned} \tag{4.33}$$

, it can be shown that knowledge of the nth-order wave function actually allows a calculation of the $(2n+1)$th-order energy.

$$W_{2n+1} = \langle\Psi_n|\mathbf{H}'|\Psi_n\rangle - \sum_{k,l=1}^{n} W_{2n+1-k-l}\langle\Psi_k|\Psi_l\rangle \tag{4.34}$$

ご利益

一次摂動

$$\Psi_1 = \sum_i c_i \Phi_i$$
$$(\mathbf{H}_0 - W_0)\left(\sum_i c_i \Phi_i\right) + (\mathbf{H}' - W_1)\Phi_0 = 0 \tag{4.35}$$

$$W_1 = \langle \Phi_0 | \mathbf{H}' | \Phi_0 \rangle \tag{4.36}$$

$$c_j = \frac{\langle \Phi_j | \mathbf{H}' | \Phi_0 \rangle}{E_0 - E_j} \tag{4.37}$$

二次摂動

$$\Psi_2 = \sum_i d_i \Phi_i$$
$$(\mathbf{H}_0 - W_0)\left(\sum_i d_i \Phi_i\right) + (\mathbf{H}' - W_1)\left(\sum_i c_i \Phi_i\right) - W_2 \Phi_0 = 0 \tag{4.38}$$

$$W_2 = \sum_i c_i \langle \Phi_0 | \mathbf{H}' | \Phi_i \rangle = \sum_{i \neq 0} \frac{\langle \Phi_0 | \mathbf{H}' | \Phi_i \rangle \langle \Phi_i | \mathbf{H}' | \Phi_0 \rangle}{E_0 - E_i}$$

$$d_j = \sum_{i \neq 0} \frac{\langle \Phi_j | \mathbf{H}' | \Phi_i \rangle \langle \Phi_i | \mathbf{H}' | \Phi_0 \rangle}{(E_0 - E_j)(E_0 - E_i)} - \frac{\langle \Phi_j | \mathbf{H}' | \Phi_0 \rangle \langle \Phi_0 | \mathbf{H}' | \Phi_0 \rangle}{(E_0 - E_j)^2} \tag{4.39}$$

Møller–Plesset Perturbation Theory

$$\begin{aligned}
\mathbf{H}_0 &= \sum_{i=1}^{N} \mathbf{F}_i = \sum_{i=1}^{N} \left(\mathbf{h}_i + \sum_{j=1}^{N} (\mathbf{J}_{ij} - \mathbf{K}_{ij}) \right) = \sum_{i=1}^{N} \mathbf{h}_i + 2\langle \mathbf{V}_{ee} \rangle \\
&= \sum_{i=1}^{N} \mathbf{h}_i + \sum_{i=1}^{N} \sum_{j=1}^{N} \langle \mathbf{g}_{ij} \rangle \\
\mathbf{H}' &= \mathbf{H} - \mathbf{H}_0 = \mathbf{V}_{ee} - \sum_{i=1}^{N} \sum_{j=1}^{N} (\mathbf{J}_{ij} - \mathbf{K}_{ij}) = \mathbf{V}_{ee} - 2\langle \mathbf{V}_{ee} \rangle \\
&= \sum_{i=1}^{N} \sum_{j>i}^{N} \mathbf{g}_{ij} - \sum_{i=1}^{N} \sum_{j=1}^{N} \langle \mathbf{g}_{ij} \rangle
\end{aligned} \tag{4.40}$$

$$W_1 = \langle \Phi_0 | \mathbf{H}' | \Phi_0 \rangle = \langle \mathbf{V}_{ee} \rangle - 2\langle \mathbf{V}_{ee} \rangle = -\langle \mathbf{V}_{ee} \rangle \tag{4.41}$$

$$\begin{aligned}
\mathrm{MP0} &= E(\mathrm{MP0}) = \sum_{i=1}^{N} \varepsilon_i \\
\mathrm{MP1} &= \mathrm{MP0} + E(\mathrm{MP1}) = E(\mathrm{HF})
\end{aligned} \tag{4.42}$$

（電子相関の入るのはMP2から）

$$\begin{aligned}
\langle \Phi_0 | \mathbf{H}' | \Phi_i^a \rangle &= \langle \Phi_0 | \mathbf{H} - \sum_{j=1}^{N} \mathbf{F}_j | \Phi_i^a \rangle \\
&= \langle \Phi_0 | \mathbf{H} | \Phi_i^a \rangle - \sum_{j=1}^{N} \langle \Phi_0 | \mathbf{F}_j | \Phi_i^a \rangle \\
&= \langle \Phi_0 | \mathbf{H} | \Phi_i^a \rangle - \varepsilon_a \langle \Phi_0 | \Phi_i^a \rangle
\end{aligned} \tag{4.43}$$

空軌道

$$W_2 = \sum_{i<j}^{\mathrm{occ}} \sum_{a<b}^{\mathrm{vir}} \frac{\langle \Phi_0 | \mathbf{H}' | \Phi_{ij}^{ab} \rangle \langle \Phi_{ij}^{ab} | \mathbf{H}' | \Phi_0 \rangle}{E_0 - E_{ij}^{ab}} \tag{4.44}$$

$$E(\mathrm{MP2}) = \sum_{i<j}^{\mathrm{occ}} \sum_{a<b}^{\mathrm{vir}} \frac{[\langle \phi_i \phi_j | \phi_a \phi_b \rangle - \langle \phi_i \phi_j | \phi_b \phi_a \rangle]^2}{\varepsilon_i + \varepsilon_j - \varepsilon_a - \varepsilon_b} \tag{4.45}$$

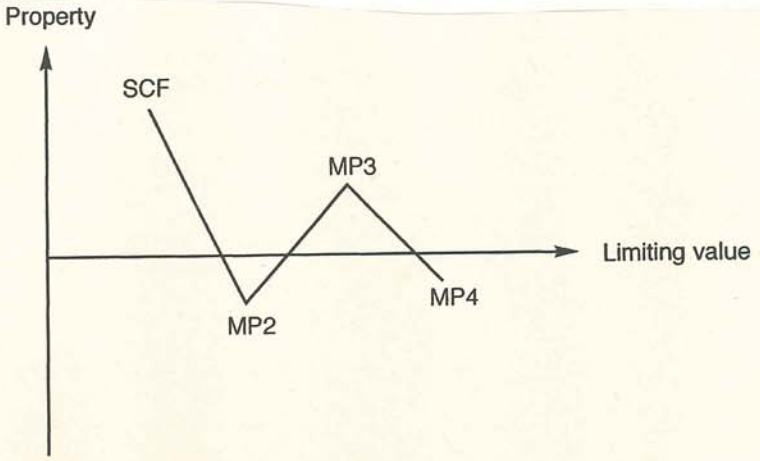

Figure 4.12 Typical oscillating behaviour of results obtained with the MP method

Coupled Cluster法

$$\Psi_{cc} = e^{\mathbf{T}}\Phi_0$$

$$e^{\mathbf{T}} = \mathbf{1} + \mathbf{T} + \frac{1}{2}\mathbf{T}^2 + \frac{1}{6}\mathbf{T}^3 + \ldots = \sum_{k=0}^{\infty}\frac{1}{k!}\mathbf{T}^k \tag{4.46}$$

where the cluster operator $\mathbf{T}$ is given by

$$\mathbf{T} = \mathbf{T}_1 + \mathbf{T}_2 + \mathbf{T}_3 + \ldots + \mathbf{T}_N \tag{4.47}$$

励起演算子

$$\mathbf{T}_1\Phi_0 = \sum_{i}^{occ}\sum_{a}^{vir} t_i^a \Phi_i^a$$
$$\mathbf{T}_2\Phi_0 = \sum_{i<j}^{occ}\sum_{a<b}^{vir} t_{ij}^{ab}\Phi_{ij}^{ab} \tag{4.48}$$

$$e^{\mathbf{T}} = \mathbf{1} + \mathbf{T}_1 + \left(\mathbf{T}_2 + \frac{1}{2}\mathbf{T}_1^2\right) + \left(\mathbf{T}_3 + \mathbf{T}_2\mathbf{T}_1 + \frac{1}{6}\mathbf{T}_1^3\right) + \left(\mathbf{T}_4 + \mathbf{T}_3\mathbf{T}_1 + \frac{1}{2}\mathbf{T}_2^2 + \frac{1}{2}\mathbf{T}_2\mathbf{T}_1^2 + \frac{1}{24}\mathbf{T}_1^4\right) + \ldots \tag{4.49}$$

$$\mathbf{H}e^{\mathbf{T}}\Phi_0 = Ee^{\mathbf{T}}\Phi_0 \tag{4.50}$$

$$\langle\Phi_0|\mathbf{H}e^{\mathbf{T}}|\Phi_0\rangle = E_{cc}\langle\Phi_0|e^{\mathbf{T}}\Phi_0\rangle \qquad E_{cc} = \langle\Phi_0|\mathbf{H}e^{\mathbf{T}}|\Phi_0\rangle \tag{4.51}$$

$$E_{cc} = \langle\Phi_0|\mathbf{H}|\left(1 + \mathbf{T}_1 + \mathbf{T}_2 + \tfrac{1}{2}\mathbf{T}_1^2\right)\Phi_0\rangle$$

$$E_{cc} = E_0 + \sum_{i}^{occ}\sum_{a}^{vir} t_i^a\langle\Phi_0|\mathbf{H}|\Phi_i^a\rangle + \sum_{i<j}^{occ}\sum_{a<b}^{vir}(t_{ij}^{ab} + t_i^a t_j^b - t_i^b t_j^a)\langle\Phi_0|\mathbf{H}|\Phi_{ij}^{ab}\rangle \tag{4.52}$$

$$E_{cc} = E_0 + \sum_{i<j}^{occ}\sum_{a<b}^{vir}(t_{ij}^{ab} + t_i^a t_j^b - t_i^b t_j^a)(\langle\phi_i\phi_j|\phi_a\phi_b\rangle - \langle\phi_i\phi_j|\phi_b\phi_a\rangle) \tag{4.53}$$

一電子励起配置と

$$\langle\Phi_m^e|\mathbf{H}e^{\mathbf{T}}|\Phi_0\rangle = E_{cc}\langle\Phi_m^e|e^{\mathbf{T}}\Phi_0\rangle$$

$$\langle\Phi_m^e|\mathbf{H}|\Phi_0\rangle + \langle\Phi_m^e|\mathbf{H}|\mathbf{T}_1\Phi_0\rangle + \langle\Phi_m^e|\mathbf{H}|\mathbf{T}_2\Phi_0\rangle + \tfrac{1}{2}\langle\Phi_m^e|\mathbf{H}|\mathbf{T}_1^2\Phi_0\rangle + \langle\Phi_m^e|\mathbf{H}|\mathbf{T}_3\Phi_0\rangle + \langle\Phi_m^e|\mathbf{H}|\mathbf{T}_1\mathbf{T}_2\Phi_0\rangle + \tfrac{1}{6}\langle\Phi_m^e|\mathbf{H}|\mathbf{T}_1^3\Phi_0\rangle = E_{cc}\langle\Phi_m^e|\mathbf{T}_1\Phi_0\rangle \tag{4.54}$$

CCSD

$$e^{\mathbf{T}_1+\mathbf{T}_2} = \mathbf{1} + \mathbf{T}_1 + \left(\mathbf{T}_2 + \tfrac{1}{2}\mathbf{T}_1^2\right) + \left(\mathbf{T}_2\mathbf{T}_1 + \tfrac{1}{6}\mathbf{T}_1^3\right) + \left(\tfrac{1}{2}\mathbf{T}_2^2 + \tfrac{1}{2}\mathbf{T}_2\mathbf{T}_1^2 + \tfrac{1}{24}\mathbf{T}_1^4\right) + \ldots \tag{4.55}$$

一電子励起配置と

$$\langle\Phi_m^e|\mathbf{H}|\left(\mathbf{1} + \mathbf{T}_1 + \left(\mathbf{T}_2 + \tfrac{1}{2}\mathbf{T}_1^2\right) + \left(\mathbf{T}_2\mathbf{T}_1 + \tfrac{1}{6}\mathbf{T}_1^3\right)\right)\Phi_0\rangle = E_{CCSD}\langle\Phi_m^e|\mathbf{T}_1\Phi_0\rangle$$

$$\langle\Phi_m^e|\mathbf{H}|\Phi_0\rangle + \sum_{ia} t_i^a\langle\Phi_m^e|\mathbf{H}|\Phi_i^a\rangle + \sum_{ijab}(t_{ij}^{ab} + t_i^a t_j^b - t_j^b t_j^a)\langle\Phi_m^e|\mathbf{H}|\Phi_{ij}^{ab}\rangle + \sum_{ijkabc}(t_{ij}^{ab}t_k^c + \ldots + t_i^a t_j^b t_k^c + \ldots)\langle\Phi_m^e|\mathbf{H}|\Phi_{ijk}^{abc}\rangle = E_{CCSD}t_m^e \tag{4.56}$$

二電子励起配置と

$$\langle\Phi_{mn}^{ef}|\mathbf{H}|\left(1 + \mathbf{T}_1 + \left(\mathbf{T}_2 + \tfrac{1}{2}\mathbf{T}_1^2\right) + \left(\mathbf{T}_2\mathbf{T}_1 + \tfrac{1}{6}\mathbf{T}_1^3\right) + \left(\tfrac{1}{2}\mathbf{T}_2^2 + \tfrac{1}{2}\mathbf{T}_2\mathbf{T}_1^2 + \tfrac{1}{24}\mathbf{T}_1^4\right)\right)\Phi_0\rangle = E_{CCSD}\langle\Phi_{mn}^{ef}|\left(\mathbf{T}_2 + \tfrac{1}{2}\mathbf{T}_1^2\right)\Phi_0\rangle$$

$$\langle\Phi_{mn}^{ef}|\mathbf{H}|\Phi_0\rangle + \sum_{ia} t_i^a\langle\Phi_{mn}^{ef}|\mathbf{H}|\Phi_i^a\rangle + \sum_{ijab}(t_{ij}^{ab} + t_i^a t_j^b - t_i^b t_j^a)\langle\Phi_{mn}^{ef}|\mathbf{H}|\Phi_{ij}^{ab}\rangle + \sum_{ijkabc}(t_{ij}^{ab}t_k^c + \ldots + t_i^a t_j^b t_k^c + \ldots)\langle\Phi_{mn}^{ef}|\mathbf{H}|\Phi_{ijk}^{abc}\rangle + \sum_{ijklabcd}(t_{ij}^{ab}t_{kl}^{cd} + \ldots + t_{ij}^{ab}t_k^c t_l^d + \ldots + t_i^a t_j^b t_k^c t_l^d + \ldots)\langle\Phi_{mn}^{ef}|\mathbf{H}|\Phi_{ijkl}^{abcd}\rangle = E_{CCSD}(t_{mn}^{ef} + t_m^e t_n^f - t_m^f t_n^e) \tag{4.57}$$

電子相関のまとめ

Table 4.5 Limiting scaling in terms of basis set size M for different methods

Scaling	CI methods	MP methods	CC methods
M^5		MP2	CC2 (iterative)
M^6	CISD	MP3, MP4(SDQ)	CCSD (iterative)
M^7		MP4	CCSD(T), CC3 (iterative)
M^8	CISDT	MP5	CCSDT (iterative)
M^9		MP6	
M^{10}	CISDTQ	MP7	CCSDTQ (iterative)

$$\text{HF} \ll \text{MP2} < \text{CISD} < \text{MP4(SDQ)} \sim \text{CCSD} < \text{MP4} < \text{CCSD(T)} \tag{4.72}$$

真のエネルギー値への外挿

As an example, the G2(MP2) method[28] involves the following steps:

(1) The geometry is optimized at the HF/6-31G(d) level, and the vibrational frequencies are calculated. To correct for the known deficiencies at the HF level, these are scaled by 0.893 to produce zero-point energies.
(2) The geometry is reoptimized at the MP2/6-31G(d) level, which is used as the reference geometry.
(3) A MP2/6–311+G(3df,2p) calculation is carried out, which automatically yields the corresponding HF energy.
(4) The energy is calculated at the QCISD(T)/6-311G(d,p) level. This automatically generates the MP2 value as an intermediate result, and the difference between the QCISD(T) and MP2 energies is taken as an estimate of the higher-order correlation energy. The G2 method (not G2(MP2)) performs additional MP4 calculations with larger basis sets to get a better estimate of the higher-order correlation energy.
(5) To correct for electron correlation beyond QCISD(T) and basis set limitations, an empirical correction is added to the total energy.

$$\Delta E(\text{empirical}) = -0.00481\,\mathrm{N}_\alpha - 0.00019\,\mathrm{N}_\beta \tag{5.6}$$

(it is assumed that the number of α-electrons is larger than or equal to the number of β-electrons). The numerical constants are determined by fitting to the reference data. It should be noted that this correction makes the G2 methods non-size-extensive.

Table 5.2 Computational levels in the G1/G2 models

Method	G1	G2	G2(MP2)	G2(MP2,SVP)
Geometry	MP2/6-31G(d)	MP2/6-31G(d)	MP2/6-31G(d)	MP2/6-31G(d)
HF and MP2	6-311G(2df,p)	6-311+G(3df,2p)	6-311+G(3df,2p)	6-311+G(3df,2p)
Higher-order correlation	MP4(SDTQ)/ 6-311G(d,p) MP4(SDTQ)/ 6-311+G(d,p) MP4(SDTQ)/ 6-311G(2df,p) QCISD(T)/ 6-311G(d,p)	MP4(SDTQ)/ 6-311G(d,p) MP4(SDTQ)/ 6-311+G(d,p) MP4(SDTQ)/ 6-311G(2df,p) QCISD(T)/ 6-311G(d,p)	QCISD(T)/ 6-311G(d,p)	QCISD(T)/ 6-31G(d)
Thermo [scale factor]	HF/6-31G(d) [0.893]	HF/6-31G(d) [0.893]	HF/6-31G(d) [0.893]	HF/6-31G(d) [0.893]
Empirical factors for electron correlation	yes	yes	yes	yes
MAD error	1.5	1.1	1.5	1.6

Geometry: level at which the structure is optimized; higher-order correlation: method(s) for estimating higher-order correlation effects; thermo: level at which the thermodynamical corrections are calculated [vibrational scale factor]; MAD: Mean Absolute Deviation for reference data set in kcal/mol.

CBS-Q

(1) The geometry is optimized at the HF/6-31 G(d†) level (d† denotes that the exponents for the d-functions are taken from the 6-311G(d) basis), and the vibrational frequencies are calculated. To correct for the known deficiencies at the HF level, these are scaled by 0.918 to produce zero-point energies.
(2) The geometry is reoptimized at the MP2/6-31G(d†) level, which is used as the reference geometry.
(3) A MP2/6-311+G(2df,2p) calculation is carried out, which automatically yields the corresponding HF energy. The MP2 result is extrapolated to the basis set limit by the pair natural orbital method.
(4) The energy is calculated at the MP4(SDQ)/6-31G(d,p) and QCISD(T)/6-31+G(d†) levels to estimate the effect from higher-order electron correlation.
(5) Corrections due to remaining correlation effects are estimated by an empirical expression.

$$\Delta E(\text{empirical}) = -0.00533 \sum_i \left(\sum_\mu C_{\mu ii} \right)^2 |S|_{ij}^2 \tag{5.7}$$

where the sum over $C_{\mu ii}$ is the trace of the first-order wave function coefficients for the natural orbital pair ii, $|S|_{ij}$ is the spatial overlap between the absolute values of MOs i and j, and the factor 0.00533 is determined by fitting to the reference data. This empirical correction is size extensive.
(6) For open-shell species the UHF method is used, which in some cases suffers from spin contamination. To correct for this an empirical correction based on the deviation of $\langle \mathrm{S}^2 \rangle$ from the theroretical value is added.

$$\Delta E(\text{empirical}) = -0.0092\left[\langle \mathrm{S}^2 \rangle - S_z(S_z - 1)\right] \tag{5.8}$$

where the factor of −0.0092 is derived by fitting.

Table 5.3 Computational levels in the CBS models

Method	CBS-4	CBS-q	CBS-Q	CBS-APNO
Geometry	HF/3-21G(*)	HF/3-21G(*)	MP2/6-31G(d†)	QCISD/ 6-311G(d,p)
HF	6-311++G(2df,p)	6-311++G(2df,p)	6-311++G (2df,2p)	[6s6p3d2f /4s2p1d]
MP2	6-31+G(d†)	6-31+G(d†)	6-311++G (2df,2p)	[6s6p3d2f /4s2p1d]
Higher-order correlation	MP4(SDQ)/ 6-31G	MP4(SDQ)/ 6-31G(d†) QCISD(T)/ 6-31G	MP4(SDQ)/ 6-31+G(d,p) QCISD(T)/ 6-31+G(d†)	QCISD(T)/ 6-311+G(2df,p)
Thermo [scale factor]	HF/3-21G (0.917)	HF/3-21G (0.917)	HF/6-31G(d†) [0.918]	HF/6-311G(d,p) [0.925]
Empirical factors for electron correlation	yes	yes	yes	yes
Empirical factors for spin contamination	yes	no	yes	no
MAD error	2.1	1.6	1.0	0.5

密度汎関数法

$E[\rho] = T[\rho] + E_{ne}[\rho] + E_{ee}[\rho] + (\text{補助反発})$

運動エネルギー（電子）　電子-核　電子-電子　ポテンシャルエネルギー

$$E_{ne}[\rho] = \sum_a \int \frac{Z_a \rho(\mathbf{r})}{|\mathbf{R}_a - \mathbf{r}|} d\mathbf{r}$$
$$J[\rho] = \frac{1}{2} \int\int \frac{\rho(\mathbf{r})\rho(\mathbf{r}')}{|\mathbf{r} - \mathbf{r}'|} d\mathbf{r}\, d\mathbf{r}' \qquad (6.1)$$

Thomas-Fermi

$$E_{TF}[\rho] = T_{TF}[\rho] + E_{ne}[\rho] + J[\rho]$$

Thomas-Fermi-Dirac

$E_{TFD}[\rho] = T_{TF}[\rho] + E_{ne}[\rho] + J[\rho] + K_D[\rho]$

$$T_{TF}[\rho] = C_F \int \rho^{5/3}(\mathbf{r}) d\mathbf{r}$$
$$K_D[\rho] = -C_x \int \rho^{4/3}(\mathbf{r}) d\mathbf{r} \qquad (6.2)$$
$$C_F = \frac{3}{10}(3\pi^2)^{2/3}$$
$$C_x = \frac{3}{4}\left(\frac{3}{\pi}\right)^{1/3}$$

Kohn-Sham の定式化

$$T_S = \sum_{i=1}^{N} \langle \phi_i | -\tfrac{1}{2}\nabla^2 | \phi_i \rangle \qquad (6.4)$$

Slater 行列式

$$E_{DFT}[\rho] = T_S[\rho] + E_{ne}[\rho] + J[\rho] + E_{xc}[\rho] \qquad (6.7)$$

$$E_{xc}[\rho] = (T[\rho] - T_S[\rho]) + (E_{ee}[\rho] - J[\rho]) \qquad (6.8)$$

小さいとする

Lagrangian

$$L[\rho] = E_{DFT}[\rho] - \sum_{ij}^{N} \lambda_{ij}[\langle \phi_i | \phi_j \rangle - \delta_{ij}] \qquad (6.9)$$

$$\mathbf{h}_{KS}\phi_i = \sum_j^N \lambda_{ij}\phi_j$$
$$\mathbf{h}_{KS} = -\frac{1}{2}\nabla^2 + \mathbf{V}_{\text{eff}} \qquad (6.10)$$
$$\mathbf{V}_{\text{eff}}(\mathbf{r}) = \mathbf{V}_{ne}(\mathbf{r}) + \int \frac{\rho(\mathbf{r}')}{|\mathbf{r} - \mathbf{r}'|} d\mathbf{r}' + \mathbf{V}_{xc}(\mathbf{r})$$

Kohn-Sham方程式

$$\mathbf{h}_{KS}\phi_i = \varepsilon_i \phi_i \qquad (6.11)$$

$$E_{xc}[\rho] = E_x[\rho] + E_c[\rho] = \int \rho(\mathbf{r})\varepsilon_x[\rho(\mathbf{r})]d\mathbf{r} + \int \rho(\mathbf{r})\varepsilon_c[\rho(\mathbf{r})]d\mathbf{r} \qquad (6.12)$$

$$\mathbf{V}_{xc}(\mathbf{r}) = \frac{\partial E_{xc}[\rho]}{\partial \rho(\mathbf{r})} = \varepsilon_{xc}[\rho(\mathbf{r})] + \rho(\mathbf{r})\frac{\partial \varepsilon_{xc}(\mathbf{r})}{\partial \rho} \qquad (6.13)$$

αスピンとβスピンに分ける

$$E_x[\rho] = E_x^{\alpha}[\rho_\alpha] + E_x^{\beta}[\rho_\beta]$$
$$E_c[\rho] = E_c^{\alpha\alpha}[\rho_\alpha] + E_c^{\beta\beta}[\rho_\beta] + E_c^{\alpha\beta}[\rho_\alpha, \rho_\beta] \qquad (6.14)$$

$$\rho = \rho_\alpha + \rho_\beta$$

$$\zeta = \frac{\rho^\alpha - \rho^\beta}{\rho^\alpha + \rho^\beta}, \quad \frac{4}{3}\pi r_S^3 = \rho^{-1} \qquad (6.15)$$

スピン分極　1電子の含まれる有効球の半径

局所密度近似（*Local Density Approximation* (LDA)

$$E_x^{LDA}[\rho] = -C_x \int \rho^{4/3}(\mathbf{r})d\mathbf{r} \qquad (6.16)$$
$$\varepsilon_x^{LDA}[\rho] = -C_x \rho^{1/3}$$

局所スピン密度近似 *Local Spin Density Approximation* (LSDA)

$$E_x^{LSDA}[\rho] = -2^{1/3} C_x \int [\rho_\alpha^{4/3} + \rho_\beta^{4/3}]d\mathbf{r} \qquad (6.17)$$
$$\varepsilon_x^{LSDA}[\rho] = -2^{1/3} C_x [\rho_\alpha^{1/3} + \rho_\beta^{1/3}]$$

$$\varepsilon_x^{LSDA}[\rho] = -\tfrac{1}{2} C_x \rho^{1/3} [(1+\zeta)^{4/3} + (1-\zeta)^{4/3}] \qquad (6.18)$$

Xα法

$$\varepsilon_{X_\alpha}[\rho] = -\tfrac{3}{2}\alpha C_x \rho^{1/3} \qquad (6.19)$$

Vosko, Wilk and Nusair (VWN)

$$\varepsilon_c^{VWN}(r_S,\zeta) = \varepsilon_c(r_S,0) + \varepsilon_a(r_S)\left[\frac{f(\zeta)}{f''(0)}\right][1-\zeta^4] + [\varepsilon_c(r_S,1) - \varepsilon_c(r_S,0)]f(\zeta)\zeta^4$$
$$f(\zeta) = \frac{(1+\zeta)^{4/3} + (1-\zeta)^{4/3} - 2}{2(2^{1/3}-1)} \qquad (6.20)$$

$$\varepsilon_{c/a}(x) = A\left\{ \ln\frac{x^2}{X(x)} + \frac{2b}{Q}\tan^{-1}\left(\frac{Q}{2x+b}\right) - \frac{bx_0}{X(x_0)}\left[\ln\frac{(x-x_0)^2}{X(x)} + \frac{2(b+2x_0)}{Q}\tan^{-1}\left(\frac{Q}{2x+b}\right)\right]\right\} \qquad (6.21)$$
$$x = \sqrt{r_S}$$
$$X(x) = x^2 + bx + c$$
$$Q = \sqrt{4c - b^2}$$

The parameters A, x_0, b and c are fitting constants, different for $\varepsilon_c(r_S,0)$, $\varepsilon_c(r_S,1)$, and $\varepsilon_a(r_S)$.

PW correlation functional

$$\varepsilon_{c/a}^{PW}(x) = -2a\rho(1+\alpha x^2)\ln\left(1 + \frac{1}{2a(\beta_1 x + \beta_2 x^2 + \beta_3 x^3 + \beta_4 x^3)}\right) \qquad (6.22)$$

Here a, α, β_1, β_2, β_3 and β_4 are suitable constants.

勾配補正法 **Gradient Corrected Methods**

Generalized Gradient Approximation (GGA) methods

PW86 交換項

$$\varepsilon_x^{PW86} = \varepsilon_x^{LDA}(1 + ax^2 + bx^4 + cx^6)^{1/15}$$
$$x = \frac{|\nabla\rho|}{\rho^{4/3}} \qquad (6.23)$$

B or B88 交換項

$$\varepsilon_x^{B88} = \varepsilon_x^{LDA} + \Delta\varepsilon_x^{B88}$$
$$\Delta_x^{B88} = -\beta\rho^{1/3}\frac{x^2}{1 + 6\beta x \sinh^{-1}x} \qquad (6.24)$$

The β parameter is determined by fitting to known atomic data

Becke and Roussel (BR) 交換項

$$\varepsilon_x^{BR} = -\frac{2 - 2e^{-ab} - abe^{-ab}}{4b}$$
$$a^3 e^{-ab} = 8\pi\rho$$
$$a(ab-2) = b\frac{\nabla^2\rho - 2D}{\rho} \qquad (6.25)$$
$$D = \sum_i^N |\nabla\phi_i|^2 - \frac{(\nabla\rho)^2}{4\rho}$$

PW91 交換項

$$\varepsilon_x^{PW91} = \varepsilon_x^{LDA}\left(\frac{1 + xa_1\sinh^{-1}(xa_2) + (a_3 + a_4 e^{-bx^2})x^2}{1 + xa_1\sinh^{-1}(xa_2) + a_5 x^2}\right) \qquad (6.26)$$

LYP 相関項

$$\varepsilon_c^{\mathrm{LYP}} = -a\frac{\gamma}{(1+d\rho^{-1/3})} - ab\frac{\gamma e^{-c\rho^{-1/3}}}{9(1+d\rho^{-1/3})\rho^{8/3}} \times \left[\begin{array}{l} 18(2^{2/3})C_F(\rho_\alpha^{8/3}+\rho_\beta^{8/3}) - 18\rho t_W \\ +\rho_\alpha(2t_W^\alpha + \nabla^2\rho_\alpha) + \rho_\beta(2t_W^\beta + \nabla^2\rho_\beta) \end{array}\right] \quad (6.27)$$

$$\gamma = 2\left[1 - \frac{\rho_\alpha^2+\rho_\beta^2}{\rho^2}\right]$$

$$t_W^\sigma = \frac{1}{8}\left(\frac{|\nabla\rho_\sigma|^2}{\rho_\sigma} - \nabla^2\rho_\sigma\right)$$

where the a, b, c and d parameters are determined by fitting to data for the helium

The t_W functional is known as the local Weizsacker kinetic energy density.

部分積分して

$$\varepsilon_c^{\mathrm{LYP}} = -4a\frac{\rho_\alpha\rho_\beta}{\rho^2(1+d\rho^{-1/3})} - ab\omega\left\{\frac{\rho_\alpha\rho_\beta}{18}\left[\begin{array}{c} 144(2^{2/3})C_F(\rho_\alpha^{8/3}+\rho_\beta^{8/3}) + (47-7\delta)|\nabla\rho|^2 \\ -(45-\delta)(|\nabla\rho_\alpha|^2+|\nabla\rho_\beta|^2) + 2\rho^{-1}(11-\delta)(\rho_\alpha|\nabla\rho_\alpha|^2+\rho_\beta|\nabla\rho_\beta|^2) \\ +\tfrac{2}{3}\rho^2(|\nabla\rho_\alpha|^2+|\nabla\rho_\beta|^2-|\nabla\rho|^2) - (\rho_\alpha^2|\nabla\rho_\beta|^2+\rho_\beta^2|\nabla\rho_\alpha|^2) \end{array}\right]\right\}$$

$$\omega = \frac{e^{-c\rho^{-1/3}}}{(1+d\rho^{-1/3})\rho^{14/3}}$$

$$\delta = c\rho^{1/3} + \frac{d\rho^{-1/3}}{(1+d\rho^{-1/3})} \quad (6.28)$$

P86. 相関項

$$\varepsilon_c^{\mathrm{P86}} = \varepsilon_c^{\mathrm{LDA}} + \Delta\varepsilon_c^{\mathrm{P86}}$$

$$\Delta\varepsilon_c^{\mathrm{P86}} = \frac{e^{\Phi}C(\rho)|\nabla\rho|^2}{f(\zeta)\rho^{7/3}}$$

$$f(\zeta) = 2^{1/3}\sqrt{\left(\frac{1+\zeta}{2}\right)^{5/3} + \left(\frac{1-\zeta}{2}\right)^{5/3}} \quad (6.29)$$

$$\Phi = a\frac{C(\infty)|\nabla\rho|}{C(\rho)\rho^{7/6}}$$

$$C(\rho) = \mathscr{C}_1 + \frac{\mathscr{C}_2 + \mathscr{C}_3 r_S + \mathscr{C}_4 r_S^2}{1 + \mathscr{C}_5 r_S + \mathscr{C}_6 r_S^2 + \mathscr{C}_7 r_S^3}$$

PW91 or P91 相関項

$$\Delta\varepsilon_c^{\mathrm{PW91}}[\rho] = \rho(H_0(t,r_S,\zeta) + H_1(t,r_S,\zeta))$$

$$H_0(t,r_S,\zeta) = b^{-1}f(\zeta)^3 \ln\left[1 + a\frac{t^2+At^4}{1+At^2+A^2t^4}\right]$$

$$H_1(t,r_S,\zeta) = \left(\frac{16}{\pi}\right)(3\pi^2)^{1/3}[C(\rho)-c]f(\zeta)^3t^2e^{-dx^2/f(\zeta)^2} \quad (6.30)$$

$$f(\zeta) = \tfrac{1}{2}((1+\zeta)^{2/3} + (1-\zeta)^{2/3})$$

$$t = \left(\frac{192}{\pi^2}\right)^{1/6}\frac{|\nabla\rho|}{2f(\zeta)\rho^{7/6}}$$

$$A = a[e^{-b\varepsilon_c(r_S,\zeta)/f(\zeta)^3} - 1]^{-1}$$

where $\varepsilon(r_S,\zeta)$ is the PW92 parameterization of the LSDA correlation energy functional (eq. (6.22)), x and $C(\rho)$ are as defined in eqs. (6.23) and (6.29), and a, b, c and d are suitable constants.

B95 相関項

$$\varepsilon_c^{\mathrm{B95}} = \varepsilon_c^{\alpha\beta} + \varepsilon_c^{\alpha\alpha} + \varepsilon_c^{\beta\beta}$$

$$\varepsilon_c^{\alpha\beta} = [1 + a(x_\alpha^2+x_\beta^2)]^{-1}\varepsilon_c^{\mathrm{PW91},\alpha\beta} \quad (6.31)$$

$$\varepsilon_c^{\sigma\sigma} = [1+bx_\sigma^2]^{-2}\frac{D_\sigma}{D_\sigma^{\mathrm{LDA}}}\varepsilon_c^{\mathrm{PW91},\sigma\sigma}$$

$$D_\sigma^{\mathrm{LDA}} = 2^{5/3}C_F\rho_\sigma^{5/3}$$

Here σ runs over α and β spins, x_σ and D_σ have been defined in eqs. (6.23) and (6.25), a and b are fitting parameters, and $\varepsilon_c^{\mathrm{PW91}}$ is the Perdew–Wang parameterization of the LSDA correlation functional (eq. (6.22)).

混成法

Hybrid Methods

the *Adiabatic Connection Formula* (ACF)[23] and involves an integration over the parameter λ which "turns on" the electron–electron interaction.

$$E_{xc} = \int_0^1 \langle \Psi_\lambda | \mathbf{V}_{xc}(\lambda) | \Psi_\lambda \rangle d\lambda \tag{6.32}$$

$$E_{xc} \simeq \tfrac{1}{2}\langle \Psi_0 | \mathbf{V}_{xc}(0) | \Psi_0 \rangle + \tfrac{1}{2}\langle \Psi_1 | \mathbf{V}_{xc}(1) | \Psi_1 \rangle \tag{6.33}$$

Half-and-Half (H+H)

$$E_{xc}^{H+H} = \tfrac{1}{2}E_x^{exact} + \tfrac{1}{2}(E_x^{LSDA} + E_c^{LSDA}) \tag{6.34}$$

Becke 3 parameter functional (B3)

$$E_{xc}^{B3} = (1-a)E_x^{LSDA} + aE_x^{exact} + b\Delta E_x^{B88} + E_c^{LSDA} + c\Delta E_c^{GGA} \tag{6.35}$$

計算法

$$\phi_i = \sum_\alpha^M c_{\alpha i}\chi_\alpha \tag{6.36}$$

(基底関数展開)

$$\begin{aligned} &\mathbf{h}_{KS}\mathbf{C} = \mathbf{S}\mathbf{C}\boldsymbol{\varepsilon} \\ &h_{\alpha\beta} = \langle \chi_\alpha | \mathbf{h}_{KS} | \chi_\beta \rangle \\ &S_{\alpha\beta} = \langle \chi_\alpha | \chi_\beta \rangle \\ &\mathbf{h}_{KS} = -\tfrac{1}{2}\nabla^2 + \mathbf{V}_{ne} + \int \frac{\rho(\mathbf{r}')}{|\mathbf{r}-\mathbf{r}'|}d\mathbf{r}' + \mathbf{V}_{xc} \end{aligned} \tag{6.37}$$

出てくる積分

$$\int \chi_\alpha(\mathbf{r})\mathbf{V}_{xc}[\rho(\mathbf{r}), \nabla\rho(\mathbf{r})]\chi_\beta(\mathbf{r})d\mathbf{r} \tag{6.38}$$

数値積分

$$\int \chi_\alpha(\mathbf{r})\mathbf{V}_{xc}[\rho(\mathbf{r}), \nabla\rho(\mathbf{r})]\chi_\beta(\mathbf{r})d\mathbf{r} \simeq \sum_{k=1}^G \mathbf{V}_{xc}[\rho(\mathbf{r}_k), \nabla\rho(\mathbf{r}_k)]\chi_\alpha(\mathbf{r}_k)\chi_\beta(\mathbf{r}_k)\nabla\mathbf{v}_k \tag{6.39}$$

Table 6.1 Comparison of the performance of DFT methods by mean absolute deviations (kcal/mol)

Method	G2	LSDA	B88	BPW91	B3PW91
Atomization Energies	1.2	35.7	3.9	5.7	2.4
Ionization Potentials	1.4	6.3	11.2	4.1	3.8
Proton Affinities	1.0	5.6	2.4	1.5	1.2

B88交換 B88交換 B3交換
+PW91相関 +PW91相関

Table 6.2 Comparison of the performance of DFT methods (kcal/mol)

Method	Mean absolute deviation	Maximum absolute deviation
G2	1.6	8.2
G2(MP2)	2.0	10.1
G2(MP2, SVP)	1.9	12.5
SVWN	90.9	228.7
BLYP	7.1	28.4
BPW91	7.9	32.2
B3LYP	3.1	20.1
B3PW91	3.5	21.8

LSDA

BLYP B88交換 + LYP相関
B3LYP B3交換 + LYP相関

MO法

$$\Phi_0 = \begin{vmatrix} \phi_1(1)\,\bar{\phi}_1(1) \\ \phi_1(2)\,\bar{\phi}_1(2) \end{vmatrix} \qquad (7.1)$$

$$\phi_1 = (\chi_A + \chi_B)\alpha$$

$$\bar{\phi}_1 = (\chi_A + \chi_B)\beta$$

1, 2番目の電子

$$\Phi_0 = \phi_1\bar{\phi}_1 - \bar{\phi}_1\phi_1 = (\phi_1\phi_1)[\alpha\beta - \beta\alpha]$$

$$\Phi_0 = (\chi_A + \chi_B)(\chi_A + \chi_B)[\alpha\beta - \beta\alpha] \qquad (7.2)$$

$$\Phi_0 = (\chi_A\chi_A + \chi_B\chi_B + \chi_A\chi_B + \chi_B\chi_A)[\alpha\beta - \beta\alpha]$$

$H^+ H^-$ $H^\bullet H^\bullet$

$$\Phi_1 = \begin{vmatrix} \phi_2(1)\,\bar{\phi}_2(1) \\ \phi_2(2)\,\bar{\phi}_2(2) \end{vmatrix}$$

$$\phi_2 = (\chi_A - \chi_B)\alpha \qquad (7.3)$$

$$\bar{\phi}_2 = (\chi_A - \chi_B)\beta$$

$$\Phi_1 = (\chi_A\chi_A + \chi_B\chi_B - \chi_A\chi_B - \chi_B\chi_A)[\alpha\beta - \beta\alpha]$$

$$\Psi_{CI} = a_0\Phi_0 + a_1\Phi_1 = ((a_0 - a_1)(\chi_A\chi_B + \chi_B\chi_A) + (a_0 + a_1)(\chi_A\chi_A + \chi_B\chi_B))[\alpha\beta - \beta\alpha] \qquad (7.4)$$

原子価結合法

Heitler–London (HL) function,

$$\Phi_{HL}(\text{cov}) = (\chi_A\chi_B + \chi_B\chi_A)[\alpha\beta - \beta\alpha] \qquad (7.5)$$

$$\Phi_{HL}(\text{ion}) = (\chi_A\chi_A + \chi_B\chi_B)[\alpha\beta - \beta\alpha] \qquad (7.6)$$

$$\Phi_{HL} = a_0\Phi_{HL}(\text{cov}) + a_1\Phi_{HL}(\text{ion}) \qquad (7.7)$$

Coulson–Fischer (CF) type

$$\Phi_{CF} = (\phi_A\phi_B + \phi_B\phi_A)[\alpha\beta - \beta\alpha]$$

$$\phi_A = \chi_A + c\chi_B \qquad (7.8)$$

$$\phi_B = \chi_B + c\chi_A$$

$$\langle\phi_A|\phi_B\rangle = (1 + c^2)\langle\chi_A|\chi_B\rangle + 2c(\langle\chi_A|\chi_A\rangle + \langle\chi_B|\chi_B\rangle)$$

$$\langle\phi_A|\phi_B\rangle = (1 + c^2)S_{AB} + 4c \qquad (7.9)$$

When c is variationally optimized, the MO-CI, VB-HL and VB-CF wave functions (eqs. (7.4), (7.7) and (7.8)) are all completely equivalent.

SCVB(スピン結合原子価結合法) CFの拡張

$$\Phi^{CH_4}_{\text{valence-MO}} = A[\phi_1\bar{\phi}_1\phi_2\bar{\phi}_2\phi_3\bar{\phi}_3\phi_4\bar{\phi}_4] \qquad (7.10)$$

$$\phi_i = \sum_{\alpha=1}^{M} c_{\alpha i}\chi_\alpha$$

$$\Phi^{CH_4}_{\text{valence-SCVB}} = \sum_{i=1}^{14} a_i A\{[\phi_1\phi_2\phi_3\phi_4\phi_5\phi_6\phi_7\phi_8]\Theta^N_{0,i}\} \qquad (7.12)$$

4つは$C\,sp^3$ 残り H 1s

$$\phi_i = \sum_{\alpha=1}^{M} c_{\alpha i}\chi_\alpha$$

組み合せの数(電子N スピン量子数S)

$$f^N_S = \frac{(2S+1)N!}{(\frac{1}{2}N + S + 1)!(\frac{1}{2}N - S)!} \qquad (7.11)$$

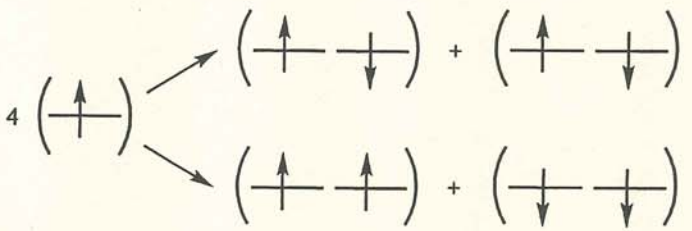

Figure 7.1 Two possible schemes for coupling four electrons to an overall singlet

Table 7.1 Number of possible spin coupling schemes for achieving an overall singlet state

N	f^N_0
2	1
4	2
6	5
8	14
10	42
12	132
14	429

計算大変

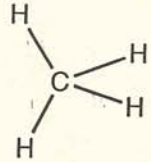

Figure 7.2 A representation of the dominating spin coupling in CH_4

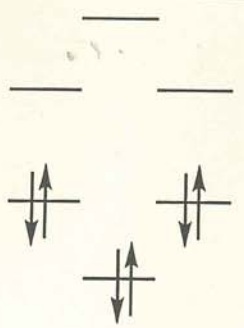

Figure 7.3 Molecular orbital energies in benzene

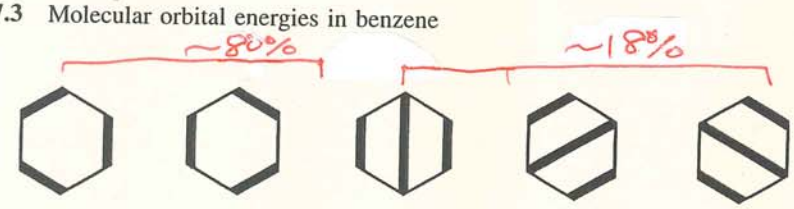

Figure 7.4 Representations of important spin coupling schemes in benzene

GVB (generalized valence bond) の要い例

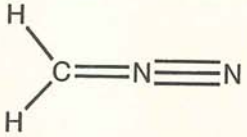

Figure 7.5 A representation of the SCVB wave function for diazomethane

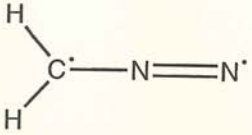

Figure 7.6 A representation of the GVB wave function for diazomethane

分子の性質

摂動

$$E(\lambda) = E(0) + \frac{\partial E}{\partial \lambda}\lambda + \frac{1}{2}\frac{\partial^2 E}{\partial \lambda^2}\lambda^2 + \frac{1}{6}\frac{\partial^3 E}{\partial \lambda^3}\lambda^3 + \dots \qquad (10.1)$$

the perturbation strength λ

外部電場

・電荷と電位（静電ポテンシャル）の相互作用

$$E = \int \rho(\mathbf{r})V(\mathbf{r})\,d\mathbf{r} \qquad (10.2)$$

$$E = qV - \boldsymbol{\mu}\mathbf{F} - \tfrac{1}{2}\mathbf{Q}\mathbf{F}' - \dots \qquad (10.3)$$

Here q is the net charge (monopole), $\boldsymbol{\mu}$ is the (electric) dipole moment, $\mathbf{Q}$ is the quadrupole moment, and $\mathbf{F}$ and $\mathbf{F}'$ are the field and field gradient ($\partial\mathbf{F}/\partial\mathbf{r}$), respectively.

$$\boldsymbol{\mu} = \langle\Psi|\mathbf{r}|\Psi\rangle \qquad (10.4)$$
$$\mathbf{Q} = \langle\Psi|\mathbf{r}\mathbf{r}^{\mathrm{t}}|\Psi\rangle$$

$$\boldsymbol{\mu} = \boldsymbol{\mu}_0 + \boldsymbol{\alpha}\mathbf{F} + \tfrac{1}{2}\boldsymbol{\beta}\mathbf{F}^2 + \tfrac{1}{6}\boldsymbol{\gamma}\mathbf{F}^3 + \dots \qquad (10.5)$$

$$E(\mathbf{F}) = E(\mathbf{0}) + \frac{\partial E}{\partial \mathbf{F}}\mathbf{F} + \frac{1}{2}\frac{\partial^2 E}{\partial \mathbf{F}^2}\mathbf{F}^2 + \frac{1}{6}\frac{\partial^3 E}{\partial \mathbf{F}^3}\mathbf{F}^3 + \frac{1}{24}\frac{\partial^4 E}{\partial \mathbf{F}^4}\mathbf{F}^4 + \dots \qquad (10.6)$$

$$E(\mathbf{F}) = E(\mathbf{0}) - \boldsymbol{\mu}_0\mathbf{F} - \tfrac{1}{2}\boldsymbol{\alpha}\mathbf{F}^2 - \tfrac{1}{6}\boldsymbol{\beta}\mathbf{F}^3 - \tfrac{1}{24}\boldsymbol{\gamma}\mathbf{F}^4 - \dots \qquad (10.7)$$

外部磁場 磁気双極子モーメント

$$E = -\mathbf{m}\mathbf{B} - \ldots \tag{10.8}$$

the orbital angular moment operator $\mathbf{L}$ and the total electron spin $\mathbf{S}$.

$$\mathbf{m} = -\tfrac{1}{2}\langle\Psi|\mathbf{L} + g_e\mathbf{S}|\Psi\rangle$$
$$\mathbf{L} = (\mathbf{r} - \mathbf{R}_G) \times \mathbf{p} \tag{10.9}$$

Here $\mathbf{R}_G$ is the gauge origin

$g_e = 2.0023$

$$E(\mathbf{B}) = E(\mathbf{0}) - \frac{\partial E}{\partial \mathbf{B}}\mathbf{B} - \frac{1}{2}\frac{\partial^2 E}{\partial \mathbf{B}^2}\mathbf{B}^2 - \ldots$$
$$E(\mathbf{B}) = E(\mathbf{0}) - \mathbf{m}_0\mathbf{B} - \frac{1}{2\mu_0}\xi\mathbf{B}^2 - \ldots \tag{10.10}$$

一般に

永久磁気双極子モーメント

The second derivative is the *magnetizability* ξ (the corresponding macroscopic quantity is called the magnetic *susceptibility* χ).

内部磁気モーメント

$$E(\mathbf{I}_1, \mathbf{I}_2, \ldots) = E(\mathbf{0}) + \frac{\partial E}{\partial \mathbf{I}_1}\mathbf{I}_1 + \frac{1}{2}\frac{\partial^2 E}{\partial \mathbf{I}_1 \partial \mathbf{I}_2}\mathbf{I}_1\mathbf{I}_2 + \ldots$$
$$E(\mathbf{I}_1, \mathbf{I}_2, \ldots) = E(\mathbf{0}) + \mathbf{g}\mathbf{I}_1 + h\mathbf{J}\mathbf{I}_1\mathbf{I}_2 + \ldots \tag{10.11}$$

The first derivative is the hyperfine coupling constant $\mathbf{g}$ (as measured by ESR), the second derivative with respect to two different nuclear spins is the NMR coupling constant, $\mathbf{J}$

構造変化

$$E(\mathbf{R}) = E(\mathbf{R}_0) + \frac{\partial E}{\partial \mathbf{R}}(\mathbf{R} - \mathbf{R}_0) + \frac{1}{2}\frac{\partial^2 E}{\partial \mathbf{R}^2}(\mathbf{R} - \mathbf{R}_0)^2 + \frac{1}{6}\frac{\partial^3 E}{\partial \mathbf{R}^3}(\mathbf{R} - \mathbf{R}_0)^3 + \ldots$$
$$E(\mathbf{R}) = E(\mathbf{R}_0) + \mathbf{g}(\mathbf{R} - \mathbf{R}_0) + \frac{1}{2}\mathbf{H}(\mathbf{R} - \mathbf{R}_0)^2 + \frac{1}{6}\mathbf{K}(\mathbf{R} - \mathbf{R}_0)^3 + \ldots \tag{10.12}$$

The first derivative is the gradient $\mathbf{g}$, the second derivative is the force constant (Hessian) $\mathbf{H}$, the third derivative is the anharmonicity $\mathbf{K}$ etc.

その他もっと複雑なもの

$$\text{IR Intensity} \propto \left(\frac{\partial \boldsymbol{\mu}}{\partial \mathbf{q}}\right)^2 \propto \left(\frac{\partial^2 E}{\partial \mathbf{R}\partial \mathbf{F}}\right)^2 \tag{10.13}$$

$$\text{Raman Intensity} \propto \left(\frac{\partial \boldsymbol{\alpha}}{\partial \mathbf{q}}\right)^2 \propto \left(\frac{\partial^3 E}{\partial \mathbf{R}\partial \mathbf{F}^2}\right)^2 \tag{10.14}$$

$$\text{NMR Shielding} \propto \left(\frac{\partial^2 E}{\partial \mathbf{B}\partial \mathbf{I}}\right) \tag{10.15}$$

$$\text{Property} \propto \frac{\partial^{n_F+n_B+n_I+n_R} E}{\partial \mathbf{F}^{n_F}\partial \mathbf{B}^{n_B}\partial \mathbf{I}^{n_I}\partial \mathbf{R}^{n_R}} \tag{10.16}$$

Table 10.1 Properties which may be calculated from derivatives of the energy

n_F	n_B	n_I	n_R	Property
0	0	0	0	Energy
1	0	0	0	Electric dipole moment
0	1	0	0	Magnetic dipole moment
0	0	1	0	Hyperfine coupling constant
0	0	0	1	Energy gradient
2	0	0	0	Electric polarizability
0	2	0	0	Magnetizability
0	0	2	0	Spin–spin coupling (for different nuclei)
0	0	0	2	Harmonic vibrational frequencies
1	0	0	1	Infra-red absorption intensities
1	1	0	0	Circular dichroism
0	1	1	0	Nuclear magnetic shielding
3	0	0	0	(first) Electric hyperpolarizability
0	3	0	0	(first) Hypermagnetizability
0	0	0	3	(cubic) Anharmonic corrections to vibrational frequencies
2	0	0	1	Raman intensities
2	1	0	0	Magnetic circular dichroism (Faraday effect)
1	0	0	2	Infra-red intensities for overtone and combination bands
4	0	0	0	(second) Electric hyperpolarizability
0	4	0	0	(second) Hypermagnetizability
0	0	0	4	(quartic) Anharmonic corrections to vibrational frequencies
2	0	0	2	Raman intensities for overtone and combination bands
2	2	0	0	Cotton–Mutton effect

摂動法

$$\mathbf{H} = \mathbf{H}_0 + \lambda \mathbf{P}_1 + \lambda^2 \mathbf{P}_2 \tag{10.17}$$

$$W_1 = \lambda \langle \Psi_0 | \mathbf{P}_1 | \Psi_0 \rangle$$
$$W_2 = \lambda^2 \left[\langle \Psi_0 | \mathbf{P}_2 | \Psi_0 \rangle + \sum_{i \neq 0} \frac{\langle \Psi_0 | \mathbf{P}_1 | \Psi_i \rangle \langle \Psi_i | \mathbf{P}_1 | \Psi_0 \rangle}{E_0 - E_i} \right] \tag{10.18}$$

導関数を用いる方法

$$E(\lambda) = \langle \Psi(\lambda) | \mathbf{H}_0 + \lambda \mathbf{P}_1 + \lambda^2 \mathbf{P}_2 | \Psi(\lambda) \rangle \tag{10.19}$$

$$\frac{\partial E}{\partial \lambda} = \left\langle \frac{\partial \Psi}{\partial \lambda} \middle| \mathbf{H}_0 + \lambda \mathbf{P}_1 + \lambda^2 \mathbf{P}_2 \middle| \Psi \right\rangle + \langle \Psi | \mathbf{P}_1 + 2\lambda \mathbf{P}_2 | \Psi \rangle + \left\langle \Psi \middle| \mathbf{H}_0 + \lambda \mathbf{P}_1 + \lambda^2 \mathbf{P}_2 \middle| \frac{\partial \Psi}{\partial \lambda} \right\rangle \tag{10.20}$$

$$\left. \frac{\partial E}{\partial \lambda} \right|_{\lambda=0} = \langle \Psi_0 | \mathbf{P}_1 | \Psi_0 \rangle + 2 \left\langle \frac{\partial \Psi_0}{\partial \lambda} \middle| \mathbf{H}_0 \middle| \Psi_0 \right\rangle \tag{10.21}$$

基底に関するパラメータ

$$\frac{\partial \Psi}{\partial \lambda} = \frac{\partial \Psi}{\partial \chi} \frac{\partial \chi}{\partial \lambda} + \frac{\partial \Psi}{\partial \mathbf{C}} \frac{\partial \mathbf{C}}{\partial \lambda} \tag{10.22}$$

摂動は基底関数に影響を及ぼさないとすると、

$$\left. \frac{\partial E}{\partial \lambda} \right|_{\lambda=0} = \langle \Psi_0 | \mathbf{P}_1 | \Psi_0 \rangle + 2 \frac{\partial \mathbf{C}}{\partial \lambda} \left\langle \frac{\partial \Psi_0}{\partial \mathbf{C}} \middle| \mathbf{H}_0 \middle| \Psi_0 \right\rangle \tag{10.23}$$

完全に変分的な波動関数(HF, MCSCF)については

$$\frac{\partial E}{\partial \mathbf{C}} = \frac{\partial}{\partial \mathbf{C}} \langle \Psi | \mathbf{H}_0 + \lambda \mathbf{P}_1 + \lambda^2 \mathbf{P}_2 | \Psi \rangle = 2 \left\langle \frac{\partial \Psi}{\partial \mathbf{C}} \middle| \mathbf{H}_0 + \lambda \mathbf{P}_1 + \lambda^2 \mathbf{P}_2 \middle| \Psi \right\rangle \tag{10.24}$$
$$\left. \frac{\partial E}{\partial \mathbf{C}} \right|_{\lambda=0} = 2 \left\langle \frac{\partial \Psi_0}{\partial \mathbf{C}} \middle| \mathbf{H}_0 \middle| \Psi_0 \right\rangle = 0$$

Variational wave functions thus obey the *Hellmann–Feynman* theorem.

$$\frac{\partial}{\partial \lambda} \langle \Psi | \mathbf{H} | \Psi \rangle = \left\langle \Psi \middle| \frac{\partial \mathbf{H}}{\partial \lambda} \middle| \Psi \right\rangle \tag{10.25}$$

二次微分

$$\frac{\partial^2 E}{\partial \lambda^2} = 2 \left\langle \frac{\partial^2 \Psi}{\partial \lambda^2} \middle| \mathbf{H}_0 + \lambda \mathbf{P}_1 + \lambda^2 \mathbf{P}_2 \middle| \Psi \right\rangle + 4 \left\langle \frac{\partial \Psi}{\partial \lambda} \middle| \mathbf{P}_1 + 2\lambda \mathbf{P}_2 \middle| \Psi \right\rangle + 2 \left\langle \frac{\partial \Psi}{\partial \lambda} \middle| \mathbf{H}_0 + \lambda \mathbf{P}_1 + \lambda^2 \mathbf{P}_2 \middle| \frac{\partial \Psi}{\partial \lambda} \right\rangle + 2 \langle \Psi | \mathbf{P}_2 | \Psi \rangle \tag{10.26}$$

$$\left. \frac{\partial^2 E}{\partial \lambda^2} \right|_{\lambda=0} = 2 \left\langle \frac{\partial^2 \Psi_0}{\partial \lambda^2} \middle| \mathbf{H}_0 \middle| \Psi_0 \right\rangle + 4 \left\langle \frac{\partial \Psi_0}{\partial \lambda} \middle| \mathbf{P}_1 \middle| \Psi_0 \right\rangle + 2 \left\langle \frac{\partial \Psi_0}{\partial \lambda} \middle| \mathbf{H}_0 \middle| \frac{\partial \Psi_0}{\partial \lambda} \right\rangle + 2 \langle \Psi_0 | \mathbf{P}_2 | \Psi_0 \rangle \tag{10.27}$$

$$\left. \frac{\partial^2 E}{\partial \lambda^2} \right|_{\lambda=0} = 2 \frac{\partial^2 \mathbf{C}}{\partial \lambda^2} \left\langle \frac{\partial \Psi_0}{\partial \mathbf{C}} \middle| \mathbf{H}_0 \middle| \Psi_0 \right\rangle + 2 \left(\frac{\partial \mathbf{C}}{\partial \lambda} \right)^2 \left\langle \frac{\partial^2 \Psi_0}{\partial \mathbf{C}^2} \middle| \mathbf{H}_0 \middle| \Psi_0 \right\rangle + 4 \left(\frac{\partial \mathbf{C}}{\partial \lambda} \right) \left\langle \frac{\partial \Psi_0}{\partial \mathbf{C}} \middle| \mathbf{P}_1 \middle| \Psi_0 \right\rangle + 2 \left(\frac{\partial \mathbf{C}}{\partial \lambda} \right)^2 \left\langle \frac{\partial \Psi_0}{\partial \mathbf{C}} \middle| \mathbf{H}_0 \middle| \frac{\partial \Psi_0}{\partial \mathbf{C}} \right\rangle + 2 \langle \Psi_0 | \mathbf{P}_2 | \Psi_0 \rangle \tag{10.28}$$

完全に変分的な波動関数について

$$\left. \frac{\partial^2 E}{\partial \lambda^2} \right|_{\lambda=0} = 2 \left\langle \frac{\partial \Psi_0}{\partial \lambda} \middle| \mathbf{P}_1 \middle| \Psi_0 \right\rangle + 2 \langle \Psi_0 | \mathbf{P}_2 | \Psi_0 \rangle \tag{10.31}$$

厳密解について

$$\frac{\partial \Psi_0}{\partial \lambda} = \sum_{i=1}^{\infty} a_i \Psi_i, \quad a_i = \frac{\langle \Psi_i | \mathbf{P}_1 | \Psi_0 \rangle}{E_0 - E_i} \tag{10.32}$$

摂動論の結果と一致

Lagrangian を用いた方法

$$L_{\mathrm{CI}} = E_{\mathrm{CI}} + \boldsymbol{\kappa} \frac{\partial E_{\mathrm{HF}}}{\partial \mathbf{c}} \tag{10.34}$$

$$\frac{\partial E_{\mathrm{CI}}}{\partial \mathbf{a}} = \frac{\partial}{\partial \mathbf{a}} \langle \Psi_{\mathrm{CI}}(\mathbf{a}, \mathbf{c}) | \mathbf{H} | \Psi_{\mathrm{CI}}(\mathbf{a}, \mathbf{c}) \rangle = 2 \left\langle \frac{\partial \Psi_{\mathrm{CI}}}{\partial \mathbf{a}} \middle| \mathbf{H} \middle| \Psi_{\mathrm{CI}} \right\rangle = 0$$
$$\frac{\partial E_{\mathrm{CI}}}{\partial \mathbf{c}} = \frac{\partial}{\partial \mathbf{c}} \langle \Psi_{\mathrm{CI}}(\mathbf{a}, \mathbf{c}) | \mathbf{H} | \Psi_{\mathrm{CI}}(\mathbf{a}, \mathbf{c}) \rangle = 2 \left\langle \frac{\partial \Psi_{\mathrm{CI}}}{\partial \mathbf{C}} \middle| \mathbf{H} \middle| \Psi_{\mathrm{CI}} \right\rangle \neq 0 \tag{10.33}$$
$$\frac{\partial E_{\mathrm{HF}}}{\partial \mathbf{c}} = \frac{\partial}{\partial \mathbf{c}} \langle \Psi_{\mathrm{HF}}(\mathbf{c}) | \mathbf{H} | \Psi_{\mathrm{HF}}(\mathbf{c}) \rangle = 2 \left\langle \frac{\partial \Psi_{\mathrm{HF}}}{\partial \mathbf{c}} \middle| \mathbf{H} \middle| \Psi_{\mathrm{HF}} \right\rangle = 0$$

Lagrangianの方法(続き)

$$\frac{\partial L_{\mathrm{CI}}}{\partial \mathbf{a}} = \frac{\partial E_{\mathrm{CI}}}{\partial \mathbf{a}} = 0 \quad \text{(CI係数)}$$
$$\frac{\partial L_{\mathrm{CI}}}{\partial \boldsymbol{\kappa}} = \frac{\partial E_{\mathrm{HF}}}{\partial \mathbf{c}} = 0 \quad \text{(MO係数)} \qquad (10.35)$$
$$\frac{\partial L_{\mathrm{CI}}}{\partial \mathbf{c}} = \frac{\partial E_{\mathrm{CI}}}{\partial \mathbf{c}} + \boldsymbol{\kappa}\frac{\partial^2 E_{\mathrm{HF}}}{\partial \mathbf{c}^2} = 0 \qquad (10.36)$$

Lagrange乗数($\frac{\partial L_{CI}}{\partial c}=0$となるように選ぶ)

$$\frac{\partial L_{\mathrm{CI}}}{\partial \lambda} = \frac{\partial E_{\mathrm{CI}}}{\partial \lambda} + \boldsymbol{\kappa}\frac{\partial}{\partial \lambda}\left(\frac{\partial E_{\mathrm{HF}}}{\partial \mathbf{c}}\right) \qquad (10.37)$$

$\hat{P}_1 \equiv \frac{\partial \hat{H}}{\partial \lambda}$

$$\frac{\partial L_{\mathrm{CI}}}{\partial \lambda} = \langle \Psi_{\mathrm{CI}}|\mathbf{P}_1|\Psi_{\mathrm{CI}}\rangle + \boldsymbol{\kappa}\left\langle \frac{\partial \Psi_{\mathrm{HF}}}{\partial \mathbf{c}}\middle|\mathbf{P}_1\middle|\Psi_{\mathrm{HF}}\right\rangle \qquad (10.39)$$

摂動に無関係

The Lagrange expression (10.39), on the other hand, contains a set of Lagrange multipliers $\boldsymbol{\kappa}$ which are independent of the perturbation, i.e. we need only solve one equation for $\boldsymbol{\kappa}$, (10.36). Furthermore, the CPHF equations involve derivatives of the basis functions, while the equation for $\boldsymbol{\kappa}$ only involves integrals of the same type as for calculating the energy itself.

Coupled Perturbed Hartree–Fock

摂動前(ゼロ次)

$$\mathbf{F}^{(0)}\mathbf{C}^{(0)} = \mathbf{S}^{(0)}\mathbf{C}^{(0)}\boldsymbol{\varepsilon}^{(0)} \qquad (10.40)$$

$$\mathbf{C}^{\dagger(0)}\mathbf{S}^{(0)}\mathbf{C}^{(0)} = \mathbf{1} \qquad (10.41)$$

摂動後(一次)

$$\mathbf{F}^{(1)}\mathbf{C}^{(0)} + \mathbf{F}^{(0)}\mathbf{C}^{(1)} = \mathbf{S}^{(1)}\mathbf{C}^{(0)}\boldsymbol{\varepsilon}^{(0)} + \mathbf{S}^{(0)}\mathbf{C}^{(1)}\boldsymbol{\varepsilon}^{(0)} + \mathbf{S}^{(0)}\mathbf{C}^{(0)}\boldsymbol{\varepsilon}^{(1)}$$
$$(\mathbf{F}^{(0)} + \mathbf{S}^{(0)}\boldsymbol{\varepsilon}^{(0)})\mathbf{C}^{(1)} = (\mathbf{F}^{(1)} + \mathbf{S}^{(0)}\boldsymbol{\varepsilon}^{(1)} + \mathbf{S}^{(1)}\boldsymbol{\varepsilon}^{(0)})\mathbf{C}^{(0)} \qquad (10.42)$$

while the orthonormality condition becomes

$$\mathbf{C}^{\dagger(1)}\mathbf{S}^{(0)}\mathbf{C}^{(0)} + \mathbf{C}^{\dagger(0)}\mathbf{S}^{(1)}\mathbf{C}^{(0)} + \mathbf{C}^{\dagger(0)}\mathbf{S}^{(0)}\mathbf{C}^{(1)} = 0 \qquad (10.43)$$

摂動により軌道の変化

$$\phi_i' = \sum_{j=1}^{M} \mathrm{U}_{ji}\phi_j \qquad (10.48)$$

これが求まればよい

$$\mathbf{C}^{(1)} = \mathbf{U}^{(1)}\mathbf{C}^{(0)} \qquad (10.50)$$

$$\langle \phi_\alpha|\mathbf{h}|\phi_\beta\rangle \rightarrow \langle \phi_\alpha|\mathbf{h}|\phi_\beta|\rangle^{(0)} + \langle \phi_\alpha|\mathbf{h}|\phi_\beta\rangle^{(1)}$$
$$\langle \phi_\alpha\phi_\beta|\mathbf{g}|\phi_\gamma\phi_\delta\rangle \rightarrow \langle \phi_\alpha\phi_\beta|\mathbf{g}|\phi_\gamma\phi_\delta\rangle^{(0)} + \langle \phi_\alpha\phi_\beta|\mathbf{g}|\phi_\gamma\phi_\delta\rangle^{(1)} \qquad (10.51)$$

次の連立方程式を解く(占有軌道数×空軌道数の変数)

$$\mathbf{A}^{(0)}\mathbf{U}^{(1)} = \mathbf{B}^{(1)} \qquad (10.52)$$

The $\mathbf{A}^{(0)}$ matrix contains only unperturbed quantities ($\langle \phi_\alpha|\mathbf{h}|\phi_\beta\rangle^{(0)}$ and $\langle \phi_\alpha\phi_\beta|\mathbf{g}|\phi_\gamma\phi_\delta\rangle^{(0)}$), while the $\mathbf{B}^{(1)}$ matrix contains first derivatives ($\langle \phi_\alpha|\mathbf{h}|\phi_\beta\rangle^{(1)}$ and $\langle \phi_\alpha\phi_\beta|\mathbf{g}|\phi_\gamma\phi_\delta\rangle^{(1)}$).

Electric Field Perturbation

電場による摂動

$\vec{F}$の一次 導関数で考えても摂動で考えても同じ

$$\frac{\partial E_{\mathrm{HF}}}{\partial \mathbf{F}} = \langle \Psi_0|\mathbf{r}|\Psi_0\rangle \qquad (10.55)$$

$\vec{F}$の二次 導関数

$$\frac{\partial^2 E_{\mathrm{HF}}}{\partial \mathbf{F}^2} = 2\left\langle \frac{\partial \Psi_0}{\partial \mathbf{F}}\middle|\mathbf{r}\middle|\Psi_0\right\rangle \qquad (10.56)$$

二次摂動論

$$W_2 = \sum_{i\neq 0} \frac{|\langle \Psi_0|\mathbf{r}|\Psi_i\rangle|^2}{E_0 - E_i} \qquad (10.57)$$

Geometry Perturbations 構造変化

$$\frac{\partial E}{\partial \mathbf{R}} = \left\langle \Psi_0 \left| \frac{\partial \mathbf{H}}{\partial \mathbf{R}} \right| \Psi_0 \right\rangle + 2\left\langle \frac{\partial \Psi_0}{\partial \mathbf{R}} \middle| \mathbf{H}_0 \middle| \Psi_0 \right\rangle \tag{10.83}$$

↑ Hellmann-Feynman項

$$\frac{\partial \Psi}{\partial \mathbf{R}} = \frac{\partial \Psi}{\partial \chi}\frac{\partial \chi}{\partial \mathbf{R}} + \frac{\partial \Psi}{\partial \mathbf{c}}\frac{\partial \mathbf{c}}{\partial \mathbf{R}} \tag{10.84}$$

↑ 基底関数に関する微分　← MO係数に関する微分 $\left(\frac{\partial E_{HF}}{\partial c}=0\right)$

Hartree-Fock エネルギー

$$E_{\mathrm{HF}} = \sum_{\alpha\beta}^{M} D_{\alpha\beta} h_{\alpha\beta} + \frac{1}{2}\sum_{\alpha\beta\gamma\delta}^{M} D_{\alpha\beta} D_{\gamma\delta} (\langle \chi_\alpha \chi_\gamma | \chi_\beta \chi_\delta \rangle - \langle \chi_\alpha \chi_\gamma | \chi_\delta \chi_\beta \rangle) + V_{\mathrm{nn}} \tag{10.85}$$

一次導関数

$$\frac{\partial E_{\mathrm{HF}}}{\partial \lambda} = \sum_{\alpha\beta}^{M} D_{\alpha\beta}\frac{\partial h_{\alpha\beta}}{\partial \lambda} + \frac{1}{2}\sum_{\alpha\beta\gamma\delta}^{M} (D_{\alpha\beta}D_{\gamma\delta} - D_{\alpha\delta}D_{\gamma\beta})\frac{\partial \langle \chi_\alpha \chi_\gamma | \chi_\beta \chi_\delta \rangle}{\delta \lambda} + \frac{\partial V_{\mathrm{nn}}}{\delta \lambda} - \sum_{\alpha\beta}^{M} W_{\alpha\beta}\frac{\partial S_{\alpha\beta}}{\partial \lambda} \tag{10.96}$$

$$W_{\alpha\beta} = \sum_{i=1}^{N} \varepsilon_i c_{\alpha i} c_{\beta i} \tag{10.97}$$

$$h_{\alpha\beta} = \langle \chi_\alpha | \mathbf{h} | \chi_\beta \rangle$$

$$\frac{\partial h_{\alpha\beta}}{\partial \lambda} = \left\langle \frac{\partial \chi_\alpha}{\partial \lambda} \middle| \mathbf{h} \middle| \chi_\beta \right\rangle + \left\langle \chi_\alpha \left| \frac{\partial \mathbf{h}}{\partial \lambda} \right| \chi_\beta \right\rangle + \left\langle \chi_\alpha \middle| \mathbf{h} \middle| \frac{\partial \chi_\beta}{\partial \lambda} \right\rangle \tag{10.89}$$

$$\langle \chi_\alpha \chi_\gamma | \chi_\beta \chi_\delta \rangle = \langle \chi_\alpha \chi_\gamma | \mathbf{g} | \chi_\beta \chi_\delta \rangle$$

$$\begin{aligned}\frac{\partial}{\partial \lambda}\langle \chi_\alpha \chi_\gamma | \chi_\beta \chi_\delta \rangle = {} & \left\langle \frac{\partial \chi_\alpha}{\partial \lambda} \chi_\gamma \middle| \mathbf{g} \middle| \chi_\beta \chi_\delta \right\rangle + \left\langle \chi_\alpha \frac{\partial \chi_\gamma}{\partial \lambda} \middle| \mathbf{g} \middle| \chi_\beta \chi_\delta \right\rangle \\ & + \left\langle \chi_\alpha \chi_\gamma \left| \frac{\partial \mathbf{g}}{\partial \lambda} \right| \chi_\beta \chi_\delta \right\rangle + \left\langle \chi_\alpha \chi_\gamma \middle| \mathbf{g} \middle| \frac{\partial \chi_\beta}{\partial \lambda} \chi_\delta \right\rangle \\ & + \left\langle \chi_\alpha \chi_\gamma \middle| \mathbf{g} \middle| \chi_\beta \frac{\partial \chi_\delta}{\partial \lambda} \right\rangle\end{aligned} \tag{10.90}$$

演算子の微分

$$\frac{\partial \mathbf{h}}{\partial X_k} = \frac{\partial}{\partial X_k}\left(-\frac{1}{2}\nabla_i^2 - \sum_a \frac{Z_a}{|\mathbf{R}_a - \mathbf{r}_i|}\right) = \frac{(X_k - x_i)Z_k}{|\mathbf{R}_k - \mathbf{r}_i|^3}$$

$$\frac{\partial \mathbf{g}}{\partial X_k} = 0 \tag{10.98}$$

$$\frac{\partial \mathbf{V}_{\mathrm{nn}}}{\partial X_k} = \frac{\partial}{\partial X_k}\left(\sum_{a>b}\frac{Z_a Z_b}{|\mathbf{R}_a - \mathbf{R}_b|}\right) = -\sum_{b\neq k}\frac{(X_k - X_b)Z_k Z_b}{|\mathbf{R}_k - \mathbf{R}_b|^3}$$

基底関数の微分

$$\chi_\alpha(\mathbf{R}_k) = N(X_k - x)^l (Y_k - y)^m (Z_k - z)^n \mathrm{e}^{-\alpha(\mathbf{r}-\mathbf{R}_k)^2}$$

$$\begin{aligned}\frac{\partial \chi_\alpha(\mathbf{R}_k)}{\partial X_k} = {} & N(X_k - x)^{l-1}(Y_k - y)^m (Z_k - z)^n \mathrm{e}^{-\alpha(\mathbf{r}-\mathbf{R}_k)^2} \\ & - 2N\alpha(X_k - x)^{l+1}(Y_k - y)^m (Z_k - z)^n \mathrm{e}^{-\alpha(\mathbf{r}-\mathbf{R}_k)^2}\end{aligned} \tag{10.99}$$

二次導関数

$$\begin{aligned}\frac{\partial^2 E_{\mathrm{HF}}}{\partial \lambda^2} = {} & \sum_{\alpha\beta}^{M} D_{\alpha\beta}\frac{\partial^2 h_{\alpha\beta}}{\partial \lambda^2} + \frac{1}{2}\sum_{\alpha\beta\gamma\delta}^{M} D_{\alpha\beta}D_{\gamma\delta}\frac{\partial^2}{\partial \lambda^2}(\langle \chi_\alpha \chi_\gamma | \chi_\beta \chi_\delta \rangle - \langle \chi_\alpha \chi_\gamma | \chi_\delta \chi_\beta \rangle) \\ & + \frac{\partial^2 V_{\mathrm{nn}}}{\partial \lambda^2} - \sum_{\alpha\beta}^{M} W_{\alpha\beta}\frac{\partial^2 S_{\alpha\beta}}{\partial \lambda^2} + \sum_{\alpha\beta}^{M}\frac{\partial D_{\alpha\beta}}{\partial \lambda}\frac{\partial h_{\alpha\beta}}{\partial \lambda} \\ & + \sum_{\alpha\beta\gamma\delta}^{M}\frac{\partial D_{\alpha\beta}}{\partial \lambda}D_{\gamma\delta}\frac{\partial}{\partial \lambda}(\langle \chi_\alpha \chi_\gamma | \chi_\beta \chi_\delta \rangle - \langle \chi_\alpha \chi_\gamma | \chi_\delta \chi_\beta \rangle) \\ & - \sum_{\alpha\beta}^{M}\frac{\partial W_{\alpha\beta}}{\partial \lambda}\frac{\partial S_{\alpha\beta}}{\partial \lambda}\end{aligned} \tag{10.100}$$

計算精度

構造の収束

Table 11.1. H_2O geometry as a function of basis set at the HF level of theory

Basis	R_{OH} (Å)	α_{HOH}
cc-pVDZ	0.9463	104.61
cc-pVTZ	0.9406	106.00
cc-pVQZ	0.9396	106.22
cc-pV5Z	0.9396	106.33
cc-pV6Z	0.9396	106.33
expt.	0.9578	104.48°

Table 11.2 H_2O geometry as a function of basis set at the MP2 level of theory

Basis	R_{OH} (Å)	α_{HOH}	ΔR_{OH} (Å)	$\Delta\alpha_{HOH}$
cc-pVDZ	0.9649	101.90	0.0186	−2.71
cc-pVTZ	0.9591	103.59	0.0185	−2.48
cc-pVQZ	0.9577	104.02	0.0181	−2.20
cc-pV5Z	0.9579	104.29	0.0184	−2.04
cc-pV6Z	0.9581	104.36	0.0185	−1.97

Table 11.3 H_2O geometry as a function of basis set at the CCSD(T) level of theory

Basis	R_{OH} (Å)	α_{HOH}	ΔR_{OH} (Å)	$\Delta\alpha_{HOH}$
cc-pVDZ	0.9663	101.91	0.0014	0.01
cc-pVTZ	0.9594	103.58	0.0003	0.06
cc-pVQZ	0.9579	104.12	0.0002	0.10
cc-pV5Z	0.9580	104.38	0.0001	0.09

Table 11.4 H_2O geometry as a function of basis set at the MP2 level of theory including all electrons in the correlation

Basis	R_{OH} (Å)	α_{HOH}	ΔR_{OH} (Å)	$\Delta\alpha_{HOH}$
cc-pCVDZ	0.9643	101.91	−0.0005	0.04
cc-pCVTZ	0.9580	103.63	−0.0008	0.11
cc-pCVQZ	0.9569	104.14	−0.0009	0.12
cc-pCV5Z	0.9570	104.41	−0.0009	0.12

Table 11.5 H_2O bond distance (Å) as a function of basis set with different DFT functionals

Basis	SVWN	BLYP	BPW91	B3LYP	B3PW91
cc-pVDZ	0.9769	0.9799	0.9762	0.9687	0.9663
cc-pVTZ	0.9706	0.9716	0.9687	0.9613	0.9596
cc-pVQZ	0.9697	0.9703	0.9677	0.9602	0.9586
cc-pV5Z	0.9698	0.9703	0.9677	0.9602	0.9586

Table 11.6 H_2O bond angle as a function of basis set with different DFT functionals

Basis	SVWN	BLYP	BPW91	B3LYP	B3PW91
cc-pVDZ	102.47	101.81	101.78	102.74	102.68
cc-pVTZ	104.34	103.77	103.60	104.52	104.36
cc-pVQZ	104.71	104.21	103.97	104.89	104.68
cc-pV5Z	104.94	104.47	104.18	105.10	104.86

エネルギーの収束

Table 11.7 % electron correlation recovered by different methods in the cc-pVDZ basis

Method	% EC
MP2	94.0
MP3	97.0
MP4	99.5
MP5	99.8
CCSD	98.3
CCSD(T)	99.7
CISD	94.5
CISDT	95.8
CISDTQ	99.9

Table 11.8 Total energy (+76 a.u.) as a function of basis set and electron correlation (valence only)

Method	cc-pVDZ	cc-pVTZ	cc-pVQZ	cc-pV5Z	cc-pV6Z	cc-pV∞Z
HF	−0.02677	−0.05713	−0.06479	−0.06704	−0.06735	−0.0676
MP2	−0.22844	−0.31863	−0.34763	−0.35860	−0.36264	−0.368
MP3	−0.23544	−0.32275	−0.34939	−0.35815	−0.36094	−0.364
MP4	−0.24067	−0.33302	−0.36104	−0.37051	−0.37357	−0.377
MP5	−0.24120	−0.33159				
CCSD	−0.23801	−0.32455	−0.35080	−0.35952		−0.366
CCSD(T)	−0.24104	−0.33219	−0.35979	−0.36904		−0.376
CISD	−0.22997	−0.31384	−0.33922	−0.34765		−0.354

Table 11.9 Total energy (+76 a.u.) as a function of basis set and electron correlation (all electrons)

Method	cc-pCVDZ	cc-pCVTZ	cc-pCVQZ	cc-pCV5Z	cc-pCV∞Z (%EC)
HF	−0.02718	−0.05731	−0.06490	−0.06706	−0.0677 (0.0)
MP2	−0.26855	−0.37486	−0.40758	−0.41939	−0.430 (97.4)
MP3	−0.27638	−0.37984	−0.41012	−0.41978	−0.430 (97.4)
MP4	−0.28194	−0.39079	−0.42240	−0.43268	−0.440 (100.0)
MP5	−0.28239	−0.38907			
CCSD	−0.27897	−0.38154	−0.41144	−0.42104	−0.428 (96.9)
CCSD(T)	−0.28226	−0.38978	−0.42096	−0.43105	−0.438 (99.5)
CISD	−0.26898	−0.36799	−0.39675	−0.40599	−0.412 (92.6)

双極子モーメント

Table 11.10 H_2O dipole moment (Debye) as a function of theory (valence correlation only), experimental value is 1.847 D

Basis	HF	MP2	CCSD(T)
cc-pVDZ	2.057	1.964	1.936
cc-pVTZ	2.026	1.922	1.903
cc-pVQZ	2.008	1.904	1.890
cc-pV5Z	2.003	1.895	
cc-pV6Z	1.990		
aug-cc-pVDZ	2.000	1.867	1.848
aug-cc-pVTZ	1.984	1.852	1.839
aug-cc-pVQZ	1.982	1.858	1.848
aug-cc-pV5Z	1.982	1.861	

Table 11.11 H_2O dipole moment (Debye) as a function of theory (all electrons)

Basis	HF	MP2	CCSD(T)
aug-cc-pCVDZ	2.001	1.868	1.849
aug-cc-pCVTZ	1.983	1.857	1.843

Table 11.12 H_2O dipole moment (Debye) as a function of DFT functional and basis set; the experimental value is 1.847 D

Basis	SVWN	BLYP	BPW91	B3LYP	B3PW91
aug-cc-pVDZ	1.853	1.796	1.803	1.855	1.859
aug-cc-pVTZ	1.857	1.799	1.800	1.854	1.854
aug-cc-pVQZ	1.855	1.798	1.797	1.854	1.852
aug-cc-pV5Z	1.856	1.799	1.798	1.855	1.852

調和振動数

Table 11.13 H_2O HF harmonic frequencies (cm^{-1}) as a function of basis set; experimental values are 3943 cm^{-1}, 3832 cm^{-1} and 1649 cm^{-1}

Basis	ω_1	ω_2	ω_3
cc-pVDZ	4212	4114	1776
cc-pVTZ	4227	4127	1753
cc-pVQZ	4229	4130	1751
cc-pV5Z	4231	4131	1748

Table 11.14 H_2O MP2 harmonic frequencies (cm^{-1}) as a function of basis set (valence electrons only); experimental values are 3943 cm^{-1}, 3832 cm^{-1} and 1649 cm^{-1}

Basis	ω_1	ω_2	ω_3
cc-pVDZ	3971	3852	1678
cc-pVTZ	3976	3855	1651
cc-pVQZ	3978	3855	1643
cc-pV5Z	3974	3849	1636

Table 11.15 H_2O CCSD(T) harmonic frequencies (cm^{-1}) as a function of basis set (valence electrons only)

Basis	ω_1	ω_2	ω_3
cc-pVDZ	3928	3822	1690
cc-pVTZ	3946	3841	1669
cc-pVQZ	3952	3845	1659

Table 11.16 H_2O MP2 harmonic frequencies (cm^{-1}) as a function of basis set (all electrons)

Basis	ω_1	ω_2	ω_3
cc-pCVDZ	3973	3853	1679
cc-pCVTZ	3976	3857	1651

Table 11.17 H_2O highest harmonic frequency (cm^{-1}) as a function of basis set with different DFT functionals; the experimental value is 3943 cm^{-1}

Basis	SVWN	BLYP	BPW91	B3LYP	B3PW91
cc-pVDZ	3787	3691	3756	3852	3898
cc-pVTZ	3825	3753	3807	3900	3937
cc-pVQZ	3826	3762	3812	3906	3941
cc-pV5Z	3827	3767	3815	3909	3943

調和振動数(続き)

Table 11.18 H_2O second lowest harmonic frequency (cm^{-1}) as a function of basis set with different DFT functionals; the experimental value is 3832 cm^{-1}

Basis	SVWN	BLYP	BPW91	B3LYP	B3PW91
cc-pVDZ	3674	3589	3651	3750	3794
cc-pVTZ	3716	3654	3704	3800	3834
cc-pVQZ	3718	3663	3709	3806	3834
cc-pV5Z	3718	3666	3712	3808	3839

Table 11.19 H_2O lowest harmonic frequency (cm^{-1}) as a function of basis set with different DFT functionals; the experimental value is 1649 cm^{-1}

Basis	SVWN	BLYP	BPW91	B3LYP	B3PW91
cc-pVDZ	1581	1629	1632	1658	1660
cc-pVTZ	1561	1611	1613	1639	1640
cc-pVQZ	1556	1605	1607	1635	1636
cc-pV5Z	1551	1599	1603	1630	1632

FOOFの構造

Table 11.20 Bond distance (Å) in FOOF. Experimental values are 1.217 and 1.575 Å

	R_{OO}			R_{FO}		
	cc-pVDZ	DZP	TZ(2d)	cc-pVDZ	DZP	TZ(2d)
HF	1.304	1.308	1.301	1.368	1.362	1.361
MP2	1.210	1.266	1.140	1.581	1.521	1.728
MP3	1.302	1.320	1.301	1.455	1.449	1.450
CCSD	1.276	1.307	1.278	1.494	1.474	1.482
CCSD(T)	1.216	1.261	1.216	1.637	1.571	1.614
CISD	1.304	1.316	1.301	1.416	1.412	1.407
SVWN	1.202	1.222	1.186	1.556	1.536	1.573
BLYP	1.224	1.243	1.207	1.622	1.604	1.643
BPW91	1.211	1.231	1.119	1.612	1.589	1.623
B3LYP	1.240	1.264	1.222	1.523	1.502	1.540
B3PW91	1.229	1.254	1.217	1.517	1.491	1.524

Table 11.20 sourced from Ref. 15.

双極子モーメント CO

Table 11.21 Dipole moment (Debye) for CO; the experimental value is 0.122 D

	aug-cc-pVDZ	aug-cc-pVTZ	aug-cc-pVQZ	aug-cc-pV5Z
HF	−0.255	−0.263	−0.265	−0.265
MP2	0.296	0.280	0.275	0.273
MP3	0.076	0.047	0.036	0.032
MP4	0.220	0.222	0.216	0.214
CCSD	0.097	0.070	0.059	0.055
CCSD(T)	0.141	0.127	0.118	0.115
CISD	0.050	0.023	0.011	
SVWN	0.232	0.226	0.229	
BLYP	0.187	0.184	0.185	
BPW91	0.221	0.217	0.218	
B3LYP	0.091	0.086	0.087	
B3PW91	0.119	0.114	0.116	

Table 11.22 Dipole moment (Debye) for CO; the experimental value is 0.122 D

	aug-DZP	10s9p4d2f	ANO [4s3p2d1f]	ANO [7s6p5d3f2g1h]
HF	−0.273	−0.266		
MP2	0.303	0.282		
MP3	0.079	0.047		
MP4	0.223	0.235		
CCSD	0.100	0.071	0.067	0.075
CCSD(T)	0.142	0.130	0.107	0.110
CCSDT	0.140			

Table 11.22 sourced from Ref. 18.

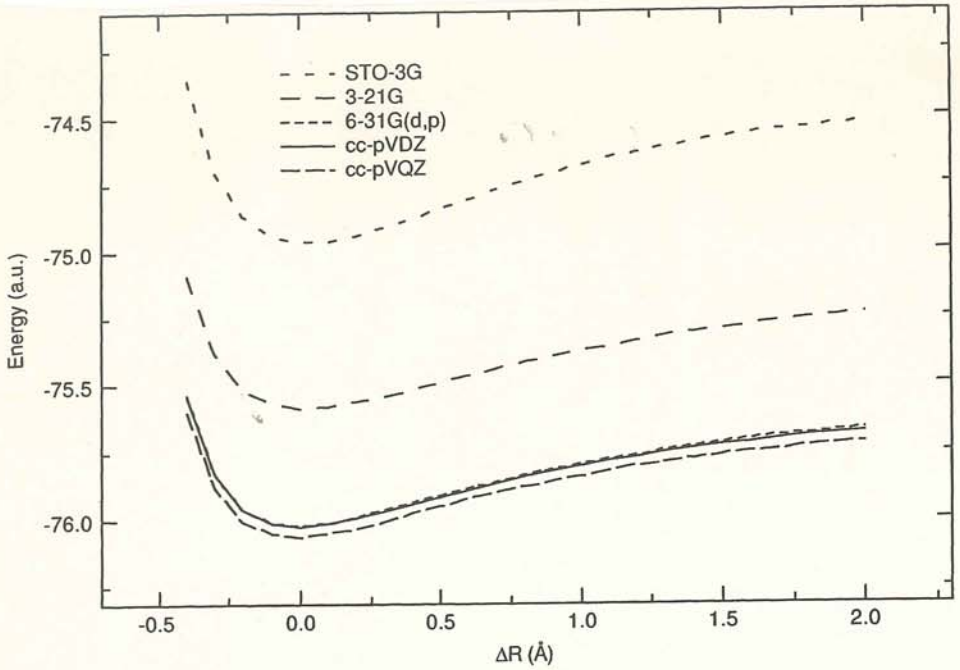

Figure 11.1 Bond dissociation curves for H_2O at the HF level, absolute energies

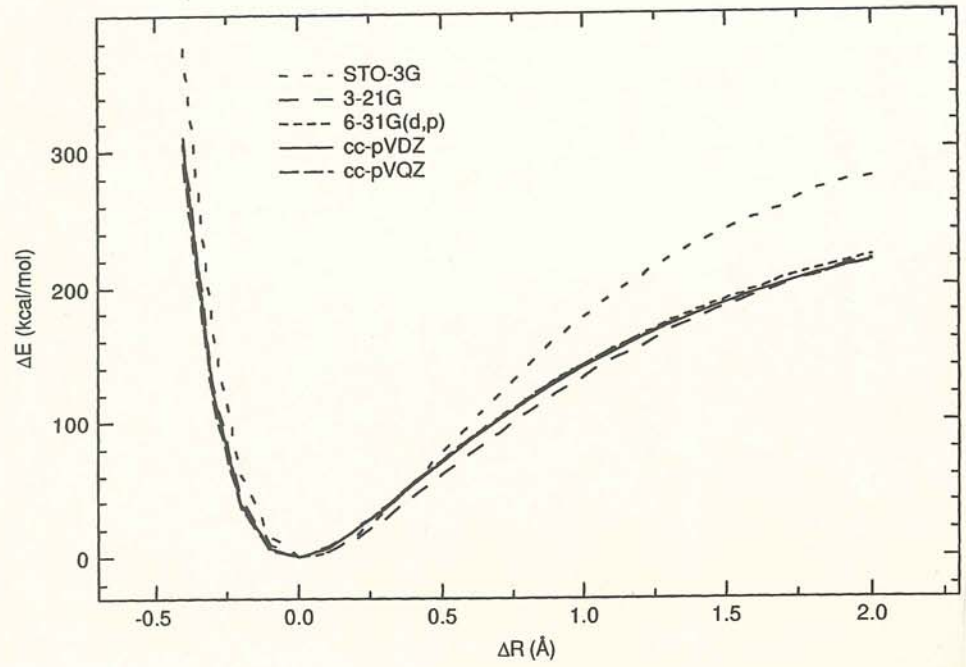

Figure 11.2 Bond dissociation curves for H_2O at the HF level, relative energies

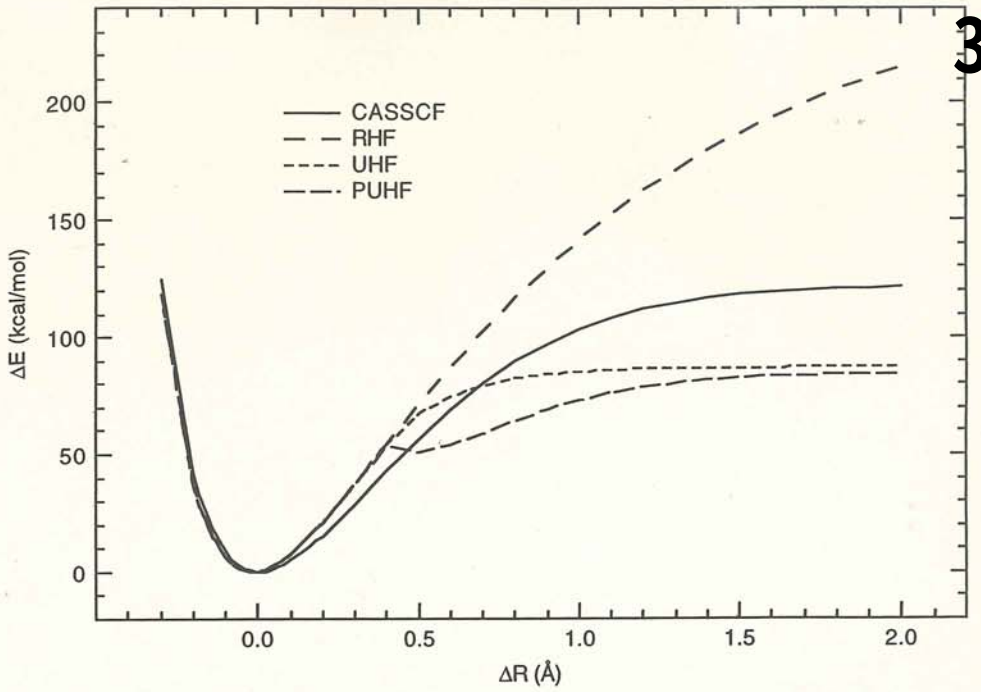

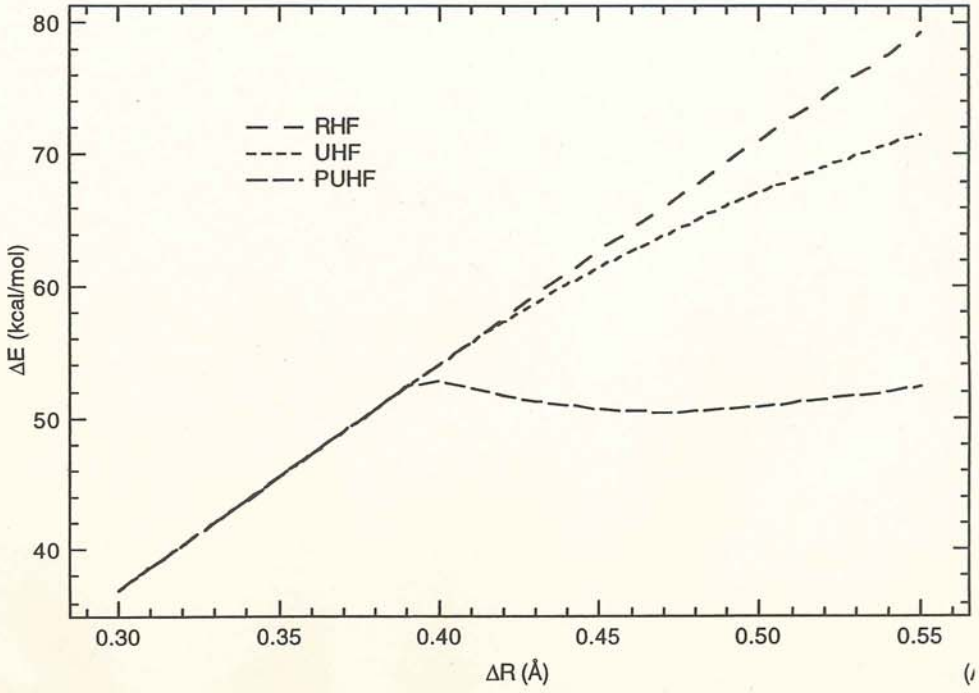

Figure 11.4 RHF, UHF and PUHF dissociation curves for H_2O near the instability point

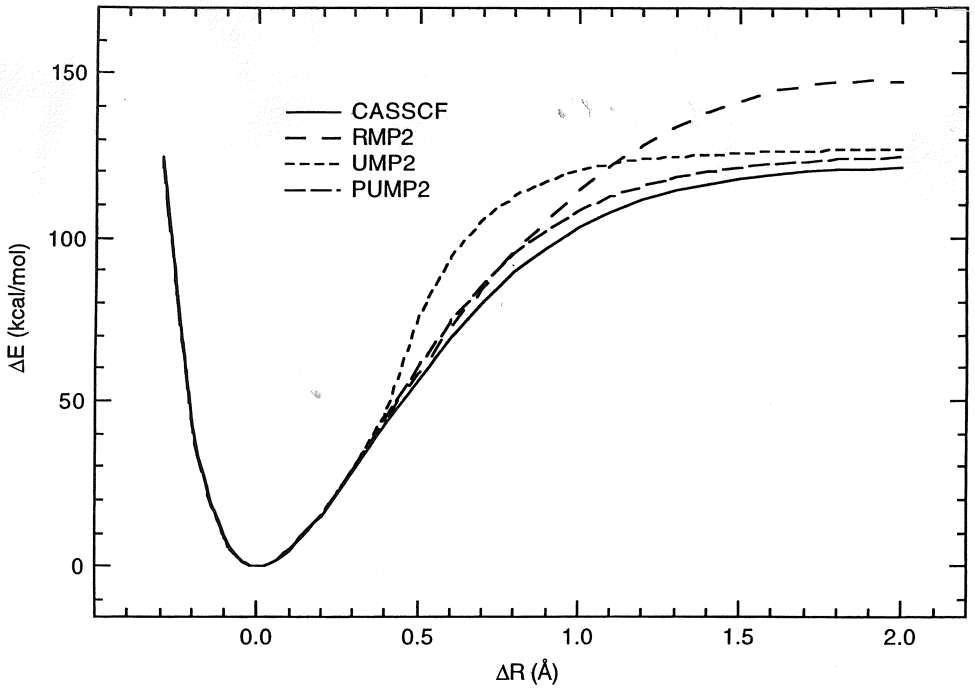

Figure 11.5 RMP2, UMP2 and PUMP2 dissociation curves for H_2O

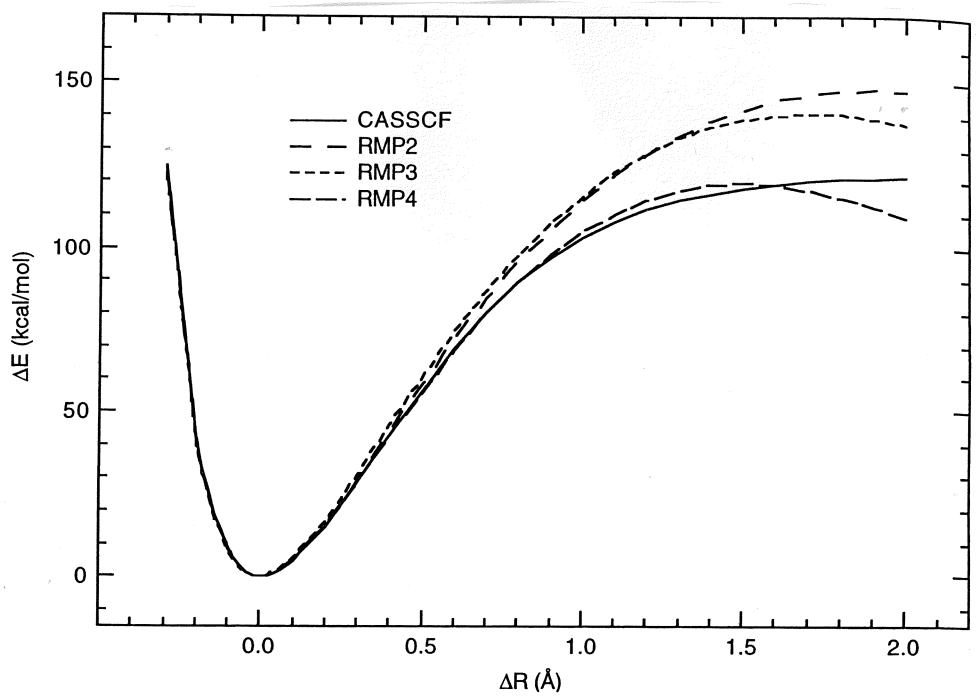

Figure 11.7 RMP2, RMP3 and RMP4 dissociation curves for H_2O

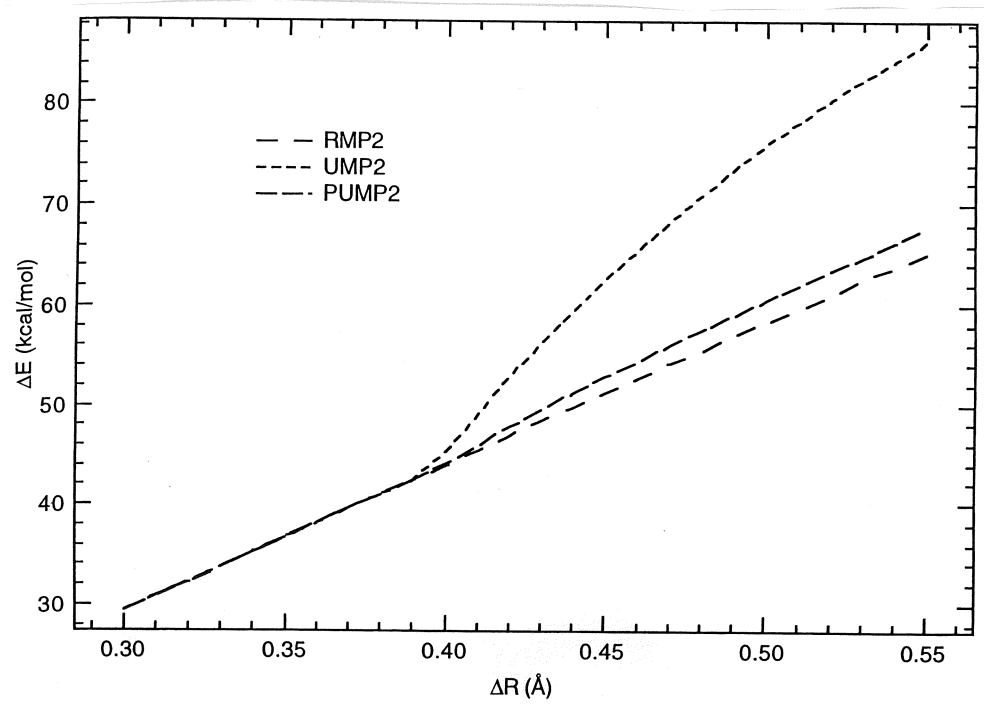

Figure 11.6 RMP2, UMP2 and PUMP2 dissociation curves for H_2O near the instability point

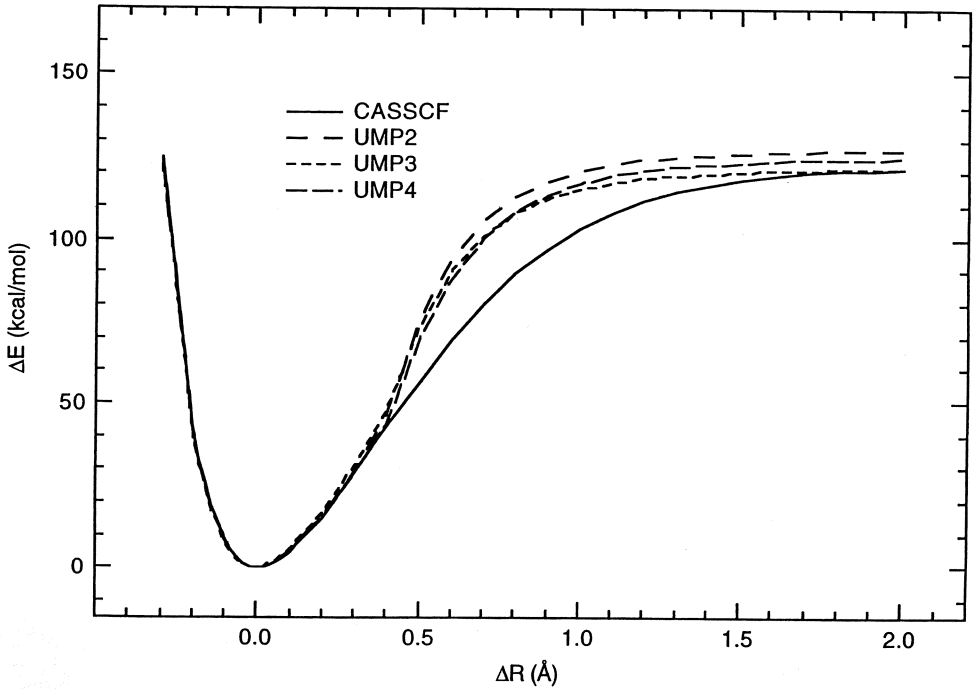

Figure 11.8 UMP2, UMP3 and UMP4 dissociation curves for H_2O

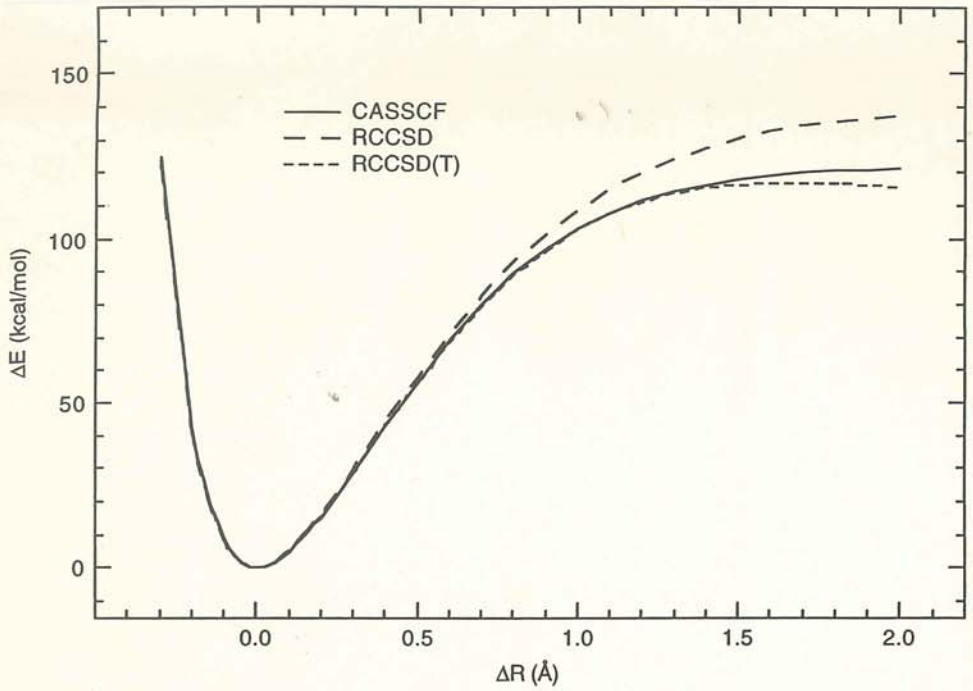

Figure 11.9 RCCSD and RCCSD(T) dissociation curves for H_2O

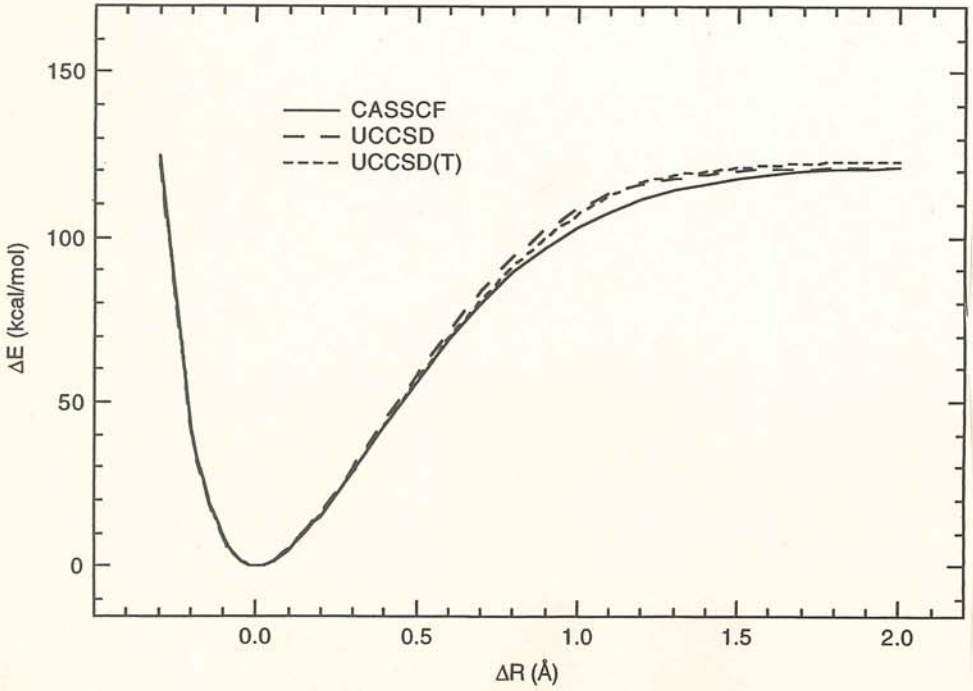

Figure 11.10 UCCSD and UCCSD(T) dissociation curves for H_2O

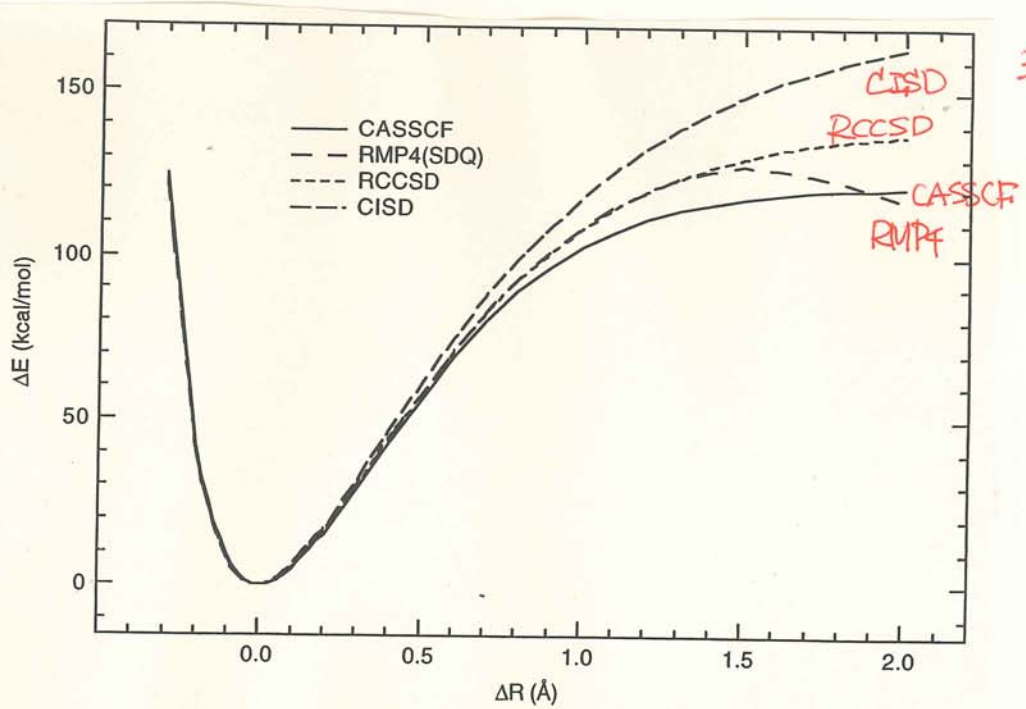

Figure 11.11 RMP4(SDQ), RCCSD and CISD dissociation curves for H_2O

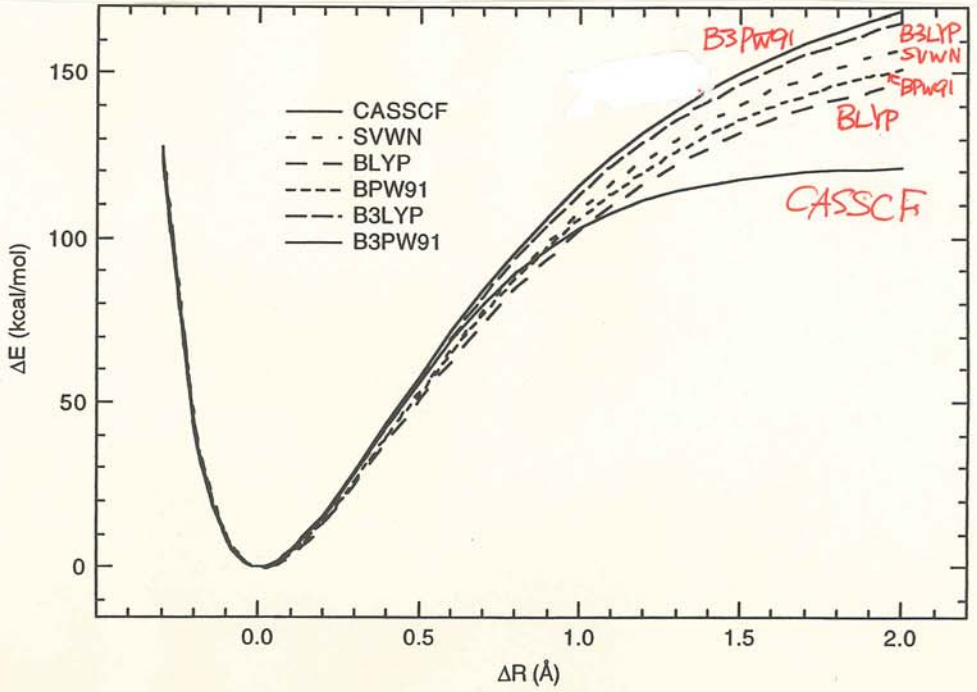

Figure 11.12 Bond dissociation curve for restricted DFT methods

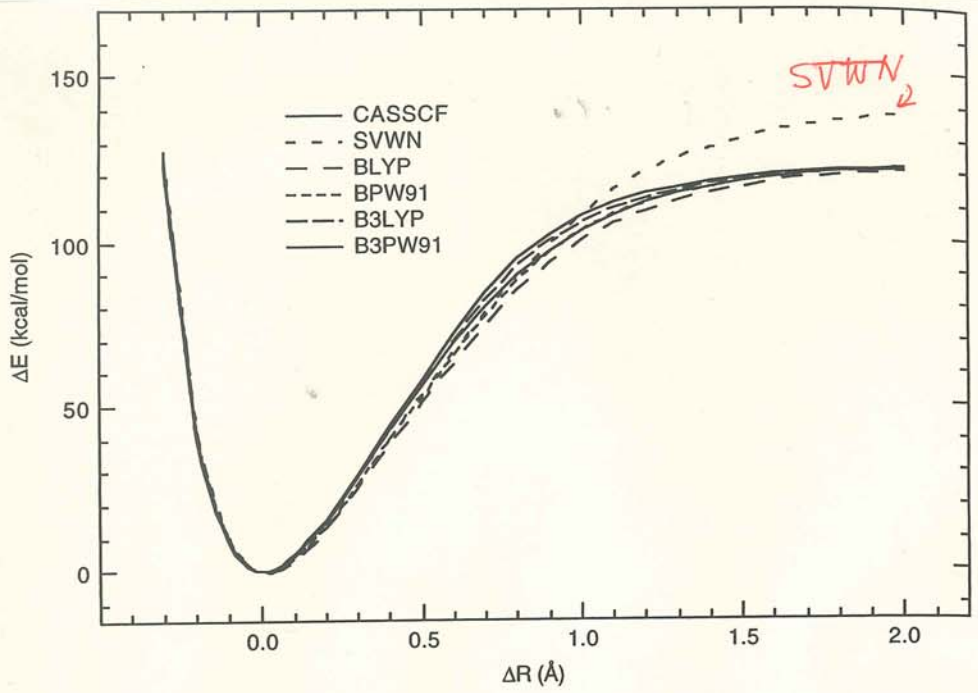

Figure 11.13 Bond dissociation curve for unrestricted DFT methods

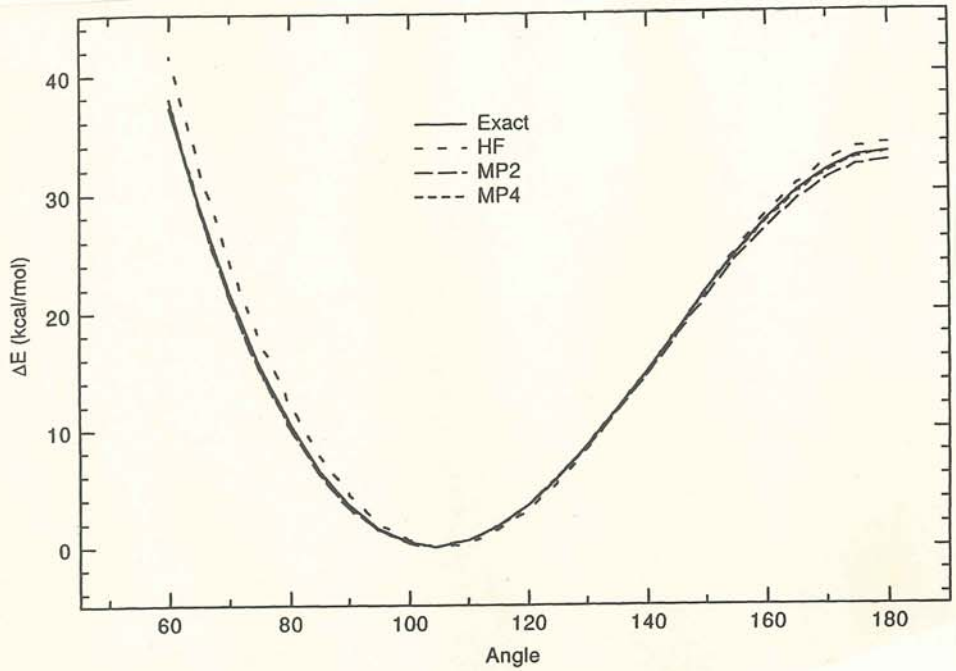

Figure 11.14 Angle bending curves for H_2O

オゾン(O_3)の振動数

Table 11.23 Harmonic frequencies for O_3 with the cc-pVTZ basis

Method	ω_1	ω_2	ω_3
HF	1537	1418	867
MP2	1166	2241	743
MP3	1364	1713	798
MP4	1106	1592	695
CCSD	1278	1267	762
CCSD(T)	1154	1067	717
CISD	1407	1535	816
[2,2]-CASSCF	1189	1497	799
SVWN	1249	1148	744
BLYP	1130	980	683
BPW91	1177	1047	706
B3LYP	1252	1194	746
B3PW91	1288	1244	762
Experimental	1135	1089	716

Table 11.24 Harmonic frequencies for O_3 with other methods

Method/basis	ω_1	ω_2	ω_3
CCSD/DZP	1256	1240	748
CCSD(T)/DZP	1129	976	703
CCSDT/DZP	1141	1077	705
CCSD/ANO [5s4p3d2f]	1280	1262	766
CCSD(T)/ANO [5s4p3d2f]	1153	1053	718
CCSD/ANO [5s4p3d2f1g]	1292	1280	771
[12,9]-CASSCF/ANO [4s3p2d1f]	1100	1039	708
[12,9]-CASPT2/ANO [4s3p2d1f]	1087	998	691
Experimental	1135	1089	716

Table 11.24 sourced from Ref. 20.

C_4H_6 異性体の相対エネルギー

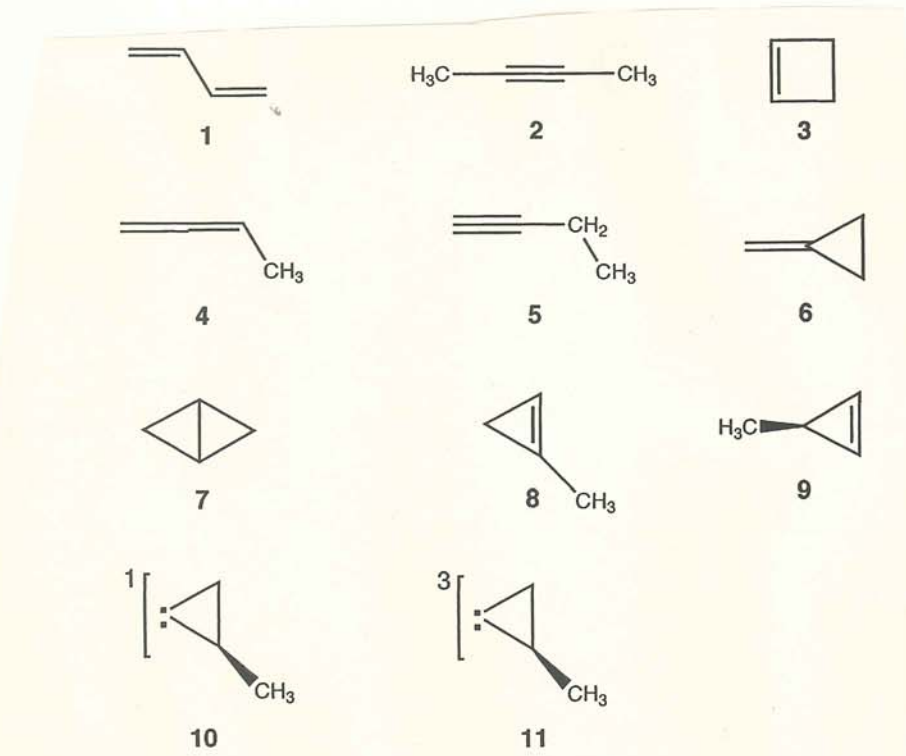

Figure 11.15 C_4H_6 isomers

Table 11.25 Energies (kcal/mol) relative to **1** calculated by semi-empirical methods

Isomer	MINDO/3	MNDO	AM1	PM3	SAM1	Exp.
2	−19.9	−4.1	2.1	−1.3	−5.5	8.6
3	1.2	2.1	15.8	6.6	13.8	11.2
4	−3.4	4.6	7.2	7.0	2.0	12.4
5	−3.8	7.2	7.6	4.7	3.7	13.2
6	1.9	8.9	17.7	13.5	15.1	21.7
7	17.8	35.1	48.2	38.2	44.1	25.6
8	10.1	24.7	34.7	26.3	28.2	31.9
9	20.0	31.6	37.8	29.2	34.2	
10	55.6	83.5	84.7	75.9	61.0	
11	54.2	84.5	90.3	80.3	80.4	
MAD	17.2	9.3	7.3	7.8	9.3	

Table 11.26 Energies relative to **1** calculated at the HF level with different basis sets

Isomer	STO-3G	3-21G	6-31G (d,p)	DZP	6-311G (2d,2p)	TZ (2d,2p)	Exp.
2	−12.8	3.6	7.1	7.8	7.5	7.7	8.6
3	−12.5	18.0	12.9	13.6	15.2	15.7	11.2
4	8.5	11.3	12.9	14.3	15.6	13.5	12.4
5	−5.3	9.2	13.4	13.4	13.2	13.4	13.2
6	5.8	25.6	20.4	21.5	22.8	23.1	21.7
7	11.6	45.7	30.1	31.8	33.8	34.7	25.6
8	22.3	47.2	37.1	39.1	39.2	39.8	31.9
9	17.3	43.5	32.6	34.4	34.8	35.3	
10	51.7	83.5	72.7	72.4	74.6	75.3	
11	45.0	77.4	70.4	71.3	73.6	74.6	
MAD	15.3	8.0	2.1	2.7	3.6	3.6	

Table 11.27 MP2/6-31G(d,p) energies relative to **1**, using either HF/6-31G(d,p) or MP2/6-31G(d,p) optimized geometries

Isomer	HF/6-31G(d,p) geometry	MP2/6-31G(d,p) geometry	Exp.
2	5.5	4.8	8.6
3	7.7	7.9	11.2
4	12.1	12.3	12.4
5	10.7	10.0	13.2
6	16.1	16.4	21.7
7	20.0	20.3	25.6
8	29.9	29.9	31.9
9	26.2	26.0	
10	81.3	81.9	
11	89.5	89.9	
MAD	3.2	3.3	

Table 11.28 Zero-point energy corrections (kcal/mol)

Isomer	HF/6-31G(d,p)	MP2/6-31 G(d,p)
2	−0.6	−0.6
3	1.0	1.2
4	−0.7	−0.3
5	−0.3	−0.3
6	0.1	0.5
7	0.9	1.4
8	−0.6	−0.2
9	−0.4	0.1
10	−1.7	−1.3
11	−0.8	−0.1

Table 11.29 Energies relative to **1** calculated at the MP2 level with different basis sets, using MP2/6-31G(d,p) optimized geometries

Isomer	6-31G (d,p)	6-311G (2d,2p)	TZ (2d,2p)	6-311G (2df,2pd)	Exp.
2	4.8	4.8	5.1	4.8	8.6
3	7.9	10.6	11.2	9.4	11.2
4	12.3	12.8	12.5	12.5	12.4
5	10.0	9.6	10.1	9.7	13.2
6	16.4	19.6	19.5	17.5	21.7
7	20.3	24.6	25.2	21.4	25.6
8	29.9	33.0	33.8	31.3	31.9
9	26.0	29.6	30.0	27.6	
10	81.9	84.0	84.8	83.3	
11	89.9	94.0	95.1	94.2	
r.m.s. error	3.3	1.8	1.6	2.6	

Table 11.30 Energies relative to **1** at different levels calculated with the 6-31G(d,p) basis sets at the MP2/6-31G(d,p) optimized geometry

Isomer	HF	MP2	MP3	MP4	CCSD	CCSD(T)	CISD	Exp.
2	7.9	4.8	9.1	7.4	8.5	9.2	7.5	8.6
3	12.6	7.9	8.9	10.1	10.1	10.6	9.1	11.2
4	12.7	12.3	12.3	12.2	12.2	12.5	12.1	12.4
5	14.2	10.0	14.0	12.5	13.5	14.1	13.2	13.2
6	20.0	16.4	17.6	18.5	18.4	19.1	17.2	21.7
7	29.8	20.3	23.7	25.2	25.8	26.5	23.8	25.6
8	37.2	29.9	32.2	32.8	33.3	33.7	32.9	31.9
9	32.6	26.0	28.5	29.0	29.6	30.1	28.7	
10	72.0	81.9	78.0	80.3	77.7	79.6	75.7	
11	70.1	89.9	88.2	91.2	88.3	90.6	82.4	
MAD	2.1	3.3	1.4	1.1	0.9	1.1	1.5	

Table 11.31 Energies relative to **1** by combining results from different calculations

Isomer	MP2 6-311G(2df,2pd)	Δ(CCSD(T)-MP2) 6-31G(d,p)	ΔZPE MP2/6-31G(d,p)	Sum	Exp.
2	4.8	4.4	−0.6	8.6	8.6
3	9.4	2.7	1.2	13.3	11.2
4	12.5	0.2	−0.3	12.4	12.4
5	9.7	4.1	−0.3	13.5	13.2
6	17.5	2.7	0.5	20.7	21.7
7	21.4	6.2	1.4	29.0	25.6
8	31.3	3.8	−0.2	34.9	31.9
9	27.6	4.1	0.1	31.8	
10	83.3	−2.3	−1.3	79.7	
11	94.2	0.7	−0.1	94.8	
MAD	2.0			1.4	

Table 11.32 Energies relative to **1** calculated at DFT levels with the 6-311G(2d,2p) basis set, using MP2/6-31G(d,p) optimized geometries

Isomer	SVWN	BLYP	BPW91	B3LYP	B3PW91	Exp.
2	8.9	9.7	8.6	9.3	8.4	8.6
3	5.4	17.0	11.1	14.6	9.8	11.2
4	9.9	10.8	10.1	11.3	10.6	12.4
5	16.2	16.4	16.0	15.9	15.4	13.2
6	13.1	22.1	17.2	20.5	16.5	21.7
7	16.5	34.8	25.3	31.3	23.5	25.6
8	29.8	38.3	33.5	37.0	33.0	31.9
9	25.5	33.8	28.7	32.6	28.4	
10	81.0	84.2	80.6	82.0	79.1	
11	92.1	95.8	89.3	93.6	87.8	
MAD	4.5	4.0	1.7	2.8	2.0	

Table 11.33 Energies relative to **1** calculated by force field methods

Isomer	MM2	MM3	MMX	Exp.
2	10.9	10.6	11.3	8.6
3	12.8	12.6	11.5	11.2
4	13.6		12.6	12.4
5	14.6	14.6	14.9	13.2
6			21.7	21.7
7	26.7	27.0	23.9	25.6
8			33.9	31.9
9			31.8	
MAD	(1.5)	(1.6)	1.2	

分子力学（力場法）

$$E_{FF} = E_{str} + E_{bend} + E_{tors} + E_{vdw} + E_{el} + E_{cross} \quad (2.1)$$

E_{str} is the energy function for stretching a bond between two atoms, E_{bend} represents the energy required for bending an angle, E_{tors} is the torsional energy for rotation around a bond, E_{vdw} and E_{el} describe the non-bonded atom–atom interactions, and finally E_{cross} describes coupling between the first three terms.

Table 2.1 MM2(91) atom types

Type	Symbol	Description	Type	Symbol	Description
1	C	sp^3-carbon	28	H	enol or amide
2	C	sp^2-carbon, alkene	48	H	ammonium
3	C	sp^2-carbon, carbonyl, imine	36	D	deuterium
4	C	sp-carbon	20	lp	lone pair
22	C	cyclopropane	15	S	sulfide (R_2S)
29	C·	radical	16	S+	sulfonium (R_3S^+)
30	C+	carbocation	17	S	sulfoxide (R_2SO)
38	C	sp^2-carbon, cyclopropene	18	S	sulfone (R_2SO_2)
50	C	sp^2-carbon, aromatic	42	S	sp^2-sulfur, thiophene
56	C	sp^3-carbon, cyclobutane	11	F	fluoride
57	C	sp^2-carbon, cyclobutene	12	Cl	chloride
58	C	carbonyl, cyclobutanone	13	Br	bromide
67	C	carbonyl, cyclopropanone	14	I	iodide
68	C	carbonyl, ketene	26	B	boron, trigonal
71	C	ketonium carbon	27	B	boron, tetrahedral
8	N	sp^3-nitrogen	19	Si	silane
9	N	sp^2-nitrogen, amide	25	P	phosphine (R_3P)
10	N	sp-nitrogen	60	P	phosphor, pentavalent
37	N	azo or pyridine (–N=)	51	He	helium
39	N+	sp^3-nitrogen, ammonium (R_4N^+)	52	Ne	neon
40	N	sp^2-nitrogen, pyrrole	53	Ar	argon
43	N	azoxy (–N=N–O)	54	Kr	krypton
45	N	azide, central atom	55	Xe	xenon
46	N	nitro ($-NO_2$)	31	Ge	germanium
72	N	imine, oxime (=N–)	32	Sn	tin
6	O	sp^3-oxygen	33	Pb	lead (R_4Pb)
7	O	sp^2-oxygen, carbonyl	34	Se	selenium
41	O	sp^2-oxygen, furan	35	Te	tellurium
47	O^-	carboxylate	59	Mg	magnesium
49	O	epoxy	61	Fe	iron(II)
69	O	amine oxide	62	Fe	iron(III)
70	O	ketonium oxygen	63	Ni	nickel(II)
5	H	hydrogen, except on N or O	64	Ni	nickel(III)
21	H	alcohol (OH)	65	Co	cobalt (II)
23	H	amine (NH)	66	Co	cobalt (III)
24	H	carboxyl (COOH)			

Note that special atom types are defined for carbon atoms involved in small rings, like cyclopropane and cyclobutane. The reason for this will be discussed in Section 2.2.2.

伸縮エネルギー E_{str}

$$E_{str}(R^{AB} - R_0^{AB}) = E(0) + \frac{dE}{dR}(R^{AB} - R_0^{AB}) + \frac{1}{2}\frac{d^2E}{dR^2}(R^{AB} - R_0^{AB})^2 \quad (2.2)$$

平衡位置のまわりでは

$$E_{str}(R^{AB} - R_0^{AB}) = k^{AB}(R^{AB} - R_0^{AB})^2 = k^{AB}(\Delta R^{AB})^2 \quad (2.3)$$

where k^{AB} is the "force constant" for the A–B bond.

Morse関数

$$E_{Morse}(\Delta R) = D[1 - e^{\alpha \Delta R}]^2 \quad (2.5)$$

Here D is the dissociation energy and α is related to the force constant ($\alpha = \sqrt{k/2D}$).

4次までの展開

$$E_{str}(\Delta R^{AB}) = k^{AB}(\Delta R^{AB})^2[1 - \alpha(\Delta R^{AB}) + \tfrac{7}{12}\alpha^2(\Delta R^{AB})^2] \quad (2.6)$$

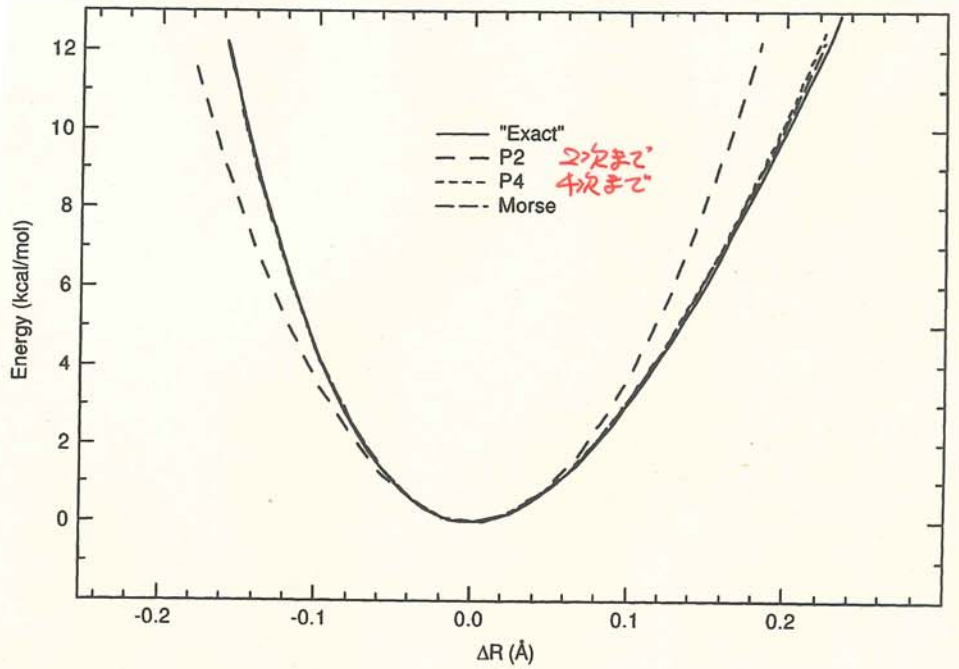

Figure 2.2 The stretch energy for CH_4

変角エネルギー E_{bend}

$$E_{\text{bend}}(\theta^{\text{ABC}} - \theta_0^{\text{ABC}}) = k^{\text{ABC}}(\theta^{\text{ABC}} - \theta_0^{\text{ABC}})^2 \qquad (2.7)$$

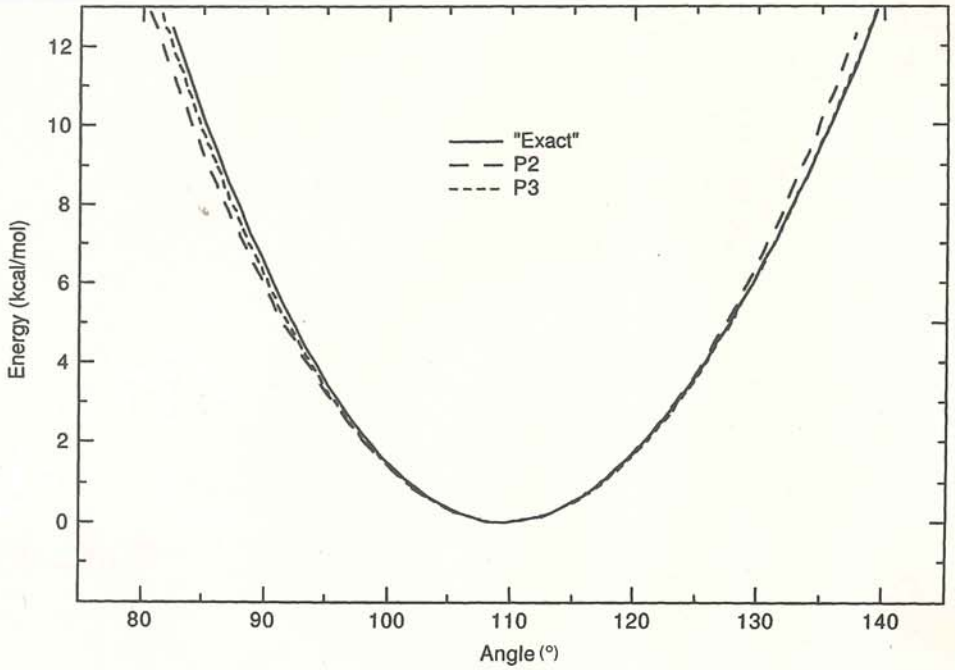

Figure 2.4 The bending energy for CH_4

面外変角エネルギー E_{oop}

$$E_{\text{oop}}(\chi^{\text{B}}) = k^{\text{B}}(\chi^{\text{B}})^2 \quad \text{or} \quad E_{\text{oop}}(d) = k^{\text{B}}d^2 \qquad (2.8)$$

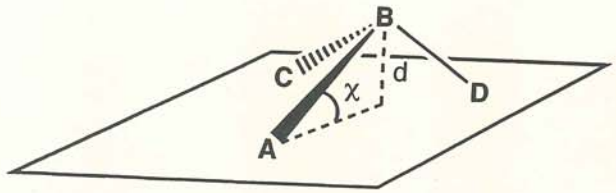

Figure 2.6 Out-of-plane variable definitions

捩れ角エネルギー

$$E_{\text{tors}}(\omega) = \sum_{n=1} V_n \cos(n\omega) \qquad (2.9)$$

$$\begin{aligned} E_{\text{tors}}(\omega^{\text{ABCD}}) = {} & \tfrac{1}{2}V_1^{\text{ABCD}}[1 + \cos(\omega^{\text{ABCD}})] \\ & + \tfrac{1}{2}V_2^{\text{ABCD}}[1 - \cos(2\omega^{\text{ABCD}})] \\ & + \tfrac{1}{2}V_3^{\text{ABCD}}[1 + \cos(3\omega^{\text{ABCD}})] \end{aligned} \qquad (2.10)$$

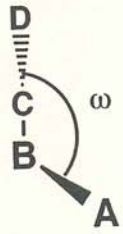

Figure 2.7 Torsional angle definition

ファンデルワールスエネルギー

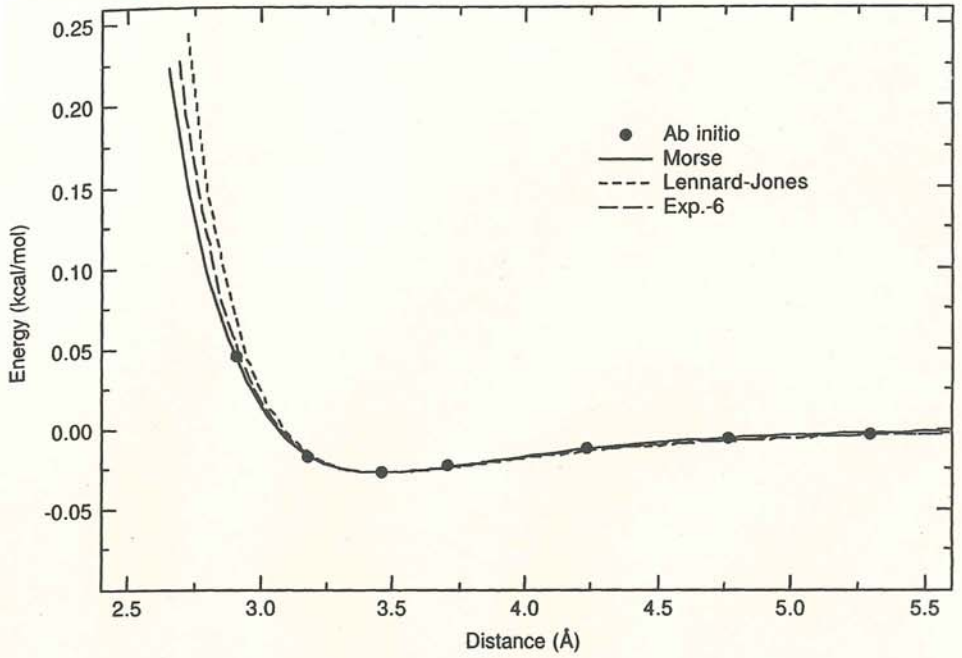

Figure 2.10 Comparison of E_{vdw} functionals for the attractive part of the H_2–He potential

ファンデルワールスエネルギー（続き）

$$E_{\text{vdw}}(R^{\text{AB}}) = E_{\text{repulsive}}(R^{\text{AB}}) - \frac{C^{\text{AB}}}{(R^{\text{AB}})^6} \tag{2.11}$$

$$E_{\text{vdw}}(R) = \varepsilon\left[\frac{6}{\alpha-6}e^{\alpha(1-R/R_0)} - \frac{\alpha}{\alpha-6}\left(\frac{R_0}{R}\right)^6\right] \tag{2.15}$$

where R_0 and ε have been defined in eq. (2.13), and α is a free parameter.

$$E_{\text{LJ}}(R) = \varepsilon\left[\left(\frac{R_0}{R}\right)^{12} - 2\left(\frac{R_0}{R}\right)^6\right] \tag{2.13}$$

where R_0 is the minimum energy distance and ε the dept of the minimum.

$$R_0^{\text{AB}} = R_0^{\text{A}} + R_0^{\text{B}}$$
$$\varepsilon^{\text{AB}} = \sqrt{\varepsilon^{\text{A}}\varepsilon^{\text{B}}} \tag{2.17}$$

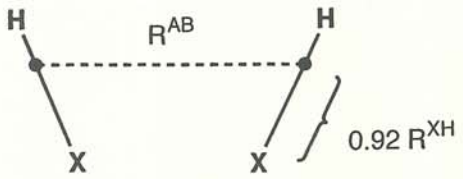

Figure 2.11 Illustration of the distance reduction which can be used for E_{vdw} involving hydrogens

$$E_{\text{H-bond}}(R) = \varepsilon\left[5\left(\frac{R_0}{R}\right)^{12} - 6\left(\frac{R_0}{R}\right)^{10}\right] \tag{2.18}$$

静電エネルギー Eel

$$E_{\text{el}}(R^{\text{AB}}) = \frac{Q^{\text{A}}Q^{\text{B}}}{\varepsilon R^{\text{AB}}} \tag{2.19}$$

交差項

$$E_{\text{str/bend}} = k^{\text{ABC}}(\theta^{\text{ABC}} - \theta_0^{\text{ABC}})[(R^{\text{AB}} - R_0^{\text{AB}}) + (R^{\text{BC}} - R_0^{\text{BC}})] \tag{2.21}$$

Other examples of such cross terms are

$$\begin{aligned}
E_{\text{str/str}} &= k^{\text{ABC}}(R^{\text{AB}} - R_0^{\text{AB}})(R^{\text{BC}} - R_0^{\text{BC}}) \\
E_{\text{bend/bend}} &= k^{\text{ABCD}}(\theta^{\text{ABC}} - \theta_0^{\text{ABC}})(\theta^{\text{BCD}} - \theta_0^{\text{BCD}}) \\
E_{\text{str/tors}} &= k^{\text{ABCD}}(R^{\text{AB}} - R_0^{\text{AB}})\cos(n\omega^{\text{ABCD}}) \\
E_{\text{bend/tors}} &= k^{\text{ABCD}}(\theta^{\text{ABC}} - \theta_0^{\text{ABC}})\cos(n\omega^{\text{ABCD}}) \\
E_{\text{bend/tors/bend}} &= k^{\text{ABCD}}(\theta^{\text{ABC}} - \theta_0^{\text{ABC}})(\theta^{\text{BCD}} - \theta_0^{\text{BCD}})\cos(n\omega^{\text{ABCD}})
\end{aligned} \tag{2.22}$$

共役系

$$\begin{aligned}
\rho_{\text{AB}} &= \sum_i^{\text{MO}} n_i c_{\text{A}i} c_{\text{B}i} \\
R_0^{\text{AB}} &= 1.503 - 0.166\rho_{\text{AB}} \\
k^{\text{AB}} &= 5.0 + 4.6\rho_{\text{AB}} \\
V_2^{\text{ABCD}} &= 15.0\rho_{\text{BC}}\beta_{\text{BC}}
\end{aligned} \tag{2.24}$$

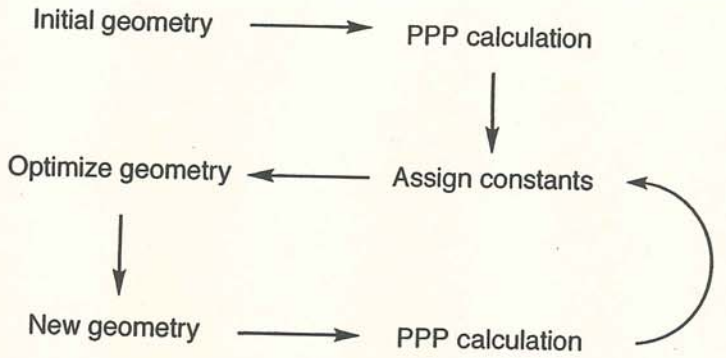

Figure 2.13 Illustration of the two-level optimization involved in a MMP2 calculation

使われているさまざまな力場

44

Table 2.3 Comparison of functional forms used in common force fields. The torsional energy, E_{tors}, is in all cases given as a Fourier series in the torsional angle

Force Field	Types	E_{str}	E_{bend}	E_{oop}	E_{vdw}	E_{el}	E_{cross}	Molecules
EAS	2	P2	P3	none	Exp.–6	none	none	alkanes
EFF	2	P4	P3	none	Exp.–6.	none	ss,bb,sb, st,btb	alkanes
MM2	71	P3	P2+6	P2	Exp.–6	dipole	sb	general
MM3	153	P4	P6	P2	Exp.–6	dipole or charge	sb,bb,st	general (all elements)
MM4	3	P6	P6	imp.	Exp.–6	charge	ss,bb,sb, tt,st,tb,btb	hydrocarbons
CVFF	53	P2 or Morse	P2	P2	6–12	charge	ss,bb,sb, btb	general
CFF 91/93/95	48	P4	P4	P2	6–9	charge	ss,bb,st, sb,bt,btb	general
TRIPOS	31	P2	P2	P2	6–12	charge	none	general
MMFF	99	P4	P3	P2	7–14	charge	sb	general
COSMIC	25	P2	P2		Morse	charge	none	general
DREIDING	37	P2 or Morse	P2(cos)	P2(cos)	6–12 or Exp.–6	charge	none	general
AMBER	41	P2	P2	imp.	6–12 10–12	charge	none	proteins, nucleic acids, carbohydrates
OPLS	41	P2	P2	imp.	6–12	charge	none	proteins, nucleic acids, carbohydrates
CHARMM	29	P2	P2	imp.	6–12	charge	none	proteins
GROMOS		P2	P2	P2(imp.)	6–12	charge	none	proteins, nucleic acids, carbohydrates
ECEPP		fixed	fixed	fixed	6–12 10–12	charge	none	proteins
MOMEC		P2	P2	P2	Exp.–6	none	none	metal coordination
SHAPES		P2	cos($n\theta$)	imp.	6–12	charge	none	metal coordination
ESFF	97	Morse	P2(cos)	P2	6–9	charge	none	all elements
UFF	126	P2 or Morse	cos($n\theta$)	imp.	6–12	charge	none	all elements

Notation: Pn: Polynomial of order n; Pn(cos): polynomial of order n in cosine to the angle; cos($n\theta$): Fourier term(s) in cosine to the angle; Exp.–6: exponential $+R^{-6}$; n–m: $R^{-n}+R^{-m}$; fixed: not a variable; imp.: improper torsional angle; ss: stretch–stretch; bb: bend–bend; sb: stretch–bend; st: stretch–torsional; bt: bend–torsional; tt: torsional–torsional; btb: bend–torsional–bend.

(*continued*)

EAS: E. M. Engler, J. D. Andose and P. v. R. Schleyer, *J. Am. Chem. Soc.*, **95** (1973), 8005; EFF: J. L. M. Dillen and *J. Comput. Chem.*, **16** (1995), 595, 610; MM2: N. L. Allinger, *J. Am. Chem. Soc.*, **99** (1977), 8127; MM3: N. L. Allinger, Y. H. Yuh and J. H. Lii, *J. Am. Chem. Soc.*, **111** (1989), 8551; J. H. Lii and N. L. Allinger, *J. Am. Chem. Soc.*, **111** (1989), 8566, 8576; "all elements" MM3: N. L. Allinger, X. Zhou and J. Bergsma, *J. Mol. Struct. Theochem.*, **312** (1994), 69; MM4: N. L. Allinger, K. Chen and J.-H. Lii, *J. Comput. Chem.*, **17** (1996), 642; N. Nevins, K. Chen and N. L. Allinger, *J. Comput. Chem.*, **17** (1996), 669; N. Nevins, J.-H. Lii and N. L. Allinger, *J. Comput. Chem.*, **17** (1996), 695; N. L. Allinger, K. Chen, J. A. Katzenellenbogen, S. R. Wilson and G. M. Anstead, *J. Comput. Chem.*, **17** (1996,) 747; CVFF: S. Lifson, A. T. Hagler and P. Dauber, *J. Am. Chem. Soc.*, **101** (1979), 5111, 5122, 5131; CFF91/93/95: M. J. Hwang, J. P. Stockfisch and A. T. Hagler, *J. Am. Chem. Soc.*, **116** (1994), 2515; TRIPOS: M. Clark, R. D. Cramer III and N. van Opdenbosch, *J. Comput. Chem.*, **10** (1989), 982; J. R. Maple, M.-J. Hwang, T. P. Stockfisch, U. Dinur, M. Waldman, C. S. Ewig and A. T. Hagler, *J. Comput. Chem.*, **15** (1994), 162; MMFF: T. A. Halgren, *J. Comput. Chem.*, **17** (1996), 490; COSMIC: S. D. Morley, R. J. Abraham, I. S. Haworth, D. E. Jackson, M. R. Saunders and J. G. Vinter, *J. Computu.-Aided Mol. Des.*, **5** (1991), 475; DREIDING: S. L. Mayo, B. D. Olafson and W. A. Goddard III, *J. Phys. Chem.*, **94** (1990), 8897; AMBER: W. D. Cornell, P. Cieplak, C. I. Bayly, I. R. Gould, K. M. Merz Jr, D. M. Ferguson, D. C. Spellmeyer, T. Fox, J. W. Caldwell and P. A. Kollman, *J. Am. Chem. Soc.*, **117** (1995), 5179; OPLS: W. Damm, A. Frontera, J. Tirado-Rives and W. L. Jorgensen, *J. Comput Chem.*, **18**, (1997), 1995; CHARMM: R. Brooks, R. E. Bruccoleri, B. D. Olafson, D. J. States, S. Swaminathan and M. Karplus, *J. Comput. Chem.* **4** (1983), 187; GROMOS: W. F. Van Gunsterenm and H. J. C. Berendsen, Groningen Molecular Simulation (GROMOS) library manual; ECEPP: G. Nemethy, K. D. Gibsen, K. A. Palmer, C. N. Yoon, G. Paterlini, A. Zagari, S. Rumsey and H. A. Sheraga, *J. Phys. Chem.*, **96** (1992) 6472; MOMEC: P. Comba and T. W. Hambley, *Molecular Modeling of Inorganic Compounds*, VCH, 1995; SHAPES: V. S. Allured, C. M. Kelly and C. R. Landis, *J. Am. Chem. Soc.*, **113** (1991), 1; ESFF: S. Barlow, A. L. Rohl, S. Shi, C. M. Freeman and D. O'Hare, *J. Am. Chem. Soc.*, **118** (1996), 7578; UFF: A. K. Rappé, C. J. Casewit, K. S. Colwell, W. A. Goddard III and W. M. Skiff, *J. Am. Chem. Soc.*, **114** (1992), 10024; C. J. Casewit, K. S. Colwell and A. K. Rappé, *J. Am. Chem. Soc.*, **114** (1992), 10035, 10046.

Table 2.6 Average errors in heat of formations (kcal/mol) by MM2

Compound type	Average error in ΔH_f
Hydrocarbons	0.42
Ethers and Alcohols	0.50
Carbonyl compounds	0.81
Aliphatic amines	0.46
Aromatic amines	2.90
Silanes	1.08

Table 2.6 is sourced from ref. 32.

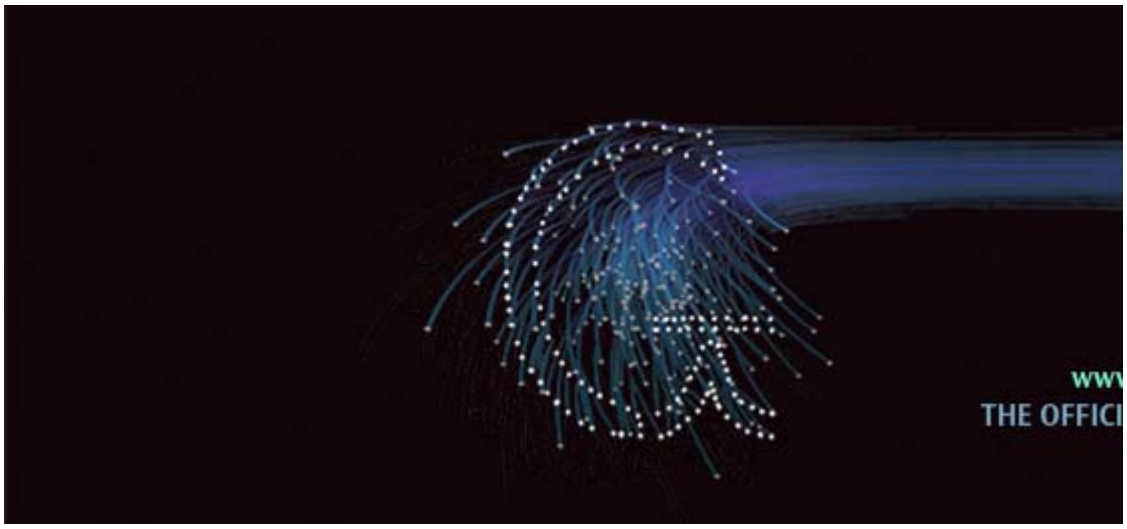

Gaussian 09 Features at a Glance

Features added since the initial release of Gaussian 03 are in scarlet.

Each section lists all relevant features; there is sometimes overlap between sections.

Fundamental Algorithms

- Calculation of 1- & 2-electron integrals over any contracted gaussian functions
- Conventional, direct, semi-direct and in-core algorithms
- Linearized computational cost via automated fast multipole methods (FMM) and sparse matrix tec
- Network/cluster and shared memory (SMP) parallelism
- Harris initial guess (much more accurate, especially for metals)
- Initial guess generated from fragment guesses or fragment SCF solutions
- Density fitting and Coulomb engine for pure DFT calculations, including automated generation of
- O(N) exact exchange for HF and hybrid DFT
- 1D, 2D, 3D periodic boundary conditions (PBC) energies & gradients (HF & DFT)

Model Chemistries

Molecular Mechanics: Amber, DREIDING and UFF energies, gradients, and frequencies; standalone MI

Ground State Semi-Empirical

- CNDO/2, INDO, MINDO3 and MNDO energies and gradients
- Newly implemented AM1, PM3, PM3MM, PM6 and PDDG energies, gradients and analytic freqs.,
- DFTB and DFTBA methods

Self Consistent Field (SCF)

- SCF restricted and unrestricted energies, gradients and frequencies, and RO energies and gradie
- Default EDIIS+CDIIS convergence algorithm and optional Quadratic Convergent SCF
- Complete Active Space SCF (CASSCF) energies, gradients & frequencies; active spaces of up to
- Restricted Active Space SCF (RASSCF) energies and gradients
- Generalized Valence Bond-Perfect Pairing energies and gradients
- Wavefunction stability analysis (HF & DFT)

Density Functional Theory

Closed shell and open shell energies, gradients & frequencies, and RO energies & gradients are availabl

- **EXCHANGE FUNCTIONALS**: Slater, Xa, Becke 88, Perdew-Wang 91, Barone-modified PW91, Gill 96
- **CORRELATION FUNCTIONALS**: VWN, VWN5, LYP, Perdew 81, Perdew 86, Perdew-Wang 91, PBE,
- **OTHER PURE FUNCTIONALS**: VSXC, HCTH functional family

- **HYBRID METHODS**: B3LYP, B3P86, P3PW91, B1 and variations, B98, B97-1, B97-2, PBE1PBE, H
  M05 & M06 and variations, X3LYP; user-configurable hybrid methods
- **EMPIRICAL DISPERSION**: B97D
- **LONG RANGE-CORRECTED**: LC-wPBE, CAM-B3LYP, WB97XD and variations, Hirao's general LC c

Electron Correlation:

*All methods/job types are available for both closed and open shell systems and may optionally use frozer
are available for MP2, MP3, MP4 and CCSD/CCSD(T) energies.*

- MP2 energies, gradients, and frequencies
- B2PLYP and MPW2PLYP double hybrid DFT energies, gradients and frequencies, with optional e
- CASSCF calculations with MP2 correlation for any specified set of states
- MP3 and MP4(SDQ) energies and gradients
- MP4(SDTQ) and MP5 energies
- Configuration Interaction (CISD) energies & gradients
- Quadratic CI energies & gradients; QCISD(TQ) energies
- Coupled Cluster methods: restartable CCD, CCSD energies & gradients, CCSD(T) energies; optic
  basis set
- Brueckner Doubles (BD) energies and gradients, BD(T) energies; optionally input amplitudes & or
- Enhanced Outer Valence Green's Function (OVGF) methods for ionization potentials & electron a
- Complete Basis Set (CBS) MP2 Extrapolation
- Douglas-Kroll-Hess scalar relativistic Hamiltonians

Automated High Accuracy Energies

- G1, G2, G3, G4 and variations
- CBS-4, CBS-q, CBS-QB3, ROCBS-QB3, CBS-Q, CBS-APNO
- W1U, W1BD, W1RO

Basis Sets and DFT Fitting Sets

- STO-3G, 3-21G, ..., 6-31G, 6-31G†, 6-311G, D95, D95V, SHC, LanL2DZ, cc-pV{D,T,Q,5,6}Z, Dc
  III, Midi!, UGBS*, MTSmall, DG{D,T}ZVP
- Effective Core Potentials (through second derivatives): LanL2DZ, CEP through Rn, Stuttgart/Dres
- Support for basis functions and ECPs of arbitrary angular momentum
- **DFT FITTING SETS**: DGA1, DGA1, W06; auto-generated fitting sets; optional default enabling of der

Geometry Optimizations and Reaction Modeling

- Geometry optimizations for equilibrium structures, transition structures, and higher saddle points,
  Cartesian, or mixed internal and Cartesian coordinates
- Redundant internal coordinate algorithm designed for large system, semi-empirical optimizations
- Newton-Raphson and Synchronous Transit-Guided Quasi-Newton (QST2/3) methods for locating
- IRCMax transition structure searches
- Relaxed and unrelaxed potential energy surface scans
- New implementation of intrinsic reaction path following (IRC), applicable to ONIOM QM:MM with t
- Reaction path optimization
- BOMD molecular dynamics (all analytic gradient methods); ADMP molecular dynamics: HF, DFT,
- Optimization of conical intersections via state-averaged CASSCF

Vibrational Analysis

- Vibrational frequencies and normal modes, including display/output limiting to specified atoms/res
- Restartable analytic HF and DFT freqs.
- MO:MM ONIOM frequencies including electronic embedding
- Analytic Infrared and static and dynamic Raman intensities (HF & DFT; MP2 for IR)
- Pre-resonance Raman spectra (HF and DFT)
- Projected frequencies perpendicular to a reaction path
- NMR shielding tensors & GIAO magnetic susceptibilities (HF, DFT, MP2) and enhanced spin-spin
- Vibrational circular dichroism (VCD) rotational strengths (HF and DFT)
- Dynamic Raman Optical Activity (ROA) intensities
- Harmonic vibration-rotation coupling
- Enhanced anharmonic vibrational analysis
- Anharmonic vibration-rotation coupling via perturbation theory
- Hindered rotor analysis

Molecular Properties

- Electronic circular dichroism (ECD) rotational strengths (HF and DFT)
- Electrostatic potential, electron density, density gradient, Laplacian, and magnetic shielding & indu generated grid
- Multipole moments through hexadecapole
- Population analysis, including per-orbital analysis for specified orbitals
- Biorthogonalization of molecular orbitals (producing corresponding orbitals)
- Electrostatic potential-derived charges
- Natural orbital analysis and natural transition orbitals
- Natural Bond Orbital (NBO) analysis, including orbitals for CAS jobs
- Electrostatic energy & Fermi contact terms
- Static and frequency-dependent analytic polarizabilities and hyperpolarizabilities (HF and DFT); n analytic 3rd derivs.)
- Approx. CAS spin orbit coupling between states
- Enhanced optical rotations and optical rotary dispersion (ORD)
- Hyperfine spectra components: electronic g tensors, Fermi contact terms, anisotropic Fermi conta terms, quartic centrifugal distortion, electronic spin rotation tensors, nuclear electric quadrupole co
- Franck-Condon analysis (photoionization)
- ONIOM integration of electric and magnetic properties

ONIOM Calculations

- Enhanced 2 and 3 layer ONIOM energies, gradients and frequencies using any available method
- Optional electronic embedding for MO:MM energies, gradients and frequencies
- Enhanced MO:MM ONIOM optimizations to minima and transition structures via microiterations in
- Support for IRC calculations
- ONIOM integration of electric and magnetic properties

Excited States

- ZINDO energies
- CI-Singles energies, gradients, & freqs.
- Restartable time-dep. HF & DFT energies and gradients
- SAC-CI energies and gradients
- EOM-CCSD energies (restartable); optionally input amplitudes computed with a smaller basis set
- Franck-Condon, Herzberg-Teller and FCHT analyses
- CI-Singles and TD-DFT in solution
- State-specific excitations and de-excitations in solution

Self-Consistent Reaction Field Solvation Models

- New implementation of the Polarized Continuum Model (PCM) facility for energies, gradients and
- Solvent effects on vibrational spectra, NMR, and other properties
- Solvent effects for ADMP trajectory calcs.
- Solvent effects for ONIOM calculations
- Enhanced solvent effects for excited states
- SMD model for ΔG of solvation
- Other SCRF solvent models (HF & DFT): Onsager energies, gradients and freqs., Isodensity Surf Isodensity Surface PCM (SCI-PCM) energies and gradients

Ease-of-Use Features

- Automated counterpoise calculations
- Automated optimization followed by frequency or single point energy
- Ability to easily add, remove, freeze, differentiate redundant internal coords.
- Simplified isotope substitution and temperature/pressure specification in the route section
- Freezing by fragment for ONIOM optimizations
- Simplified fragment definitions on molecule specifications
- Many more restartable job types
- Atom freezing in optimizations by type, fragment, ONIOM layer and/or residue
- QST2/QST3 automated transition structure optimizations
- Saving and reading normal modes

Last update: 13 May 2010

1. 適当なコマンドを使って *Gaussian* の環境を設定する。

プログラムを実行する前に、*Gaussian* の中に入っている初期化ファイルをまず実行する必要がある。このファイルは、プログラムに必要な環境の変数値（UNIX）や論理名（VMS）を設定する。通例、このファイルはユーザーの初期化ファイル（.login、.profile、や LOGIN.COM など）の中で実行されるが、もちろん、コマンドをタイプして行ってもよい。

下記のコマンドを用いて、*Gaussian 94* を実行する。†

UNIX: C シェル
```
% setenv g94root ディレクトリ名
% source $g94root/g94/bsd/g94.login
```

UNIX: Bourne シェル
```
$ g94root=ディレクトリ名 ; export g94root
$ . $g94root/g94/bsd/g94.profile
```

VMS
```
$ @ディスク名:[G94.VMS.EDT]G94Login.Com
```

UNIX ユーザーは、システム上で *Gaussian 94* のツリーの場所を指定する。VMS ユーザーは、[G94] ディレクトリの入っているディスクの場所を与える。

もしこれらのコマンドが、ユーザーの初期化ファイルにない場合は、今加えるとよいだろう。VMS ユーザーは、ワークセットを最大に設定するために LOGIN.COM に次のような行を挿入することをお薦めする。

```
$ Set Work/NoAdjust/Quota=65536/Limit=65536
```

次に、水分子のエネルギー計算のための *Gaussian* インプットファイルの作成について説明する。

2. テキストエディターをスタートし、下の行を新しいファイルにタイプする。

UNIX
```
#T RHF/6-31G(d) Test
```

VMS
```
$ RunGauss
#T RHF/6-31G(d) Test
```

† ほとんどの場合、Gaussian 98 では、これらのコマンドを "4" の代わりに、"8" を使って実行できる。

VMS ユーザーは、*Gaussian* を実行するためのコマンドを使って入力を始める。UNIX ユーザーは、UNIX コマンドの標準インプットのところに *Gaussian* のインプットファイルを入れる。

で始まる行は、このジョブのルートセクションである。ルートセクションの最初の行の始めのカラムは、 常にこのシャープサイン（#）で始まる（UNIX ユーザーへ：これはコメントのマーカーではない）。#T は、簡略化されたアウトプットが欲しいとき（最低限必要な結果）に用いる。 # だけであると通常の *Gaussian* のアウトプット、また #P は、より詳細なアウトプットを与えるためのもの。

ルートセクションは、計算の操作と基底系を指定するところである。

キーワード	意味
RHF	制限されたHartree-Fock（*制限*されたというのは、取り扱う分子が不対電子を持たないという意味）
6-31G(d)	6-31G(d) の基底系を用いる（便利でかつよく用いられる基底系）

つまり、ここでは制限された(R) Hartree-Fock (HF) 計算を、6-31G(d) (6-31G(d)) の基底系で計算せよと指定したことになる。

すべてのルートセクションは、操作キーワードと基底系キーワードを含まなければならない。他のキーワードは、計算の種類や種々のオプションを指定する。

ここでは，一つだけ他のキーワード Test を含めた。これは、この計算がテスト計算であり、その結果は、*Gaussian* のアーカイブに入るものではないという意味である（ユーザーのサイトで用いられている場合）。

3. 次に、空行を一行入れて、計算のコメントを一行入れる。

そうすると、インプットファイルは次のようになる。

```
#T RHF/6-31G(d) Test

My first Gaussian job: water single point energy
```

この行は、ジョブのための*タイトルセクション*になり、アウトプットに現われる計算の説明とアーカイブのエントリーとなる。それ以外では、プログラムによって用いられることはない。

4. タイトルの後、空行をもう一つ入れ、以下の四行をタイプする。

```
0  1
O -0.464   0.177   0.0
H -0.464   1.137   0.0
H  0.441  -0.143   0.0
```

これは、*分子指定セクション*に相当する。これは、水分子の場合である。 最初の行に、分子の電荷とスピン多重度を自由形式でタイプする。この場合、分子は中性（電荷０）、スピン多重度は１（一重項）である。スピン多重度は、第二章で詳しく説明されており、分子指定についての一般的な議論は、付録Ｂに与えられている。

残りの三行には、元素のタイプと分子中原子のカーテシアン (x,y,z) 座標を指定する。

5. 最後に、もう一度空行を一行入れて インプットを終える。

最終的なインプットファイルは、以下のようになる。

演習 QS.1: 水分子のシングルポイントエネルギー
ファイル : qs.com

```
#T RHF/6-31G(d) Test

My first Gaussian job: water single point energy

0 1
O -0.464   0.177   0.0
H -0.464   1.137   0.0
H  0.441  -0.143   0.0
```

VMS ユーザーは、RunGauss コマンドをこのインプットの頭に置くこと。

6. このファイルを、h2o.com としてセーブし、エディターを終了する。

このインプットでは、どのような計算をするのか指定していない。何も指定しないと、*Gaussian* はエネルギー計算を行う。今の場合は、エネルギー計算がこのインプットの目的である。

さて、これで本計算の準備ができた。

7. 適当なコマンドを用いて、この *Gaussian* ジョブを実行する。

UNIX
```
% g94 <h2o.com >& h2o.log          C シェル
$ g94 <h2o.com 2>&1 >h2o.log      Bourne シェル
```

VMS
```
$ @H2O.Com/Output=H2O.Log
```


このジョブは、簡単に終わるもので、以下のようなコマンドを用いてバックグランドでジョブを流してもよい。

UNIX
```
% g94 <h2o.com >& h2o.log &          C シェル
$ g94 <h2o.com 2>&1 >h2o.log &      Bourne シェル
```

VMS
```
$ Spawn/NoWait/Notify/In=H2O.Com/Out=H2O.Log
```

このジョブのアウトプットは、h2o.log というファイルにセーブされる。後でこのアウトプットをより詳しく見ることになるが、ここで簡単に見ておくことにする。

8. 端末のスクリーン上にログファイルの内容を表示してみる。

一旦すべての内容を見た後、ジョブが問題なく終了したことを確認する。これは、ファイルの最後にある次のような行でわかる。

```
Normal termination of Gaussian 94.
```

CPU 時間などの計算機使用量に関する情報もここに含まれている。

次に、先程のインプットによる計算の結果、つまり系のエネルギーを見ることにする。

9. アウトプットファイル中で “SCF Done” という部分を探してみる .

適当な探索コマンドを用いて探すと、次のような行が出てくる。

```
SCF Done: E(RHF) = -76.0098706218 A.U. after  6 cycles
```

これは、系のエネルギーは Hartree-Fock のレベルで -76.00987hartree であることを示す。

グラフィックプログラムからの分子構造の変換

分子指定は、タイプしてもいいし、またグラフィックプログラムからも変換できる。ここでは、Brookhaven Protein Data Bank (PDB) のフォーマットでセーブされた水分子を変換する簡単な例を示そう。 サブディレクトリの quick の下にある water.pdb というファイルに、水分子の PDB フォーマットの構造が入っている。

演習 QS.2: PDB ファイルの変換

ファイル : water.pdb

種々のファイル間の変換をするために NewZMat という機能が *Gaussian* に備わっている。ここでは、この水分子の PDB ファイルを *Gaussian* のインプットファイルに変換するために用いることにする。

10. 次の NewZMat コマンドを実行する。

UNIX

```
% newzmat -ipdb $g94root/g94/tutor/quick/water.pdb water.com
```

VMS

```
$ NewZMat -IPDB ディスク名:[G94.Tutor.Quick]Water.PDB []Water.Com
```

このコマンドにより、新しい *Gaussian* インプットファイルが作られる。NewZMat は、電荷と多重度を聞いてくることがあるが、デフォルトの値 (0,1) をここでは用いる。

11. 新しいインプットファイルをエディットする。

NewZMat は、6-31G(d) 基底系を用いた Hartree-Fock 計算を設定するようにできている。作られたファイルの分子指定は、カーテシアンではなく、Z マトリックスになっている。このファイルをエディットして、計算方法や Z マトリックス、それに基底系を指定する。このジョブは、上と同じ計算なのでここでは繰り返さない。

バッチプロセス

上では水分子の計算を対話的に直接行ったが、一人以上のユーザーで計算機を共有しバッチ計算のできる環境では、バッチで *Gaussian* の計算を行うことをお薦めする。スーパーコンピューターセンターのような所では、バッチプロセスだけが唯一の実行方法である。VMS のユーザーは `Submit` コマンドを用いてバッチジョブとして water.com を実行するとよいだろう。NQS バッチをサポートしている UNIX 上では、*Gaussian 94* に入っている **subg94** コマンドを用いるとよい。ここに例を示す。

```
% subg94 キュー名 h2o.com
```

キュー名はバッチキューの名前。ジョブのアウトプットは自動的に water.log というファイルにセーブされる。UNIX 上では、*Gaussian* ジョブは **nice** コマンドを用いて、低いプライオリティのバックグランドで実行することもできる。

```
% nice g94 <h2o.com >h2o.log &
```

これで、UNIX と VMS に関するチュートリアルの部分を終える。読者はさらに *Gaussian* を学習するために、ページ liii へお進み願いたい。そこでは *Gaussian* のアウトプットが説明してある。

ウインドウズ版のためのチュートリアル

ここでは、読者がウインドウズ上での操作の知識を持っており、読者の PC に既に *Gaussian* をインストールし、ウインドウズに慣れているものとする。

Gaussian の計算のステップは次のようなものである。

- プログラムのスタート。
- *Gaussian* インプットのロード或いはタイプ。
- ジョブの実行開始。
- アウトプットのチェックと解釈。

1. プログラムをスタートする。

Gaussian 94W

メインのプログラムウインドウがオープンする。

2. スクリーンのウインドウ中で、下に示してあるような箇所を探す。

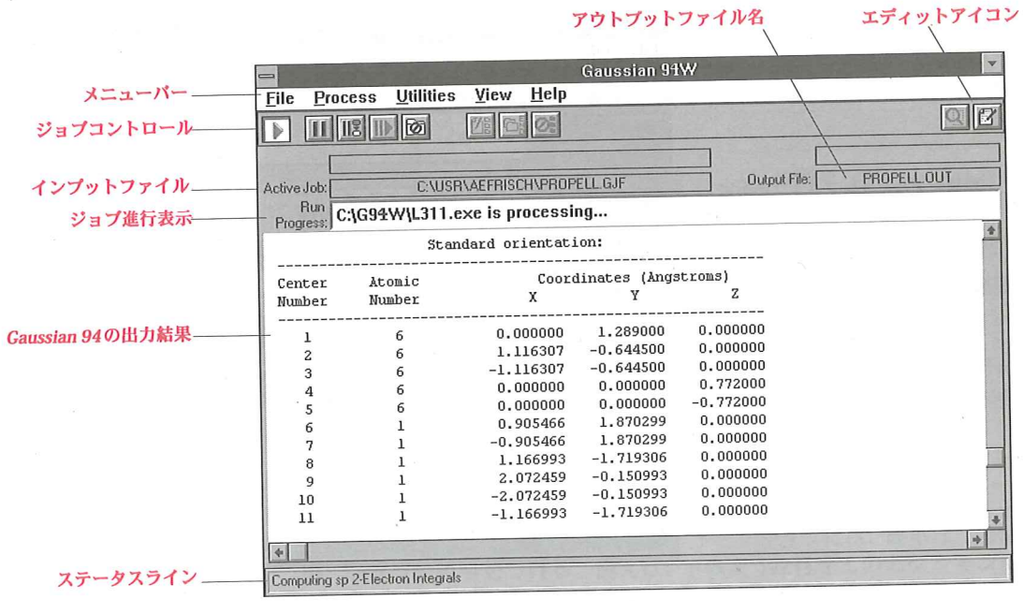

これらの項目を順を追って説明する。

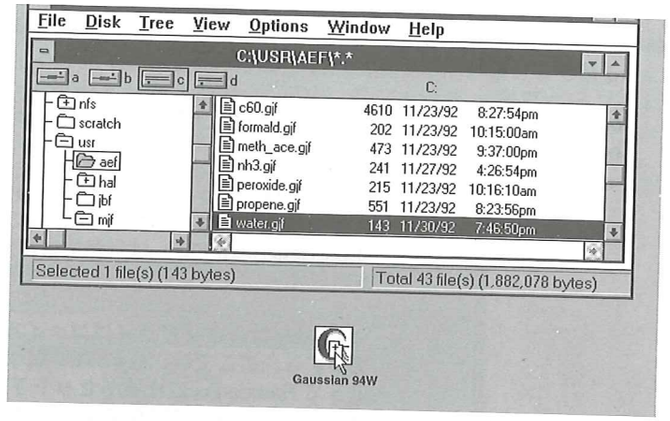

✦ マウスボタンを離すとジョブがロードされる。

もし **Run Dropped Files** の preference が設定されていると、ジョブはドロップされるとすぐに実行が開始される。

20. このテクニックを先にセーブした Water.GJF インプットファイルに用いてみる。

Gaussian のアウトプットの見方を扱う次の節で、このセットアップを用いるので、プログラムをオープンしたまま、ジョブが完了するのを待つ。

Gaussian は、バッチプロセスの機能も持ち合わせている。詳しくは、*Gaussian 94W Reference* の資料を参照のこと。

これで、ウインドウズ用のチュートリアルを終える。次の節では *Gaussian* を引き続き学習していく意味で、そのアウトプットを詳しく見てみよう。

Gaussian アウトプットのクイックツアー

Edit Output File アイコン

この節では、エディターを使って、上で行った水分子のシングルポイントエネルギー計算のアウトプットを詳しく見ていくことにする。UNIX と VMS のユーザーは、エディターを使って h2o.log のファイルをオープンする。*Gaussian* のユーザーは、どんなエディターを使ってもいいが、メインプログラムの右上にある**Edit Output File** のアイコンをクリックして、アウトプットをオープンすることもできる。† このアイコンは、*Gaussian* のジョブが終了した後アクティブになる。

演習 QS.3: Gaussian アウトプットのサンプル

このアウトプットの主な特徴を見て行くことにする。読者はエディターで相当するところを探しながら、欄外にあるそれぞれのコメントを読んでもらいたい。アウトプットの結果が、システムによって少し違うかも知れないが、大きな差ではない。最後の桁の数値が違っていることもあり得るが、その違いは少数点五桁以下のものである。これで、*Gaussian* の簡単なチュートリアルを終える。読者は、これで *Gaussian* が提供する種々のモデル化学を学ぶ準備ができたことになる。

これは *Gaussian* の著作権に関するものである。これが出てくると、プログラムの実行が始まったことがわかる。

```
Entering Gaussian System, Link 0=g94
Input=h2o.com
Output=h2o.log
Initial command:
/mf/g94/l1.exe /scratch/g94-17042.inp -scrdir=/scratch/
Entering Link 1 = /mf/g94/l1.exe PID=     18580.

      Copyright (c) 1988,1990,1992,1993,1995 Gaussian, Inc.
                    All Rights Reserved.

This is part of the Gaussian 94(TM) system of programs. It is
based on the Gaussian 92(TM) system (copyright 1992
Gaussian, Inc.), the Gaussian 90(TM) system (copyright 1990
Gaussian, Inc.), the Gaussian 88(TM) system (copyright 1988
Gaussian, Inc.), the Gaussian 86(TM) system (copyright 1986
Carnegie Mellon University), and the Gaussian 82(TM) system
(copyright 1983 Carnegie Mellon University). Gaussian is a
federally registered trademark of Gaussian, Inc.

This software is provided under written license and may be
used, copied, transmitted, or stored only in accord with that
written license.

...
```

† このエディターは、そのアイコンをクリックするとノートパッドで始まるようになっているが、Preferences ウインドウにある ASCII Editor を用いて、どんなエディターを使ってもよい。File メニューから Preferences を選択すると、Gaussian 94W Preferences のウインドウになる。ノートパッドを含めた他のエディターには長さの制限があり、*Gaussian* のアウトプットが入り切れない場合もあるので注意。

これは *Gaussian 94* プログラムの公式な引用である。この引用は、読者のバージョンの *Gaussian 94* 或いは *Gaussian 94W* を用いて得られた結果を掲載した論文に含めなくてはならない。

この部分は *Gaussian 94* のバージョンが Revision C.3 であることを示す。Gaussian 社に送る質問には必ずこの情報を含めること。

次にインプットファイルからのルートセクション、タイトルセクション、分子指定が表示される。

計算の効率を最適化するために、プログラムの内部では計算の際に標準配向が座標系として用いられている。座標の原点は、分子中の核の電荷の中心に置かれている。ここでは、酸素原子が 原点の上の Y　軸上にあり、二つの水素原子はその下の XY 面上に置かれている。

```
Gaussian, Inc.
Carnegie Office Park, Building 6, Pittsburgh, PA 15106 USA

Cite this work as:
Gaussian 94, Revision C.3,
M. J. Frisch, G. W. Trucks, H. B. Schlegel, P. M. W. Gill,
B. G. Johnson, M. A. Robb, J. R. Cheeseman, T. Keith,
G. A. Petersson, J. A. Montgomery, K. Raghavachari,
M. A. Al-Laham, V. G. Zakrzewski, J. V. Ortiz, J. B. Foresman,
J. Cioslowski, B. B. Stefanov, A. Nanayakkara, M. Challacombe,
C. Y. Peng, P. Y. Ayala, W. Chen, M. W. Wong, J. L. Andres,
E. S. Replogle, R. Gomperts, R. L. Martin, D. J. Fox,
J. S. Binkley, D. J. Defrees, J. Baker, J. P. Stewart,
M. Head-Gordon, C. Gonzalez, and J. A. Pople,
Gaussian, Inc., Pittsburgh PA, 1995.

*********************************************
Gaussian 94:  IBM-RS6000-G94RevC.3 26-Sep-1995
                25-Nov-1995
*********************************************
------------------
#T RHF/6-31G(d) Test
------------------
---------------
Water HF Energy
---------------
Symbolic Z-matrix:
   Charge = 0 Multiplicity = 1
O      -0.464     0.177     0.
H      -0.464     1.137     0.
H       0.441    -0.143     0.
---------------------------------------------------------------------
                     Z-MATRIX (ANGSTROMS AND DEGREES)
CD Cent Atom  N1    Length/X    N2     Alpha/Y    N3      Beta/Z     J
---------------------------------------------------------------------
  1   1  O     0    -.464000          .177000           .000000
  2   2  H     0    -.464000         1.137000           .000000
  3   3  H     0     .441000         -.143000           .000000
---------------------------------------------------------------------
Framework group  CS[SG(H2O)]
Deg. of freedom    3
                    Standard orientation:
---------------------------------------------------------------------
Center      Atomic                  Coordinates (Angstroms)
Number      Number              X           Y           Z
---------------------------------------------------------------------
   1           8           .000000     .110843     .000000
   2           1           .783809    -.443452     .000000
   3           1          -.783809    -.443294     .000000
---------------------------------------------------------------------
```


この行はシングルポイントエネルギー計算で予測されたエネルギーを示す。また SCF 計算での収斂の条件も与えてある。付録 A では SCF 法についてより詳しく説明してある。

Mulliken population 解析が SCF エネルギー計算結果の後に続く。この解析は分子の電荷を原子によって分割するやり方である。

Total atomic charges と記された部分は分子中のそれぞれの原子の全電荷を示す。ここでは、酸素原子は負の電荷を持ち，二つの水素原子のわずかの正の電荷と打ち消し合っている。

この部分は標準座標での分子のダイポールモーメントを与える。このダイポールモーメントは負の Y 軸成分を持ち、その大きさは 1.69 デバイである。慣習に従って、ダイポールモーメントは正の電荷を指す方向を向く。この分子の標準配向によると、酸素原子は 正の Y 軸上に位置している。これはダイポールモーメントは酸素原子から分子の正に荷電した部分に向かっていることを示す。

成功の内に終わった *Gaussian* ジョブでは、アウトプットの終わりに内部に収納されているコレクションから種々の引用文がアトランダムにプリントされる。

CPU 時間とファイル等の他の計算資源の使用量に関する情報がジョブの最後にプリントされる。

以下はこのジョブの結果を要約したアーカイブのエントリー

```
Rotational constants (GHZ):  919.1537631  408.1143172  282.6255042
Isotopes: O-16,H-1,H-1
   19 basis functions        36 primitive gaussians
    5 alpha electrons         5 beta electrons
      nuclear repulsion energy       9.1576073710 Hartrees.
Projected INDO Guess.
Initial guess orbital symmetries:
      Occupied  (A') (A') (A') (A') (A")
      Virtual   (A') (A') (A') (A') (A") (A') (A') (A') (A')
                (A') (A') (A") (A")
Warning!  Cutoffs for single-point calculations used.
SCF Done:  E(RHF) =  -76.0098706218     A.U. after    6 cycles
             Convg  =      .3332D-04             -V/T =  2.0027
             S**2   =      .0000

*************************************************************
          Population analysis using the SCF density.
*************************************************************
Orbital Symmetries:
      Occupied  (A') (A') (A') (A') (A")
      Virtual   (A') (A') (A') (A') (A') (A") (A') (A') (A") (A')
                (A") (A') (A') (A')
 The electronic state is 1-A'.
Alpha occ. eigenvals-- -20.55796 -1.33618 -.71426 -.56023  -.49562
Alpha virt. eigenvals--    .21061   .30388 1.04585 1.11667  1.15963
Alpha virt. eigenvals--  1.16927  1.38460 1.41675 2.03064  2.03551
Alpha virt. eigenvals -- 2.07410  2.62759 2.94215 3.97815
          Condensed to atoms (all electrons):
Total atomic charges:
             1
 1  O    -.876186
 2  H     .438090
 3  H     .438096
Sum of Mulliken charges=     .00000
...
Electronic spatial extent (au):  <R**2>=     18.9606
Charge=       .0000 electrons
Dipole moment (Debye):
   X=    -.0001    Y=  2.1383    Z=    .0000  Tot=  2.1383
 Test job not archived.
 1\1\GINC-MJF\SP\RHF\6-31G(d)\H2O1\AEFRISCH\25-Nov-1995\0\\#T
RHF/6-31G(
 d) TEST\\Water HF
Energy\\0,1\O,0,-0.464,0.177,0.\H,0,-0.464,1.137,0.\H

,0,0.441,-0.143,0.\\Version=IBM-RS6000-G94RevC.3\State=1-A'\H
F=-76.0098
 706\RMSD=3.332e-05\Dipole=0.6868725,0.4857109,0.\PG=CS
[SG(H2O1)]\\@
```